AD-761 524

FINITE ELEMENT ANALYSIS OF PAVEMENT STRUCTURES USING AFPAV CODE (LINEAR ELASTIC ANALYSIS)

Raman Pichumani

New Mexico University

Prepared for:

Air Force Weapons Laboratory

May 1973

AFWL-TR-
72-186

FINITE ELEMENT ANALYSIS OF PAVEMENT STRUCTURES USING AFPAV CODE (LINEAR ELASTIC ANALYSIS)

Raman Pichumani

University of New Mexico

TECHNICAL REPORT NO. AFWL-TR-72-186

May 1973

AIR FORCE WEAPONS LABORATORY
Air Force Systems Command
Kirtland Air Force Base
New Mexico

90

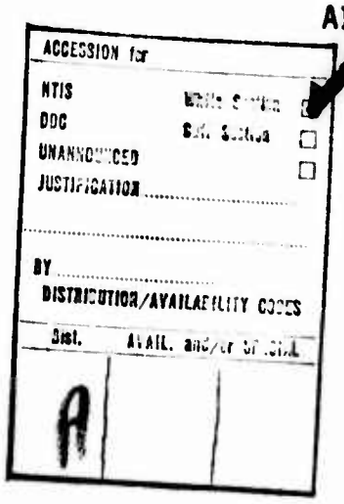

AIR FORCE WEAPONS LABORATORY
Air Force Systems Command
Kirtland Air Force Base
New Mexico 87117

UNCLASSIFIED

Security Classification

DOCUMENT CONTROL DATA - R & D

(Security classification of title, body of abstract and indexing annotation must be entered when the overall report is classified)

1. ORIGINATING ACTIVITY (Corporate author) University of New Mexico Albuquerque, New Mexico 87106	2a. REPORT SECURITY CLASSIFICATION UNCLASSIFIED 2b. GROUP

3. REPORT TITLE

FINITE ELEMENT ANALYSIS OF PAVEMENT STRUCTURES USING AFPAV CODE (LINEAR ELASTIC ANALYSIS)

4. DESCRIPTIVE NOTES (Type of report and inclusive dates)

August 1970 through March 1972

5. AUTHOR(S) (First name, middle initial, last name)

Raman Pichumani

6. REPORT DATE	7a. TOTAL NO. OF PAGES	7b. NO. OF REFS
May 1973	90	22

8a. CONTRACT OR GRANT NO	9a. ORIGINATOR'S REPORT NUMBER(S)
F29601-72-C-0024 b. PROJECT NO. 683M c. Task 04 d.	AFWL-TR-72-186 9b. OTHER REPORT NO(S) (Any other numbers that may be assigned this report)

10. DISTRIBUTION STATEMENT

Approved for public release; distribution unlimited.

11. SUPPLEMENTARY NOTES	12. SPONSORING MILITARY ACTIVITY
	AFWL (DEZ) Kirtland AFB, NM 87117

13. ABSTRACT

(Distribution Limitation Statement A)

This report deals with the structural analysis part of the rational pavement evaluation procedure being developed by the U.S. Air Force. It describes the research effort directed toward evaluating the Airfield Pavement (AFPAV) Code and conducting parametric studies of pavement systems using this code. The AFPAV code, which is an analytical model based on the finite element structural analysis technique, has been developed to represent all types of pavement systems. To evaluate the performance of the code, the data from the full-scale pavement tests sections at the Waterways Experiment Station, Vicksburg, Mississippi, were anlyzed using this code. Although agreement between theoretical predictions and field data was not as good as desired, it was reasonable considering the limitations of the linear elastic model and the difficulty in determingin the elastic constants of the pavement layers. The code was also used to conduct parametric studies of rigid and flexible pavement systems to determine the effect of changes in pav ement layer properties on the pavement response. These results revealed that the AFPAV code can be used effectively in the rational pavement evaluation program, once the properties of the various layers of the pavement systems are accurately determined.

DD FORM 1 NOV 68 1473

UNCLASSIFIED

Security Classification

14. KEY WORDS	LINK A		LINK B		LINK C	
	ROLE	WT	ROLE	WT	ROLE	WT
Civil engineering						
Airfields						
Pavements						
Flexible pavement						
Rigid pavement						
Computer code						

AFWL-TR-72-186

FINITE ELEMENT ANALYSIS OF PAVEMENT STRUCTURES USING AFPAV CODE (LINEAR ELASTIC ANALYSIS)

Raman Pichumani

University of New Mexico

TECHNICAL REPORT NO. AFWL-TR-72-186

ib

FOREWORD

This report was prepared by the Civil Engineering Research Facility, University of New Mexico, Albuquerque, New Mexico, under Contract F29601-72-C-0024. The work was performed under Program Element 63723F, Project 683M, Subtask 4A07.

Inclusive dates of research were August 1970 through March 1972. The report was submitted 20 April 1973 by the Air Force Weapons Laboratory Project Officer, Major Donald V. Harnage (DEZ).

The author wishes to acknowledge the assistance of Mr. John Crawford of the Naval Civil Engineering Laboratory in using the AFPAV code for the successful performance of this research. Ann Stough, Research Associate Mathematician, aided in making the code (particularly the movie option in the postprocessor of the code) operational on the AFWL CDC-6600 computer.

Donald V. Harnage

DONALD V. HARNAGE
Major, USAF
Project Officer

OREN G. STROM
Lt Colonel, USAF
Chief, Aerospace Facilities Branch

William B. Liddicoet

WILLIAM B. LIDDICOET
Colonel, USAF
Chief, Civil Engineering Research Division

CONTENTS

ILLUSTRATIONS

ILLUSTRATIONS (Concl'd)

TABLES

ABBREVIATIONS AND SYMBOLS

B	half-width of pavement structure
E	modulus of elasticity
$\{F_n\}$	global nodal force vector of n^{th} harmonic
F_y	applied load in y-direction
H	half-length of single wheel load
$[K_n]$	structural stiffness matrix of n^{th} harmonic
L	half-span; half-period; half-characteristic length
M	bandwidth
N	number of nodes; number of equations; number of Fourier terms
P_i $(i = 1,2,3...)$	applied loading
$\{U_n\}$	nodal displacement vector of n^{th} harmonic
W	half-width of single wheel load
b	half-width of prismatic solid
d	half-depth of prismatic solid
f_{ym}, f_{yn}	Fourier coefficients of applied vertical loading function
h	layer thickness
ℓ	half-length of prismatic solid
m, n	m^{th} and n^{th} Fourier terms, respectively
p	contact pressure
u_{xn}, u_{yn}, u_{zn}	Fourier coefficients of displacements in x, y, and z directions of n^{th} harmonic, respectively
u, v, w	displacements in x, y, and z directions, respectively
x, y, z	Cartesian coordinates
α_{in} $(i = 1$ through $9)$	generalized coordinates of n^{th} harmonic
ν	Poisson's ratio

SECTION I

INTRODUCTION

1. BACKGROUND

In 1968 the United States Air Force initiated a comprehensive research program to develop a rational pavement evaluation procedure. Three capabilities expected from this evaluation procedure were as follows (ref. 1):

(1) A technique which could be used to determine the stresses, strains, and deflections at any point within a pavement structure loaded by the multiple wheels of various gear configurations of modern aircraft

(2) An analytical capability by which the influence of varying the strength and thickness of the various pavement components could be compared in terms of the stress and strain response of the pavement system

(3) Applicability of this procedure to both rigid and flexible pavements, composite pavements, and pavement overlays

The Air Force Weapons Laboratory (AFWL) in 1969 assigned the task of developing an analytical model to the Naval Civil Engineering Laboratory (NCEL). Crawford at NCEL developed a finite element computer code, called *Airfield Pavement (AFPAV)* code, which models the layered pavement system as a prismatic solid (ref. 2). The theoretical basis for this analytical model is derived from Herrmann's three-dimensional elasticity solution for continuous beams (ref. 3). The central part of this code is based on a finite element program which Herrmann developed for three-dimensional elasticity analysis of periodically loaded prismatic solids.

While the AFPAV code was being developed by NCEL, the Eric H. Wang Civil Engineering Research Facility (CERF) operated by the University of New Mexico for the U.S. Air Force evaluated some existing computer codes to determine their applicability for theoretical analysis of general pavement systems. The results of this evaluation are reported in reference 4. The central part of the AFPAV code was compared with computer codes such as BISTRO (ref. 5), VISAB3 (ref. 6), and WIL67 (ref. 7). The AFPAV code was found to be the most suitable

and efficient of these codes for obtaining a complete picture of the stress distribution in layered pavement systems, both rigid and flexible, and for plotting pavement deflection basins under multiple-wheel aircraft gears (e.g., C-5A and Boeing 747). Furthermore, the AFPAV code can be used to analyze efficiently certain complex pavement structures, which could be idealized as prismatic solids, without having to use three-dimensional finite element programs. Since the AFPAV code uses only a two-dimensional finite element mesh, but solves special types of three-dimensional problems, it is also referred to as an extended two-dimensional code. In view of the great promise of the AFPAV code it was decided to examine its full potentialities by using it for further analyses of structural response of pavement systems subjected to heavy aircraft loads.

A linear elastic model is used for the entire pavement system in the original version of the AFPAV code (refs. 2,4). Since the inadequacy of this simplified constitutive relationship to represent all of the pavement components is realized, the code is currently being modified to consider not only nonlinear material properties but also vertical joints in rigid pavement systems and discontinuities at layer interfaces, etc. This task has been given to NCEL by AFWL, and is expected to be completed in FY73. After checking out the performance of the modified AFPAV code and establishing its usefulness as an analytical tool for airfield pavement evaluation, a report containing complete documentation of the final version of the code along with a user's manual and computer graphic displays of the analytical results of some sample problems will be published.

2. OBJECTIVES

The first objective of this research effort was to conduct a theoretical analysis of airfield pavement systems to determine the pavement response* to multiple wheel loads using the finite element analysis technique. The rigid and flexible pavements of the Multi-Wheel Heavy-Gear Load (MWHGL) test sections constructed and tested at the Waterways Experiment Station (WES) were analyzed using the original AFPAV code. The predicted responses were compared with the measured stresses and deflections in the test sections.

The second objective was to perform a parametric study of the properties of the different pavement components of the MWHGL test sections using the first version of the AFPAV code to determine the changes in pavement response due to changes in the properties of the different pavement components.

*Elastic deflections, strains, and stresses.

While implementing the above objectives, the capabilities and the limitations of the original AFPAV code were examined in some detail. Its applications to theoretical analysis of pavement structures were then assessed by (1) analyzing the MWHGL test sections and comparing the computed results with the experimental data, and (2) conducting parametric studies of both flexible and rigid pavement systems.

3. APPROACH

The objectives of this research effort which relate only to finite element analysis of pavement structures, were accomplished in two phases using the original version of the AFPAV code in which a linear elastic model was used for the entire pavement system.

a. Phase I--Evaluation of AFPAV Code

The AFPAV code consists of three parts: (1) AFPRE (preprocessor), (2) AFPAV (main program), and (3) AFPOST (postprocessor). The different parts of the code were evaluated by analyzing the MWHGL test sections at WES. Although the finite element analysis technique can handle nonlinear material properties, only linear elasticity theory was assumed in the first version of the AFPAV code which was used for the analyses conducted in this effort. The moduli of elasticity of the various pavement layers were estimated from the available laboratory and field data. The computed response (i.e., deflections and stresses) was compared with the pavement response measured by WES in the full-scale testing of pavement sections loaded with a 12-wheel assembly of the main landing gear of the C-5A aircraft.

b. Phase II--Parametric Study

The AFPAV code was used to perform a parametric study to determine the effects of varying the properties of pavement structure layers on the size and shape of the deflection basin of a pavement under multi-wheeled aircraft. Rigid and flexible pavement systems of the MWHGL test sections were studied. The thicknesses of the pavement layers, as well as the elastic constants (i.e., the modulus of elasticity, E, and Poisson's ratio, ν), were varied and the effects of changing these properties were examined. In addition to pavement deflection basins, variations of vertical and horizontal normal stresses, and shear stresses caused by variations in pavement layer properties were examined.

SECTION II

DESCRIPTION OF AFPAV CODE

The finite element structural analysis technique used in the AFPAV code is discussed in detail in reference 2 and also described briefly in reference 4. Therefore, only a brief account of the salient features of the theory is given here. This section also describes the three component parts of the AFPAV code as well as the special features of the code to show how it can perform analyses of certain pavement problems that cannot be accomplished by other codes such as BISTRO and WIL67.

1. THEORY OF PRISMATIC SOLID ANALYSIS

The AFPAV code is based on a finite element analysis computer program originally written by Herrmann for performing three-dimensional elasticity analysis of periodically loaded prismatic solids (ref. 8). Before writing this program, Herrmann presented the theory of periodically loaded structures in a paper on three-dimensional analysis of continuous beams (ref. 3), in which he defines a prismatic solid (fig. 1) as a body (1) that is infinite in extent in the

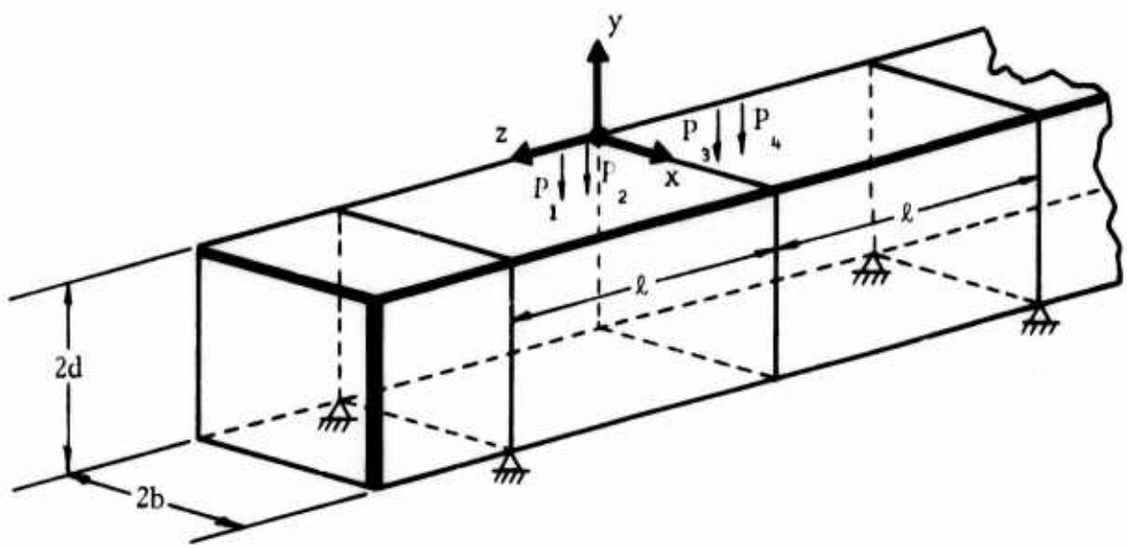

Figure 1. Prismatic Solid (Continuous Beam)

longitudinal direction, z; (2) whose cross section is identical for all values of z; and (3) whose material properties do not vary in the z-direction. The cross-sectional dimensions, compared to the length of the prismatic solid, 2ℓ, are such* that it is necessary to analyze the solid by the three-dimensional elasticity theory. Furthermore, the analysis is restricted to those problems in which the spatial dependence of the loading may be approximated as being periodic in the z-direction. The period of the loading, however, can be made sufficiently large so that the effects of isolated single loads (or groups of closely spaced loads) can be analyzed with reasonable accuracy. For example, the prismatic solid analysis may be used to determine the effect of a point load on a long tunnel or culvert by considering a series of point loads separated by sufficiently long distances, 2L, to prevent or minimize any interaction (figs. 2 and 3).

In the AFPAV code the layered pavement system is idealized as a prismatic solid which is described in a rectangular Cartesian coordinate system (x, y, and z); the z-axis is assumed to be perpendicular to the transverse section of the pavement structure (fig. 4).

The analysis of the effects of any arbitrary gear loads acting on a pavement structure is made tractable by expressing the concentrated loads, which are functions of z, as a Fourier series in z. Figure 5 shows the configuration of a 12-wheel assembly of a C-5A landing gear. If the loads are symmetric with respect to the $z = 0$ plane (fig. 5a), the loading can be represented by a Fourier cosine series. If for some reason such as the particular location of a discontinuity in the pavement structure the z-axis must be taken in a different direction (fig. 5b), the same loading as in figure 5a will be represented by a complete Fourier series consisting of both cosine and sine terms. It is not necessary to express the arbitrary gear loading as a Fourier series when the general three-dimensional solid analysis program (ref. 9) is used; however, the advantage in using the prismatic solid analysis technique in the AFPAV code is that it is simpler and less expensive than the general three-dimensional solid analysis for solving a majority of practical airfield pavement problems (refs. 1,2,4,10).

*The relative dimensions of the width, 2b, and the depth, 2d, with respect to the length of the prismatic solid, 2ℓ, determine the appropriate analytical method (e.g., if $b/\ell \ll 1$ and $d/\ell \ll 1$, conventional beam theory is adequate).

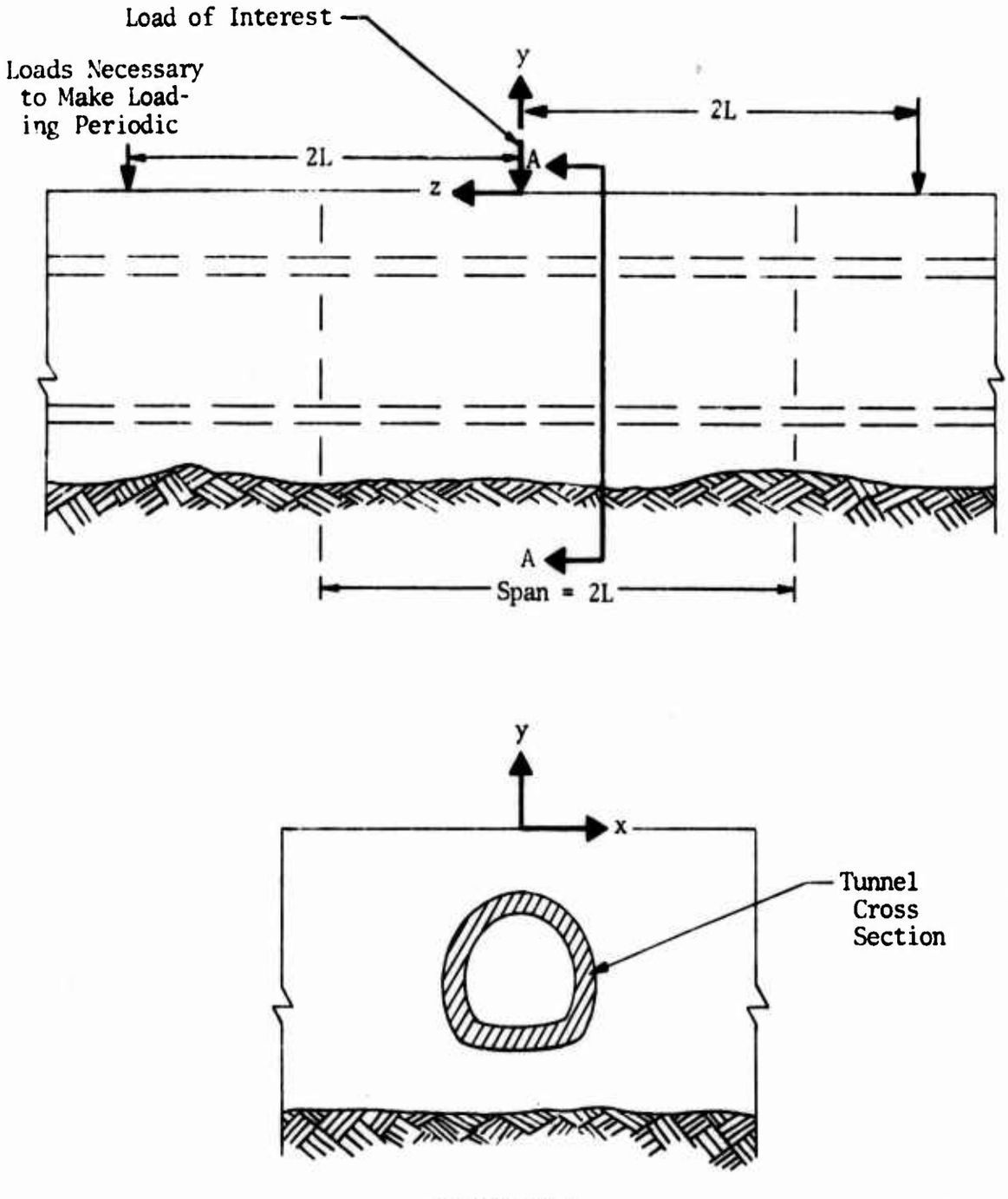

Figure 2. Tunnel Subjected to Point Load at Surface [after Herrmann (ref. 8)]

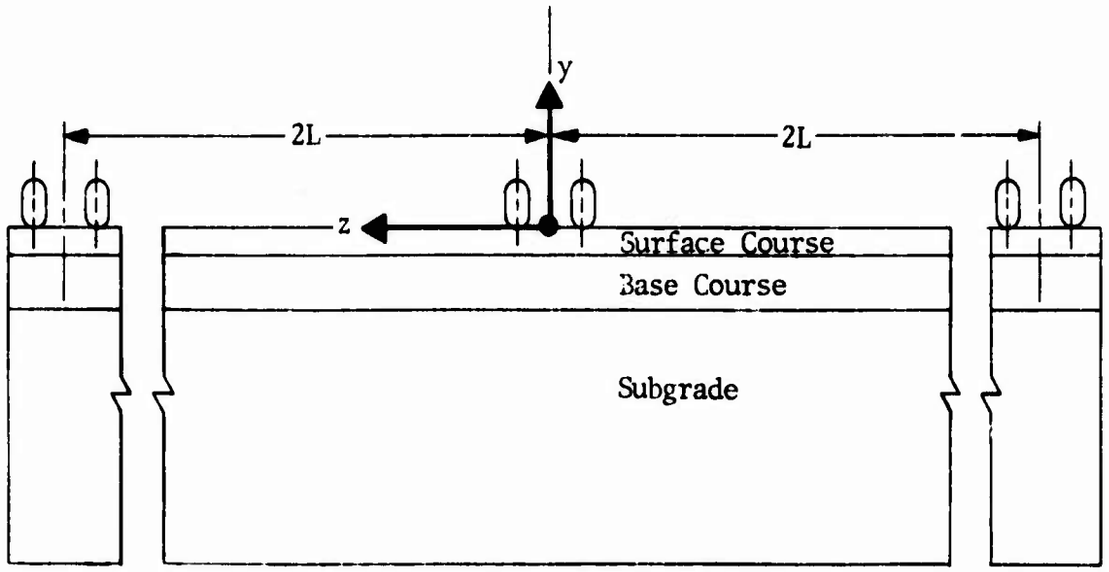

Longitudinal Section

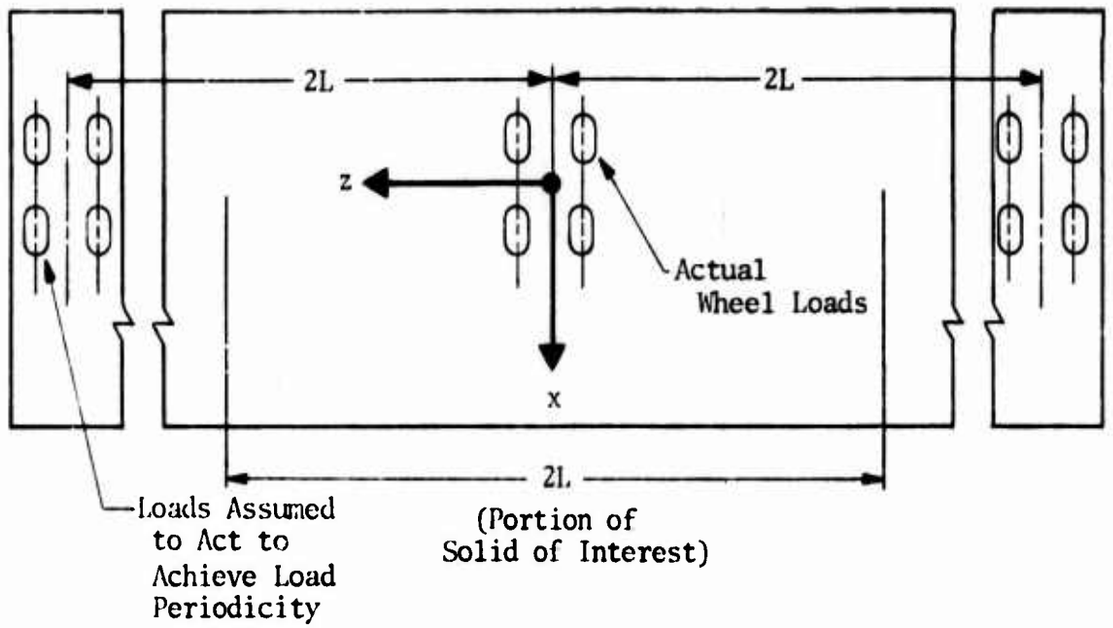

Plan

Figure 3. Pavement System Loaded by Group of Wheels

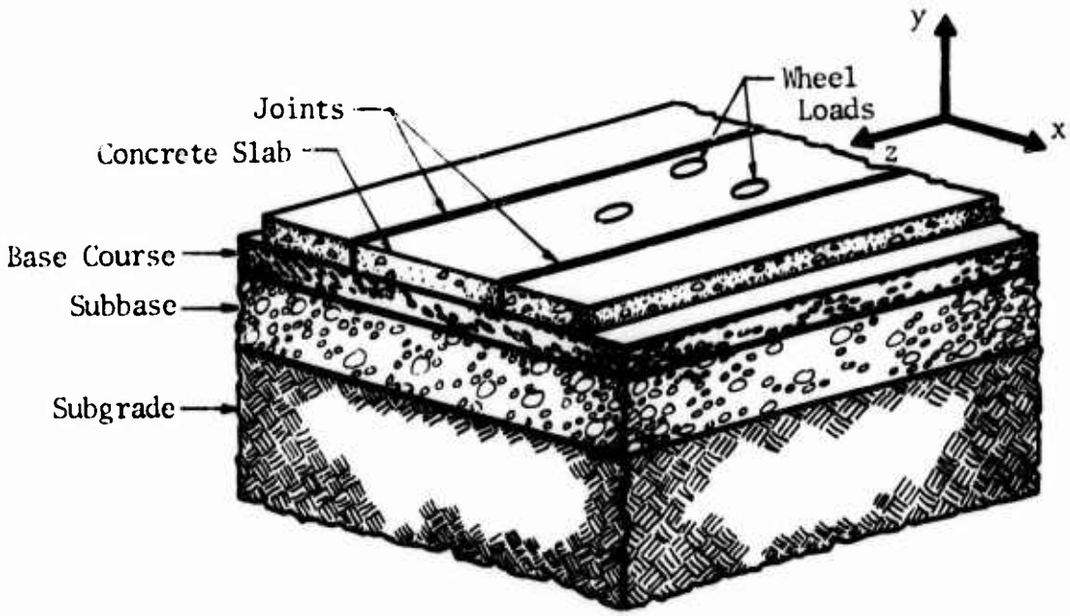

Figure 4. Pavement Structure Idealized as Prismatic Solid

Figure 6 shows an idealization of a typical pavement structure loaded by the 24 wheels of the landing gear and the 4 wheels of the nose gear of a C-5A aircraft. Figure 7 shows the finite element grid pattern of this idealized pavement structure. In this idealization, it is assumed that the cross section of the prismatic solid is as shown in figure 7 with the width equal to 2B. The period of the applied loading is equal to 2L as shown in figure 6. (The numerical values of L and B were chosen as described in section III.) All the actual infinite dimensions of the pavement system were assumed to be finite as shown by the dashed boundary lines as required by this analysis technique. Although all 24 wheels of the main landing gear are included in figures 6 and 7, it is not always necessary to consider all the wheels in the analysis. In most instances, only one group of the closely spaced wheels need be included (fig. 8) since the interaction between the different groups of loads is usually insignificant. Furthermore, the direction of the longitudinal axis can be altered as required by the circumstances of the problem as in the two cases shown in figure 8. For instance, case 2 would be the required idealization if a culvert running under the runway were to be analyzed, since the z-axis should coincide with the longitudinal axis of the culvert.

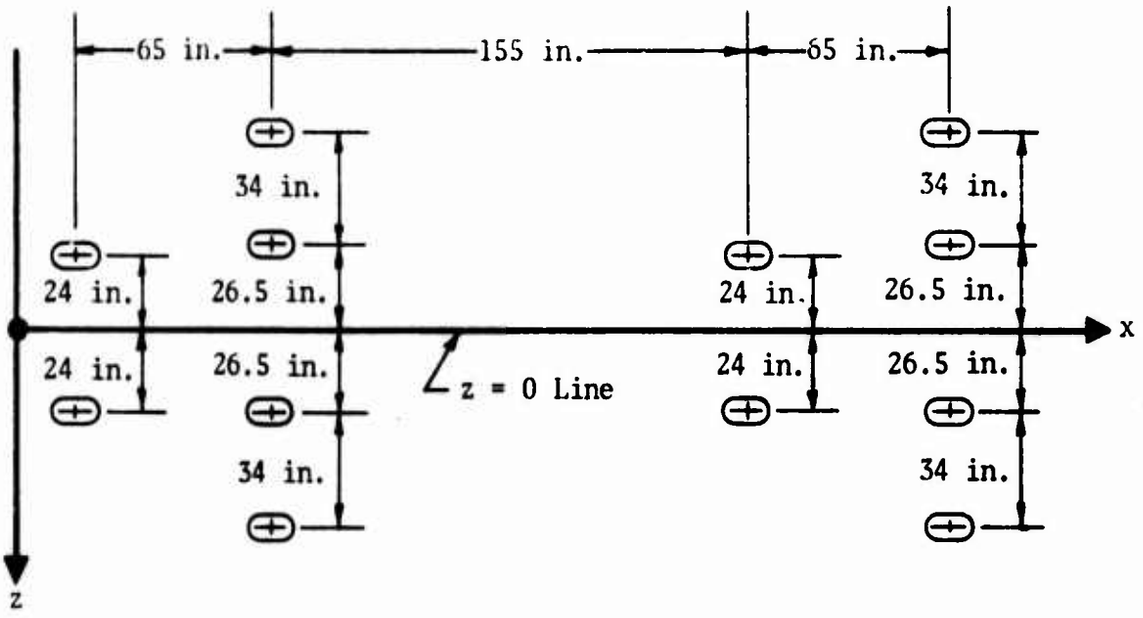

(a) Loading Symmetric About z = 0 Plane

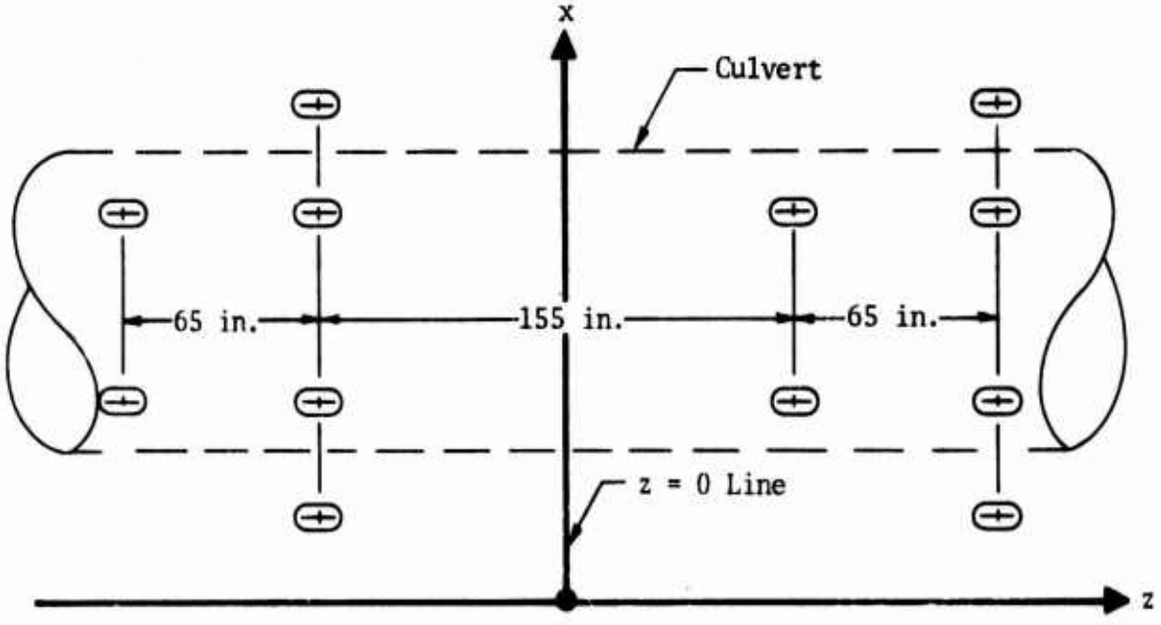

(b) Loading Unsymmetric About z = 0 Plane

Figure 5. Twelve-Wheel Assembly of C-5A Landing Gear

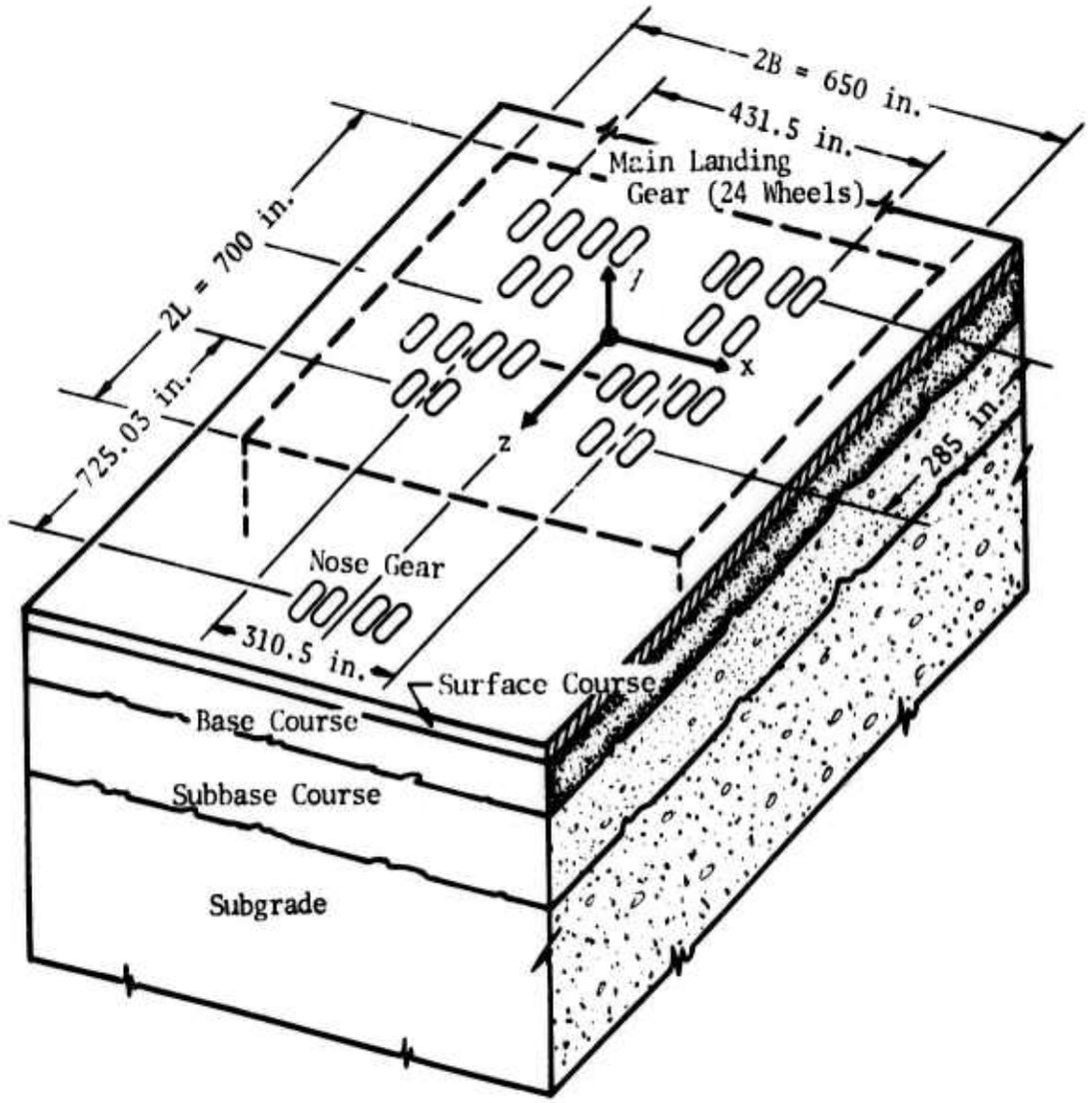

Figure 6. Idealization of Pavement Structure Loaded by C-5A Aircraft

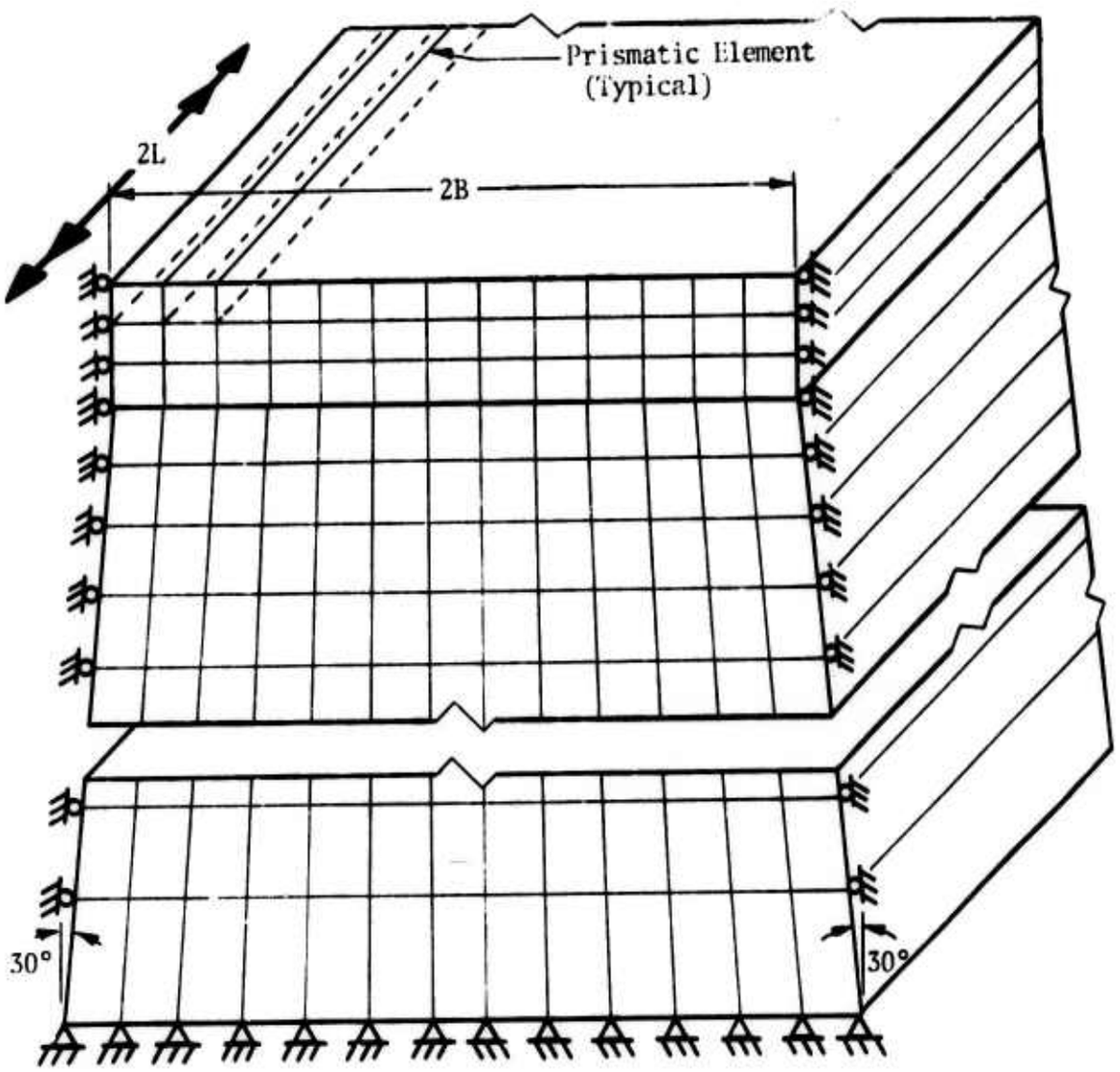

Figure 7. Finite Element Grid Pattern of Idealized Pavement Structure

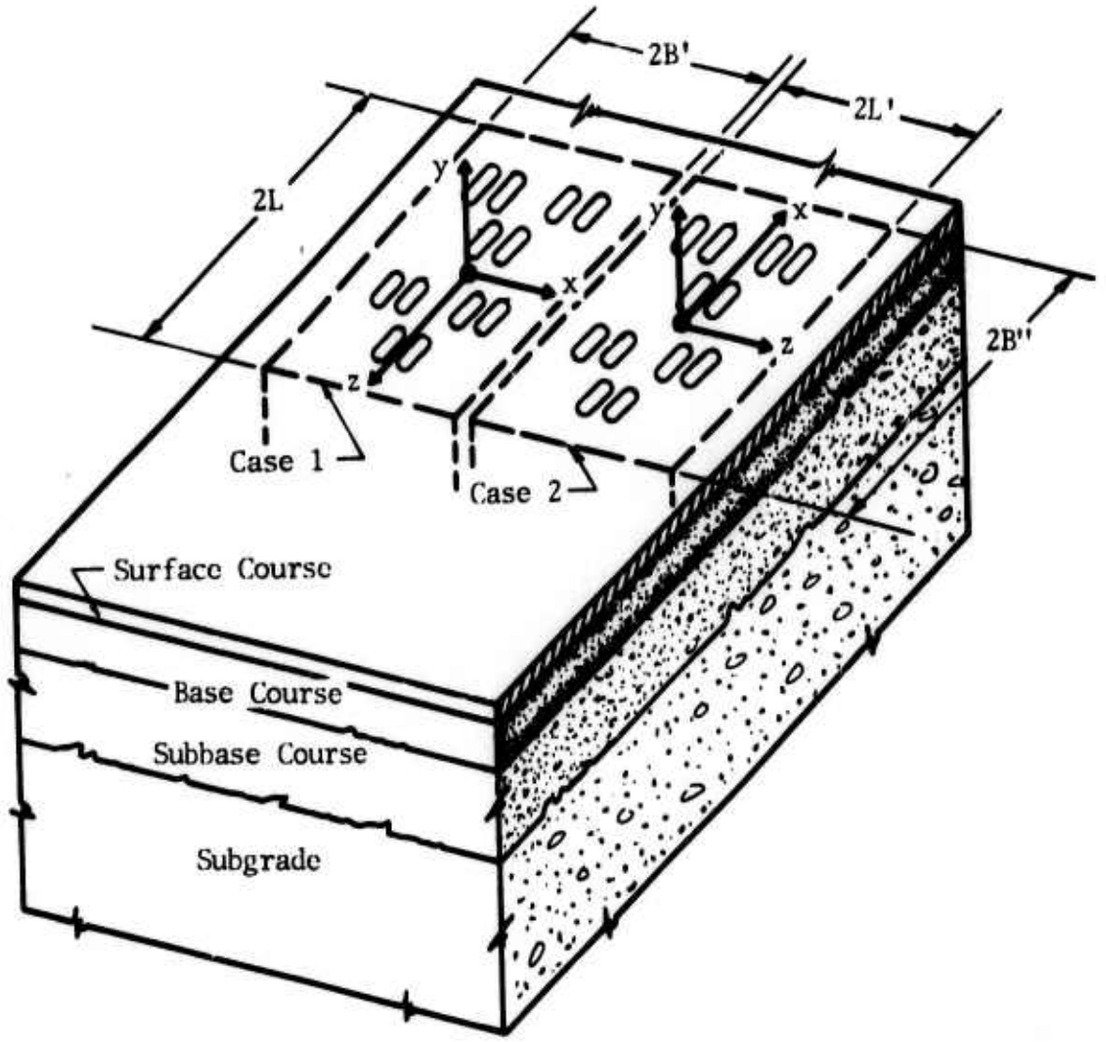

Figure 8. Alternate Idealization of Pavement Structure Loaded by C-5A Aircraft

2. THEORY OF AFPAV CODE

Crawford at NCEL developed the AFPAV code for AFWL as a model for analyzing airfield pavements by adding a preprocessor (AFPRE) and a postprocessor (AFPOST) to the prismatic solid analysis program (AFPAV) which is the central or main part of the code. The structural analysis of the problem is performed by AFPAV, and the theory described in the following paragraphs pertains to that part only. AFPRE simplifies the enormous amount of input data pertaining to the multi-wheel gear loads and the pavement structure properties; AFPOST prints the output data or produces a graphic display of the output either in a movie or in microfilm plots.

As the term *finite element analysis* indicates, the layered pavement structure with *infinite* dimensions is first reduced (idealized) to a structure with finite dimensions as shown in figure 6 and then subdivided into a system of discrete, but interconnected substructures as shown in figure 7. Each rectangle/quadrilateral in figure 7 represents a prismatic* element (substructure) with a length of 2L (fig. 6). The corners of these elements represent the nodal lines and are simply called *nodes*.

Structural analysis of the complicated layered pavement system is performed by assuming that the unknowns in the problem are the displacements at the nodes. The applied loading is broken up into concentrated forces acting at the nodes. By applying the minimum potential energy theorem and using appropriate kinematic assumptions for the distribution of displacements within each element as described below, equilibrium equations for nodal forces are developed in terms of the unknown nodal displacements. Solution of this set of simultaneous equations gives the nodal displacements from which the strains and stresses in the different elements of the structure are determined.

In the first version of the code, each quadrilateral element (fig. 9) was divided into four triangular elements, and a linear distribution of displacement field was assumed within each triangular element. After forming the stiffness matrices of the triangular elements, the quadrilateral element stiffness was

*Henceforth, in this report, the use of the adjective *prismatic* to describe the element is dispensed with for convenience; it must, however, be remembered that in the AFPAV code the author is always referring to three-dimensional prismatic elements of the prismatic solid and not to two-dimensional plane elements.

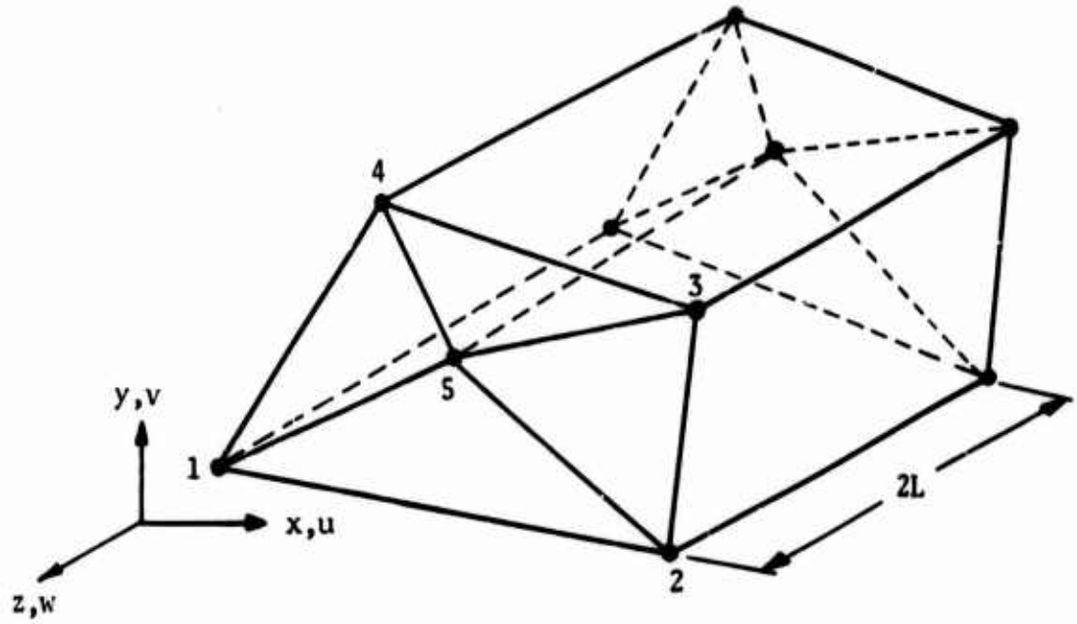

Figure 9. Prismatic Quadrilateral Element Composed of Triangular Elements

formed by condensing out (i.e., by eliminating the unknown displacements of) the interior node.

Since the nodal displacements due to arbitrary gear wheel loads are functions of x, y, and z, the displacements are expanded into Fourier series having a period of 2L, as given in the following equations:

$$u(x,y,z) = \sum_{n=0}^{N} u_{xn}(x,y) \cos\left(\frac{n\pi z}{L}\right) + \sum_{m=1}^{M} u_{xm}(x,y) \sin\left(\frac{m\pi z}{L}\right) \tag{1a}$$

$$v(x,y,z) = \sum_{n=0}^{N} u_{yn}(x,y) \cos\left(\frac{n\pi z}{L}\right) + \sum_{m=1}^{M} u_{ym}(x,y) \sin\left(\frac{m\pi z}{L}\right) \tag{1b}$$

$$w(x,y,z) = \sum_{n=0}^{N} u_{zn}(x,y) \sin\left(\frac{n\pi z}{L}\right) + \sum_{m=1}^{M} u_{zm}(x,y) \cos\left(\frac{m\pi z}{L}\right) \tag{1c}$$

where u, v, and w represent displacements in the x, y, and z directions, respectively (ref. 2). The Fourier coefficients u_{xn}, u_{xm}, etc., are functions of x and y only, and the displacement variation along the z-axis is accounted

for by the Fourier series expansion in terms of z. If the loading is symmetrical about the x-axis (i.e., z = 0 plane), the second terms on the right side of eqs. (1) are omitted since they are required for unsymmetrical loading only.

The following form of the Fourier coefficients can be assumed to give a linear variation of displacements within the triangular elements in the x-y plane:

$$u_{xn}(x,y) = \alpha_{1n} + \alpha_{2n}x + \alpha_{3n}y \tag{2a}$$

$$u_{yn}(x,y) = \alpha_{4n} + \alpha_{5n}x + \alpha_{6n}y \tag{2b}$$

$$u_{zn}(x,y) = \alpha_{7n} + \alpha_{8n}x + \alpha_{9n}y \tag{2c}$$

The αs are called *generalized coordinates*. The linear displacement field in eqs. (2) ensures a linear variation of displacements along the edges of the triangles thus forcing continuity between elements since edges initially straight will remain straight in the deformed position. Furthermore, displacement continuity throughout the structure is ensured by having common displacements at the two node points along each element edge.

From the assumed displacement functions, the element strains are derived by using the appropriate strain/displacement relationships of elasticity theory. Strains must also be expanded in Fourier series since displacements are expressed in this manner. By using the appropriate constitutive equations, the element stresses can be derived from the element strains. Stresses, like strains, are expanded in Fourier series.

The equilibrium equations of the structure are derived by applying the theory of minimum potential energy. In this process, when the total strain energy is computed by integrating over the volume of the body, the orthogonality conditions of the trigonometric functions help to uncouple eqs. (1) (ref. 2, appendix I). Thus a set of governing equilibrium equations in the following form is obtained for each Fourier term:

$$[K_n]\{U_n\} = \{F_n\} \tag{3}$$

where $[K_n]$ is the structure stiffness matrix, $\{F_n\}$ is the global nodal force vector, and $\{U_n\}$ is the nodal displacement vector, for the n^{th} harmonic. The displacement vector in eq. (3) is a function of x and y only. The structure

stiffness matrix is obtained by summing the quadrilateral element stiffness matrices; the quadrilateral element stiffness matrix itself is obtained from the four triangle stiffness matrices.

The discrete wheel loads of the landing gear of an aircraft are expressed in a Fourier series as functions of the z-coordinate in the same manner as the displacement functions. These Fourier loads are broken down into an equivalent set of concentrated loads acting at the nodal points. In a general case, both cosine and sine Fourier terms are included in the Fourier series expansion:

$$F_y(z) = \sum_{n=0}^{N} f_{yn} \cos\left(\frac{n\pi z}{L}\right) + \sum_{m=1}^{M} f_{ym} \sin\left(\frac{m\pi z}{L}\right) \tag{4}$$

where f_{yn} and f_{ym} are the Fourier coefficients of the applied vertical loading function. In eq. (4), the subscript y refers to the vertical component of the applied load. If loads in the horizontal direction are to be considered, similar expressions can be written. If the wheel loads are symmetric about the x-axis (i.e., z = 0 plane), eq. (4) can be reduced to

$$F_y(z) = \sum_{n=0}^{N} f_{yn} \cos\left(\frac{n\pi z}{L}\right) \tag{5}$$

The choice of the coordinate axes shown in figure 6 and in case 1 of figure 8 requires the use of eq. (4); case 2 in figure 8 needs only eq (5).

For each harmonic of the loading function, there are a corresponding harmonic of the displacement function and an associated stiffness matrix. The equilibrium equations are solved for each harmonic to obtain the Fourier coefficients of the corresponding harmonic of the displacement function. The nodal displacements are finally computed by substituting these coefficients in eqs. (1). The strains are derived from the displacements. The linear displacement functions assumed in eqs. (2) give constant strains in a given element. The stresses are then computed from the strains. Since the stresses are constant over a given (constant-strain) element, great care must be exercised in idealizing the pavement structure by having smaller elements in areas of high-strain gradients and having as many elements in the whole structure as computer capacity and computer cost will permit. However, because of the limitations in computer capacity, it is not possible to increase the number of elements too much; therefore, it is necessary to replace the constant-strain elements by higher-order elements where greater accuracy is desired (ref. 11). Details of the

higher-order elements and a comparison of the pavement responses predicted by constant-strain element formulation and higher-order element formulation will be given in a subsequent report.

3. STRUCTURE OF AFPAV CODE

The AFPAV code contains three parts each of which performs a significant function: AFPRE (preprocessor) generates the finite element mesh and determines the Fourier coefficients of the applied wheel loading for input into the main program; AFPAV (main program) uses the linear elasticity theory to predict the response of layered pavement systems subjected to the static loadings of MWHGL of aircraft such as the C-5A and the Boeing 747; AFPOST (postprocessor) is capable of either producing a graphic display of the stresses and displacements or of printing out the stresses, strains, and displacements in the entire cross section of the structure at any desired location in the pavement.

a. AFPRE Program

The main program of the AFPAV code considers the effect of multiple wheel loads without converting them into an equivalent single-wheel load or without using the principle of superposition as in the BISTRO code (ref. 5). Furthermore, the Air Force has developed this code as an analytical model to represent the special three-dimensional nature of the pavement structure (i.e., prismatic solid) and to consider the actual gear configuration of any type of aircraft. Because of this versatility, a large amount of manual input will be required to define the pavement structure and the Fourier coefficients of applied loading if only the original prismatic solid finite element analysis program developed by Herrmann is used. Therefore, AFPRE was developed to automate the input of structure dimensions and the calculation of the Fourier coefficients of the applied loading.

AFPRE contains several options and special features. There are two distinct segments in the preprocessor (viz., single-wheel and multi-wheel load analysis). In the single-wheel analysis, only one-half of the layered pavement system (fig. 10) need be considered. The main restriction in this analysis is that the thickness of each layer of the pavement system be uniform. For ease in expressing the wheel loads in Fourier series, the tire contact area is assumed to be rectangular. The multi-wheel load option in AFPRE is more versatile than the single-wheel option. There are two cases in the multi-wheel load

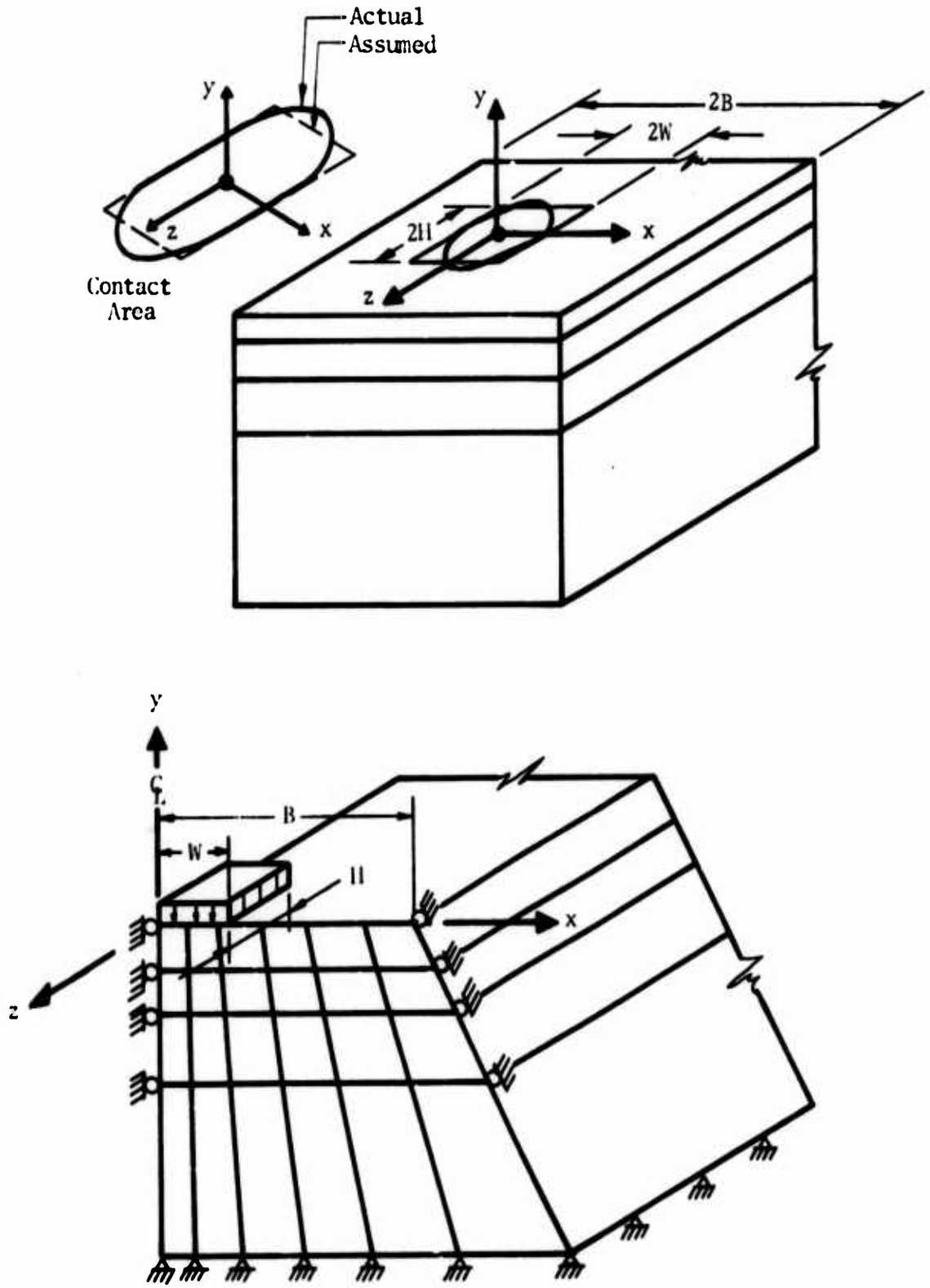

Figure 10. Single-Wheel Load Option in AFPRE

option, depending on the choice of the z-axis with respect to the gear wheel configuration in a given problem. They are symmetric and unsymmetric wheel configuration. Figure 11 shows a 6-wheel assembly symmetric with respect to the longitudinal z-axis.* Because of symmetry, it is sufficient to consider only one-half of the pavement system loaded by one-half of the wheel assembly. This feature is similar to the single-wheel load option in AFPRE and reduces the number of node points and elements. Of course, this assumes symmetry of not only the loads but also of the pavement layers. The same 6-wheel assembly is shown again in figure 12, but the orientation of the z-axis is different from that in figure 11 because of the inclusion of the culvert in the pavement structure. Therefore, the entire wheel assembly must be included in the analysis.

There is a significant difference between the single-wheel option and the multi-wheel option in respect to the capability for automatic mesh generation. In the single-wheel option, the finite element mesh data for the entire structure is automatically generated; however, to achieve this capability, a sacrifice must be made in that the pavement layers must be horizontal and of uniform thickness. If nonuniform thicknesses are encountered in a problem, the multi-wheel load option can be used to input the structure data even for a single wheel load. In the multi-wheel option, the following three distinct regions are assigned to cover the different layers of the pavement systems:

(1) Surface region
(2) Base region
(3) Subgrade region

Even though the names of the different regions appear to be the same as those commonly used by pavement engineers, they do not necessarily refer to the same thing in the AFPAV code. For example, in figure 11 there are four different pavement material layers, viz., surface course, base course, subbase, and subgrade. In each of these material layers, there are more than one element layer. In the AFPAV code, however, the first of the element layers of the surface course is called the *surface region;* the remaining element layers of the

*However, the loading is not symmetric about the z = 0 plane in this case and, therefore, eq. (4) containing both cosine and sine Fourier terms would be used to determine the Fourier coefficients of the loading.

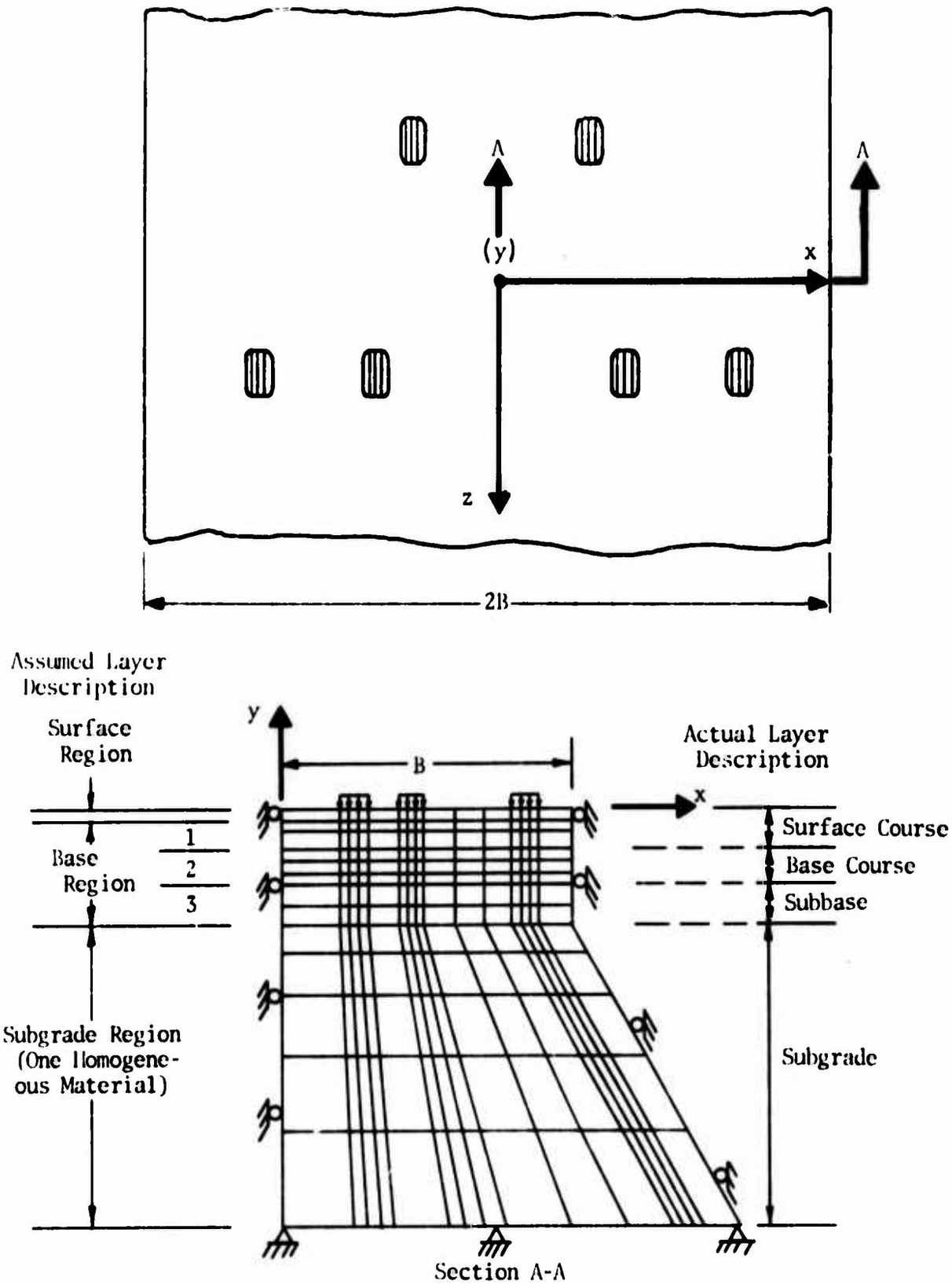

Figure 11. Symmetric Multi-Wheel Load Option in AFPRE

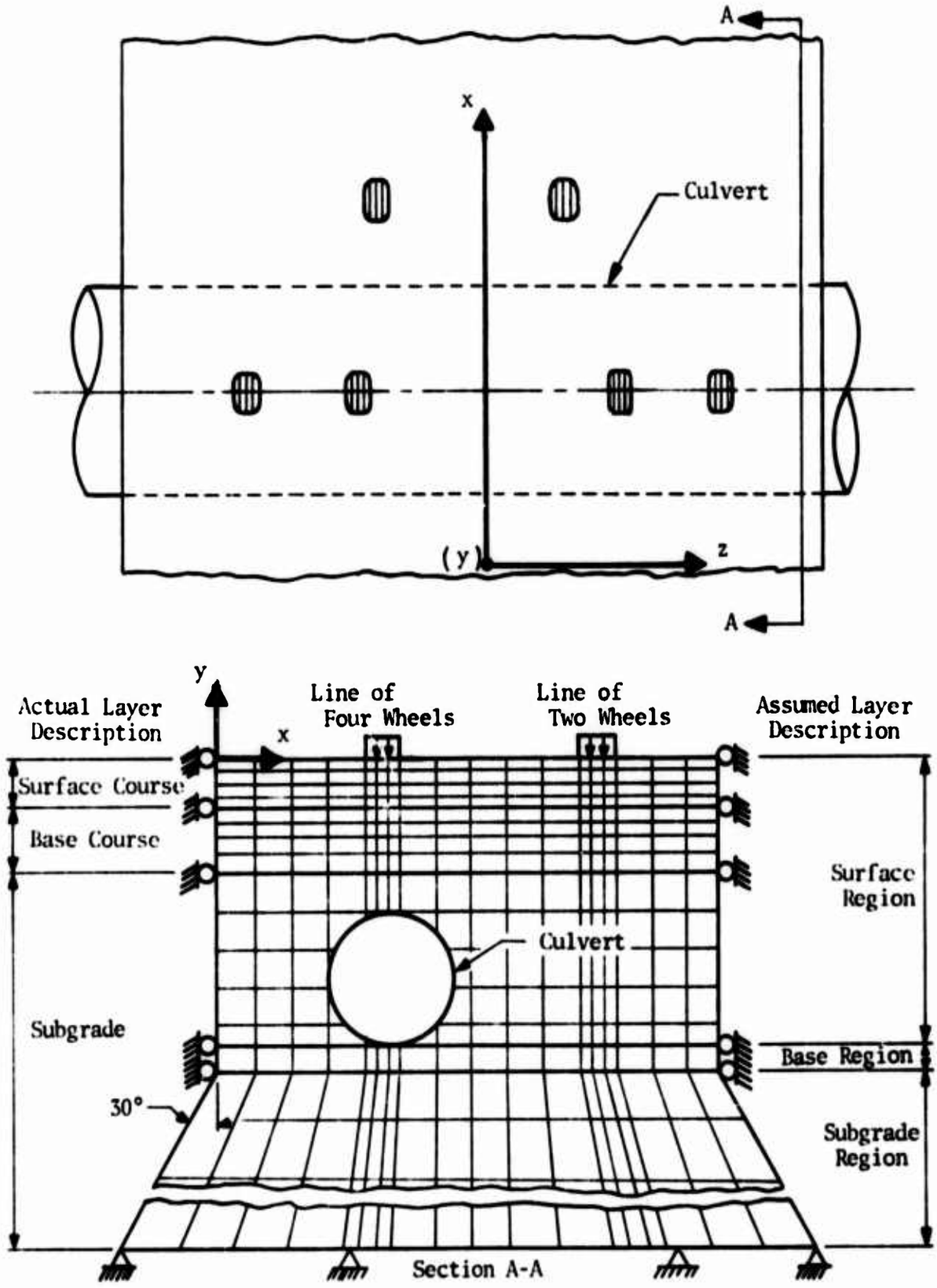

Figure 12. Unsymmetric Multi-Wheel Load Option in AFPRE

surface course and all the element layers of the base course and subbase are designated as the *base region*; and the subgrade, which is always assumed to be of one homogeneous material in this code for the purpose of automation of element layers, is called the *subgrade region*. This division of the different pavement layers into three regions has been arbitrarily made to achieve very desirable objectives. While inputting the information in AFPRE concerning different layers for generating the finite element mesh, it is necessary to give the coordinates of the nodes and the node numbers of the elements in the surface region only. Then, if the number of element layers required in each of the component material layers of the base region* and the thicknesses of the material layers are specified, AFPRE automatically calculates all the information concerning the elements and the nodes in the entire structure. The sides of the surface and the base regions are assumed to be vertical; the subgrade region has sloping sides.

In some special cases the surface region, like the base region, can have more than one material. (This can be seen in figure 12 where the surface course, the base course, the culvert, and even a part of the subgrade are included in the surface region.) This, however, increases the amount of input data to describe the complicated structure to AFPRE.

In the present version of AFPRE, the nodes are first numbered automatically in a horizontal direction. Then, if desired, the nodes can be renumbered in the vertical direction as shown in figure 13. This results in a reduction of the computer time required for the solution of the set of simultaneous equations represented by eq. (3) because of the reduction in the *bandwidth* of the matrix equation. Figure 13 shows the finite element idealization of a typical pavement system with 14 element layers (and 3 or 4 material layers as the case may be). When the numbering of the 40 columns of nodes is done horizontally, the bandwidth in this three-dimensional problem is 126. However, by renumbering the nodes in a vertical direction as shown in figure 13, the bandwidth is reduced to 51. Since the number of arithmetic operations involved in

*The number of element layers in the subgrade region is automatically calculated; however, the user must specify certain information to guide the program in determining the depths of the element layers.

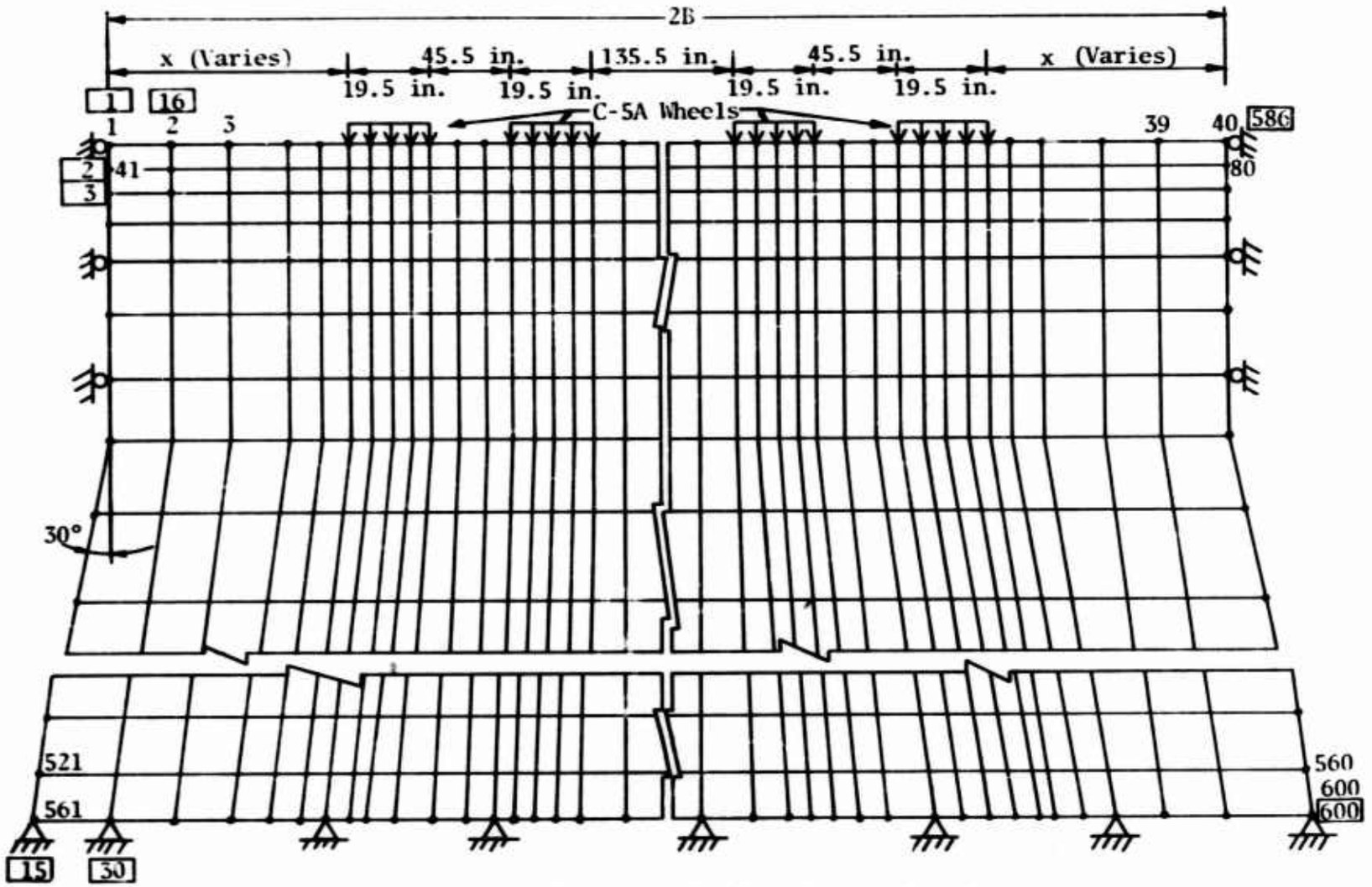

Note: Nodes renumbered in the vertical direction are boxed.

Figure 13. Renumbering of Nodes of Idealized Pavement Structure

solving a set of N simultaneous equations with a bandwidth, M, is proportional to NM^2, the renumbering reduces the number of operations to about 16 percent of that required without renumbering. (If the number of element layers were 20 instead of 14, the reduction in the number of operations would be about 30 percent. The saving due to renumbering is obviously a function of the number of horizontal layers for a given number of vertical columns.) This results in considerable savings in computer time, particularly when solving a multi-layered pavement system loaded by multi-wheel-geared aircraft such as the C-5A. At present, this renumbering scheme requires the running of AFPRE twice; however, AFPRE could be modified to eliminate this double run. (AFPRE takes a very insignificant part of the total computer time compared with that taken by the complete AFPAV code.)

b. AFPAV Main Program

The main part of the AFPAV code takes the input data concerning the aircraft loading and the pavement structure from AFPRE and performs the finite element structural analysis computations. In the present version of this code, this program performs only static analysis of linear elastic problems; however, this part of the code is being modified to consider nonlinear stress/strain relationships of certain pavement layer materials.

There are two options for feeding the input data to the main program: (1) using AFPRE for generating the finite element mesh data and determining the Fourier coefficients of the applied loading; and (2) determining the input data by separate calculations and feeding them to the main program manually by cards. Since the purpose of adding AFPRE to the original prismatic solid analysis program was to eliminate the need for manual input of an enormous amount of data relating to the finite element mesh and multiple loads, it is not now necessary to use the second input option. Furthermore, AFPRE does not take much computer time.

There are two options for obtaining the output data: (1) using AFPOST; and (2) using the main program only. Using the main program to print the output, one can specify one or more nodes or elements at one or more cross sections of the pavement system and the following information pertaining to any specified cross section of the pavement system can be obtained:

(1) The displacements in three directions at any specified node of the finite element mesh

(2) The three normal strains, the three shear strains, and the three normal stresses in any specified element

Using AFPOST, however, one can limit the number of cross sections but not the number of elements and nodes in a given cross section. Once the cross sections are specified, the results relating to all the nodes and the elements in those cross sections are printed. When using AFPOST, the core storage required increases depending on the number of cross sections at which results are desired.

c. AFPOST Program

To eliminate the need to examine the enormous amount of printed output generated either by AFPOST or by the main program itself, certain plot capabilities were developed to do the following for any specified cross section:

(1) Plot contours of stresses and displacements in the x-y plane

(2) Plot stresses and displacements as *surfaces* over the x-y plane providing a three-dimensional view of the distribution of stresses, etc., in a cross section

These plots can be obtained for the entire cross section of the pavement system or for only a part of the cross section as desired by the user.

In addition to the above capabilities, AFPOST can plot the finite element mesh input data (such as the material description, mesh geometry, node numbers, etc.) so that the user can check the accuracy of the input. Examples of most of the plots that can be obtained using AFPOST are given in reference 2.

AFPOST can also help the user make a movie showing all the plots mentioned above. This movie does not show the variation of stresses, etc., as a function of time, since only static analysis can presently be performed. However, it does afford an excellent graphic display of the changes in stresses and displacements as a function of space. In the case of a C-5A aircraft, this graphic display could be assumed to represent, without any significant error, the changes in stresses, etc., at a given cross section of the pavement system as the different rows of the 24-wheel assembly of the landing gear moved very slowly over that cross section. Such a movie has been made, and prints of the

frames will be included in a subsequent report which will contain documentation of the program and sample problems.

In addition to the graphic displays mentioned, AFPOST can print out in tabular form all the stresses and displacements in all of the elements at desired cross sections of the pavement structure as stated earlier. However, while it is possible to print out displacements, strains, and stresses pertaining to only a select number of nodes or elements using the main program, it is not possible to achieve this using the present version of AFPOST. Experience has shown that it is not advisable to use AFPOST if the pavement response at only a few points is desired. For graphic displays of contours of stresses, etc., however, AFPOST is very useful.

The preceding description of the capabilities of AFPOST covers only those features originally included in the code developed by NCEL. While analyzing practical pavement problems, it was realized that it would be useful if linear plots of stresses and displacements as functions of depth could also be made. Therefore, a subroutine for obtaining such plots was written at CERF by Ann Stough. This subroutine can be used in conjunction with the main program of the AFPAV code. Similarly it would be useful to have the capability to plot the surface deflection basins of pavement systems loaded by multi-wheeled aircraft gears using the output data given by the main program. A subroutine to obtain such a plot was also prepared at CERF. In order not to make AFPOST a very unwieldy part of the AFPAV code, these two subroutines are kept separate and can be used in conjunction with the main program whenever required.

4. SPECIAL FEATURES AND LIMITATIONS

A special feature of the AFPAV code is that the culvert shown in figure 12 is considered a part of the pavement structure in the prismatic solid analysis; this cannot be done with other codes used for pavement analysis. Similarly, edge loading, discontinuities in pavement systems such as longitudinal joints, and nonuniform thickness of certain layers (e.g., thickened edges and keel sections in Portland cement concrete slabs) can be considered by the AFPAV code and not by other codes such as BISTRO. For a detailed comparison of the AFPAV code with other codes, see reference 4.

Although the AFPAV code is a good tool for three-dimensional analysis of pavement systems idealized as periodically loaded prismatic structures, a

general three-dimensional analysis of pavement structures cannot be performed with this code. Specifically, the presence of intersecting joints in Portland cement concrete slabs cannot be accounted for, since the main assumption of a prismatic solid is that the cross section of the solid does not vary in the longitudinal direction. In the present version of the AFPAV code, only linear elastic, static analysis can be performed. However, this code is currently being modified to consider nonlinear stress/strain relationships of certain pavement layer materials.

SECTION III

SIGNIFICANCE OF SYSTEM IDEALIZATION PARAMETERS

Both the pavement structure and the discrete loads of the multi-wheeled aircraft gear must be properly idealized in order to analyze a layered airfield pavement problem. The structure idealization of pavement systems for finite element analysis has been discussed in detail elsewhere (refs. 1,2,4, 10,12,13). Briefly, the layered half-space is idealized as a finite structure with boundaries consisting of rollers and pin supports as shown in figures 10 through 13, and the discrete loads are expressed in a Fourier series. The influence of these boundary conditions and the significance of the loading function parameters are discussed in this section. The two parameters pertaining to the Fourier series expansion of the loading function are (1) the number of Fourier terms, N, and (2) the characteristic length, or the period, 2L, as in eq. (1). Linked with these two parameters is the fineness of the finite element mesh used to represent the given pavement cross section. The interaction of these three parameters has been investigated by Herrmann whose findings on this subject are discussed by Crawford in some detail in reference 2. In this connection, it is worthwhile to make the following general observations based on experience gained in using the code.

1. ELEMENT SIZE

Crawford (ref. 2) has stated that, when the decreasing importance of the higher-order terms to the total solution is accounted for, about the same fineness of grid is needed for all values of N. Therefore, it is sufficient to draw up a finite element grid with element sizes under, and adjacent to, the loads as small as the computer capacity will permit and to use the same grid for all values of N.

Figure 13 shows a finite element mesh used to determine the response of a pavement system loaded by a C-5A aircraft. The distance of the vertical rollers from the edge of the outer wheels, x, should be as great as possible so as to include as much of the pavement cross section in the idealized structure as is convenient. This distance should be at least 7 to 10 times the width of the wheel, and preferably greater in the case of rigid pavement systems. It may be difficult to achieve this for multiple wheels because of the increase in the number of nodes that will result from an excessively large value of x. If in

figure 13 the top element layers are taken as 1 in. thick in a 3-in.-thick material such as an asphalt cement concrete layer, it would be desirable to restrict the maximum width of an element in this element layer at either edge of the structure to about twenty times the thickness (i.e., 20 in.) to obtain a proper definition of stresses in that element. If this restriction is adhered to and if the distance, x, chosen is 200 in. or more, the number of nodes in a horizontal layer will increase to considerably more than that shown in figure 13. The increase in the number of nodes in a horizontal layer will restrict the number of element layers since there is a limit on the total number of nodes that the program can handle. Since the computer time depends on the number of nodes in the grid, it is desirable to minimize the number of nodes in a given problem. Therefore, care should be exercised in choosing the finite element grid to idealize a given pavement system loaded by a particular aircraft.

2. NUMBER OF FOURIER TERMS

The number of Fourier terms, N, required to express a loading function with reasonable accuracy must be determined in relation to the problem to be solved. In reference 4 the author shows that the elastic (recoverable) surface deflections are predicted fairly accurately in a particular problem with as little as six Fourier terms. Although the subgrade stresses were predicted as accurately with 6 Fourier terms as with 31, the stresses in the surface layer were not predicted properly with a small number of Fourier terms. The reason for this is clear from figure 14 which shows the Fourier series representation of a line of four wheel loads of a C-5A gear by 9, 17, and 31 Fourier terms. Figure 15, which compares the loading function represented by 9, 17, and 31 terms, also shows that a smaller number of Fourier terms does not predict the surface stresses accurately since large tensile (upward) loading is given by Fourier expansion with a smaller N. The stresses in deep layers, however, will be accurately predicted as can be explained by the Saint-Venant's principle. (A unit value is assumed in figures 14 and 15 for contact pressures, and a constant period is used for the three different Fourier terms.)

3. PERIOD OF LOADING FUNCTION

The period of the Fourier series representing the discrete wheel loads affects the pavement response just as the number of Fourier terms does. Figure 16 shows the effect of the period on the loading function of a line of four

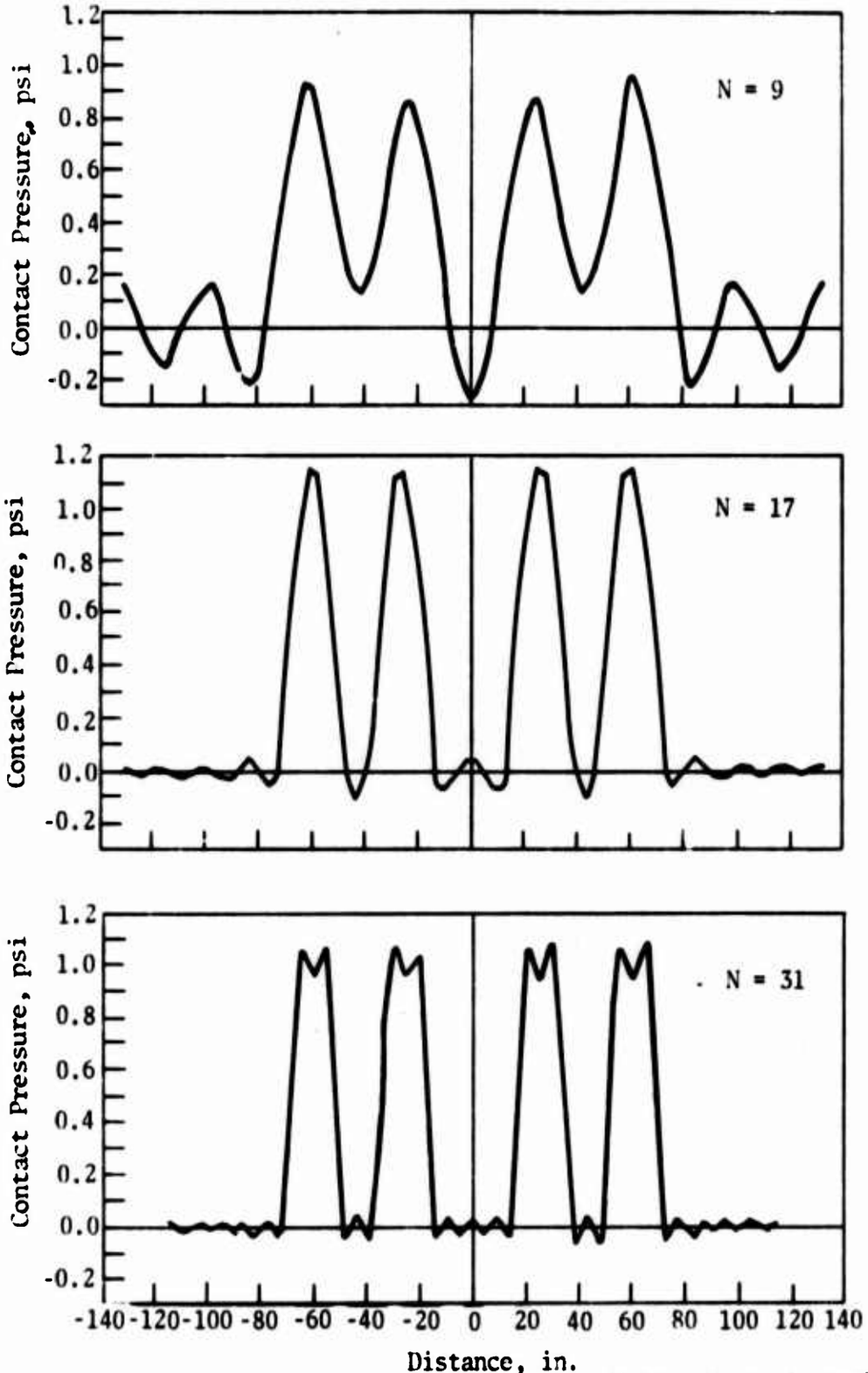

Note: N equals number of Fourier terms.

Figure 14. Fourier Series Representation of Four Wheel Loads of C-5A Landing Gear

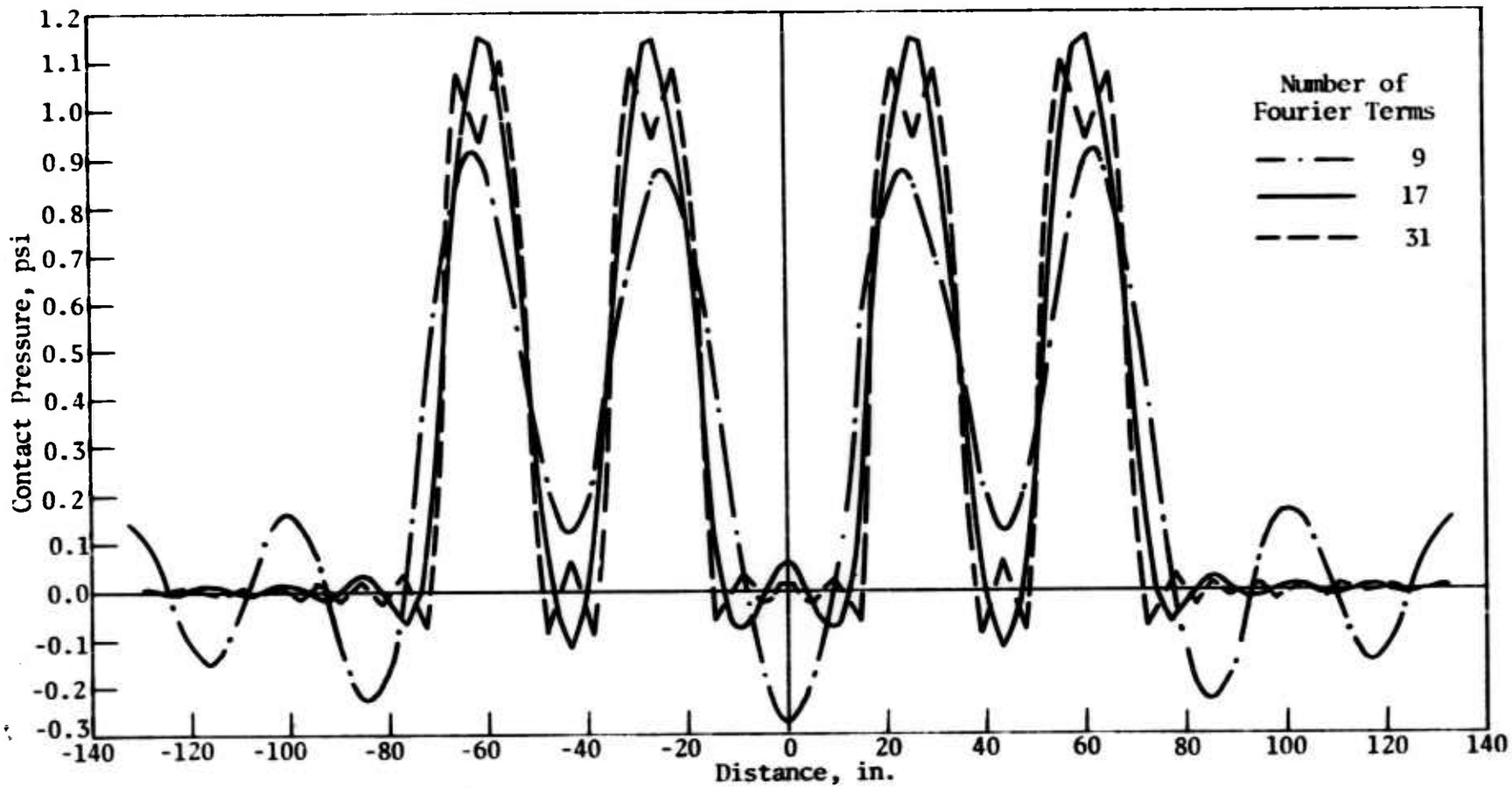

Figure 15. Effect of Number of Fourier Terms on Loading Function

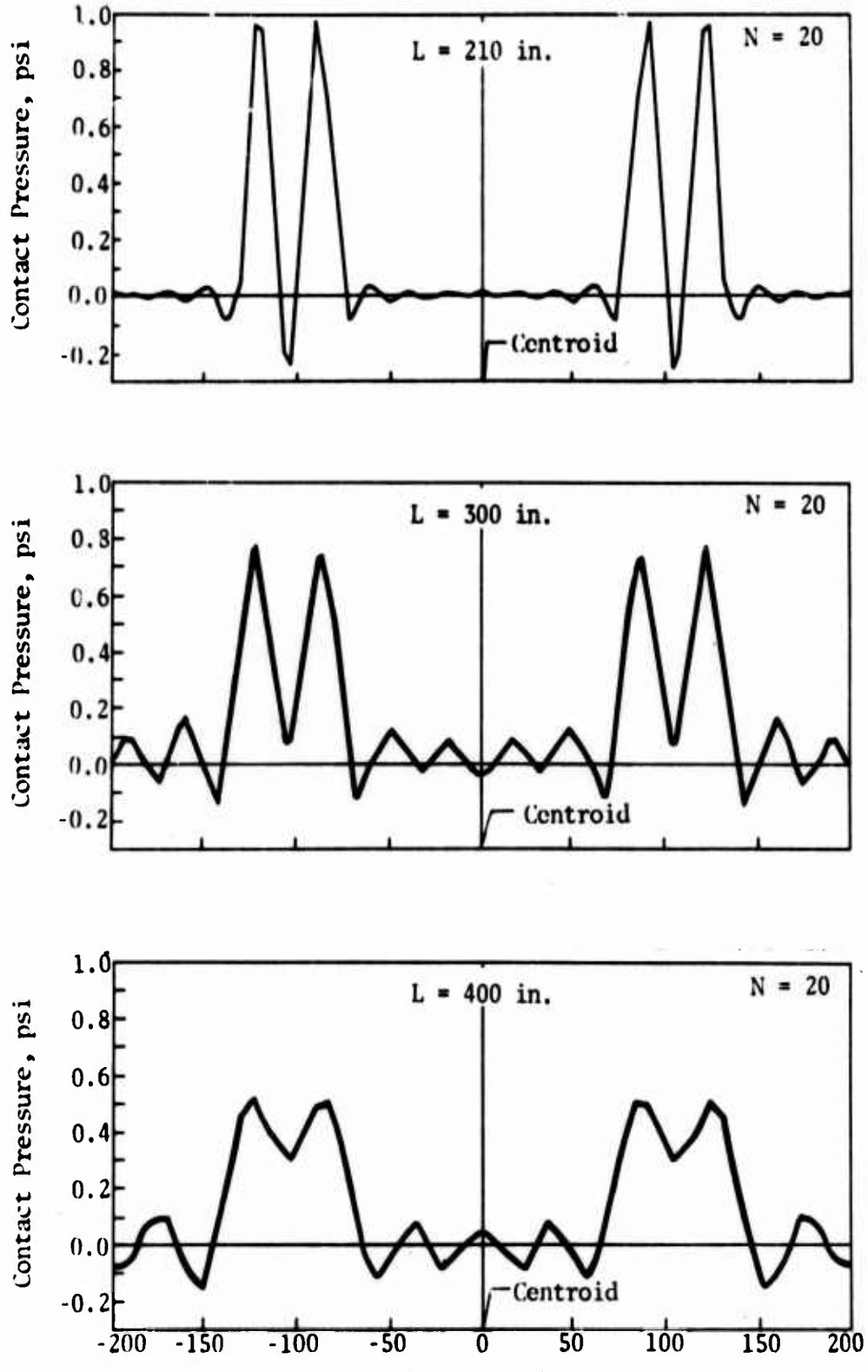

Note: N equals number of Fourier terms; L equals half-period.

Figure 16. Effect of Period on Fourier Series Representation of Four Wheel Loads of C-141A Landing Gear

wheels of a C-141A aircraft. When the half-period is 210 in., which is equal to the tread, i.e., the distance between the centroids of the two sets of four wheels of the main landing gear (ref. 14), the maximum value of the loading function (with N = 20) is 0.986 which is almost the assumed contact pressure of 1.0. However, when the half-period is increased to 300 in. and 400 in., the corresponding maximum values of the loading function (with N = 20) become 0.766 and 0.502. This adversely affects the prediction of surface layer stresses. Figure 17 shows a comparison of the loading functions for the wheel loads of the C-141A aircraft for the three values of 2L. As L increases, an increasing number of Fourier terms are required to obtain a better approximation of the loading function; but, since this increases computer time, judgment based on experience in using AFPRE should be exercised in choosing an appropriate characteristic length for a given problem.

Figures 18 and 19 show, respectively, the effect of the half-period on the elastic surface deflection and on the horizontal stresses at the bottom (i.e., at a depth of 7.2 in.) of an 8-in. Portland cement concrete slab loaded by the eight wheels of the C-141A aircraft landing gear. There is almost no difference in the maximum surface deflection for the various half-periods, although there is an increase of about 12 percent in the maximum horizontal stress (fig. 19). Even though this percentage is small, it may be important to know the correct maximum tensile stress if it approaches the modulus of rupture.

The effects of the period of the loading function on flexible pavement response may differ quantitatively from those on the rigid pavement response. But even in flexible pavement systems, only the response of the upper layers is affected by the number of Fourier terms and the period of the loading function, which is also called the *characteristic length*. It is, therefore, necessary to exercise reasonable judgment in selecting proper values of N and L when analyzing a given problem, keeping in mind the nature of the information required. As stated earlier, if the total surface deflection is all that is required from an analysis, any set of reasonable N and L values will serve the purpose, and no time need be wasted in representing the loading function very accurately.

4. BOUNDARY CONDITIONS

Another important consideration when idealizing a layered pavement structure is the selection of an appropriate width for the idealized structure.

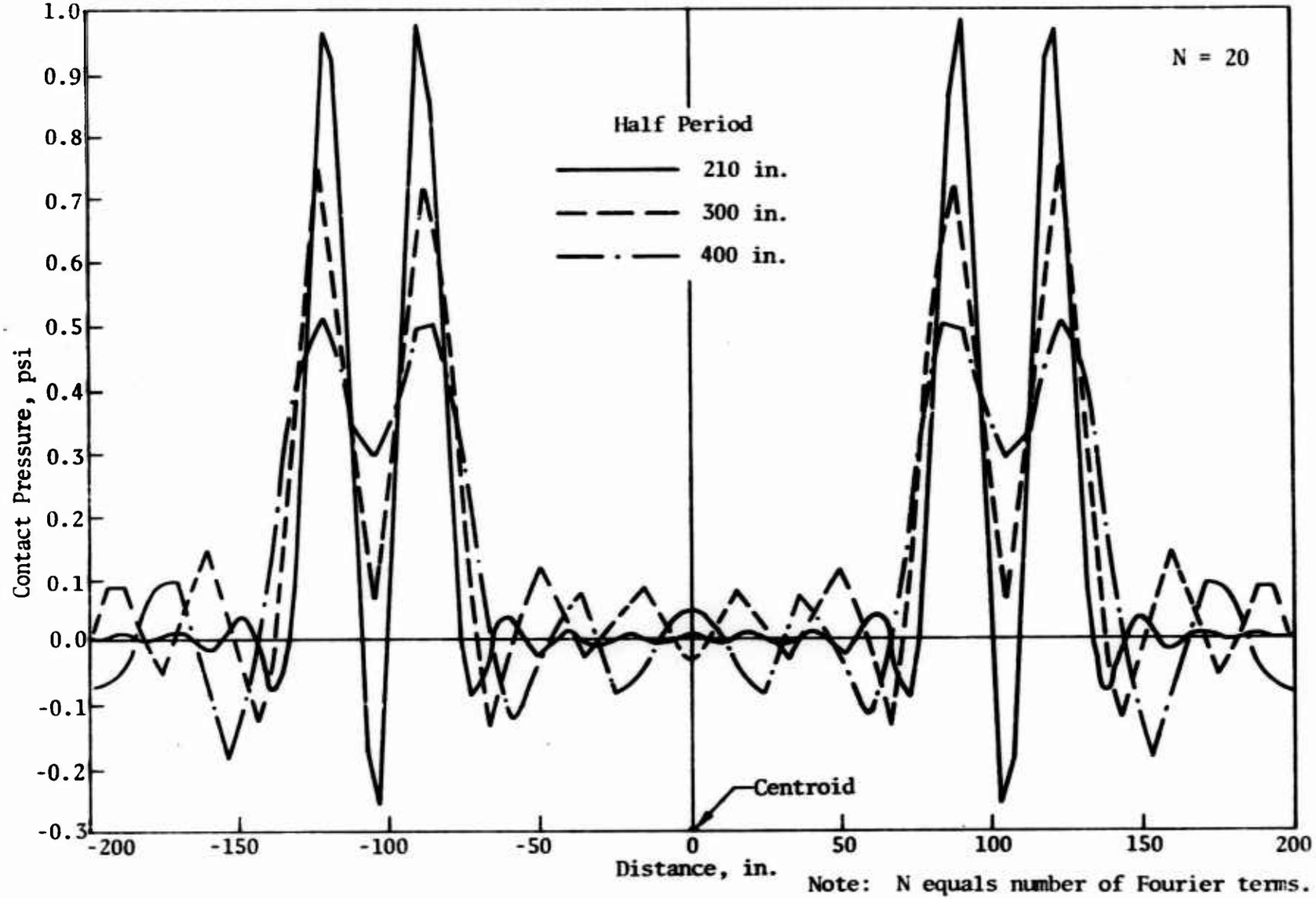

Figure 17. Effect of Period on Loading Function of C-141A Landing Gear

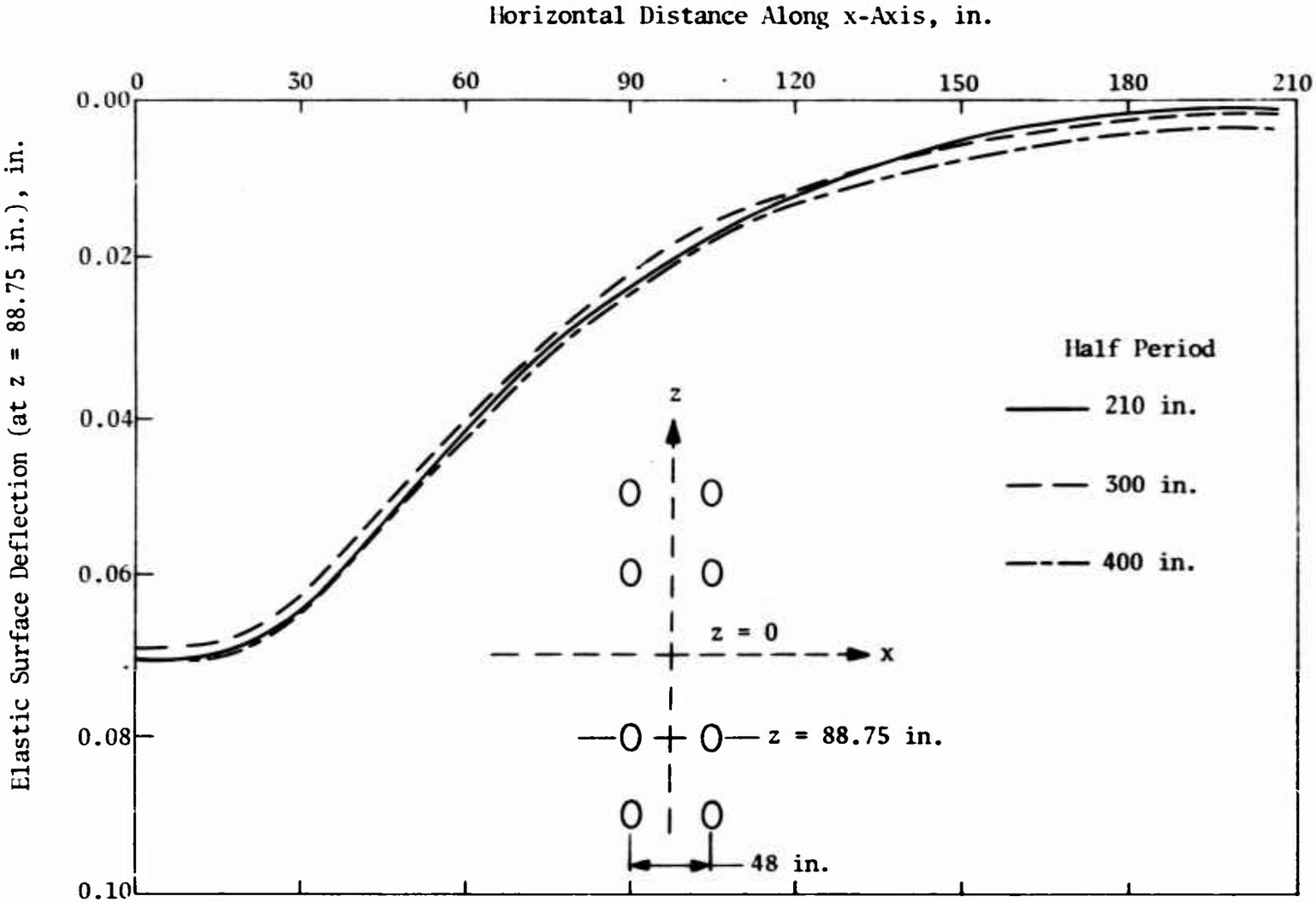

Figure 18. Effect of Period on Elastic Surface Deflection of Rigid Pavement

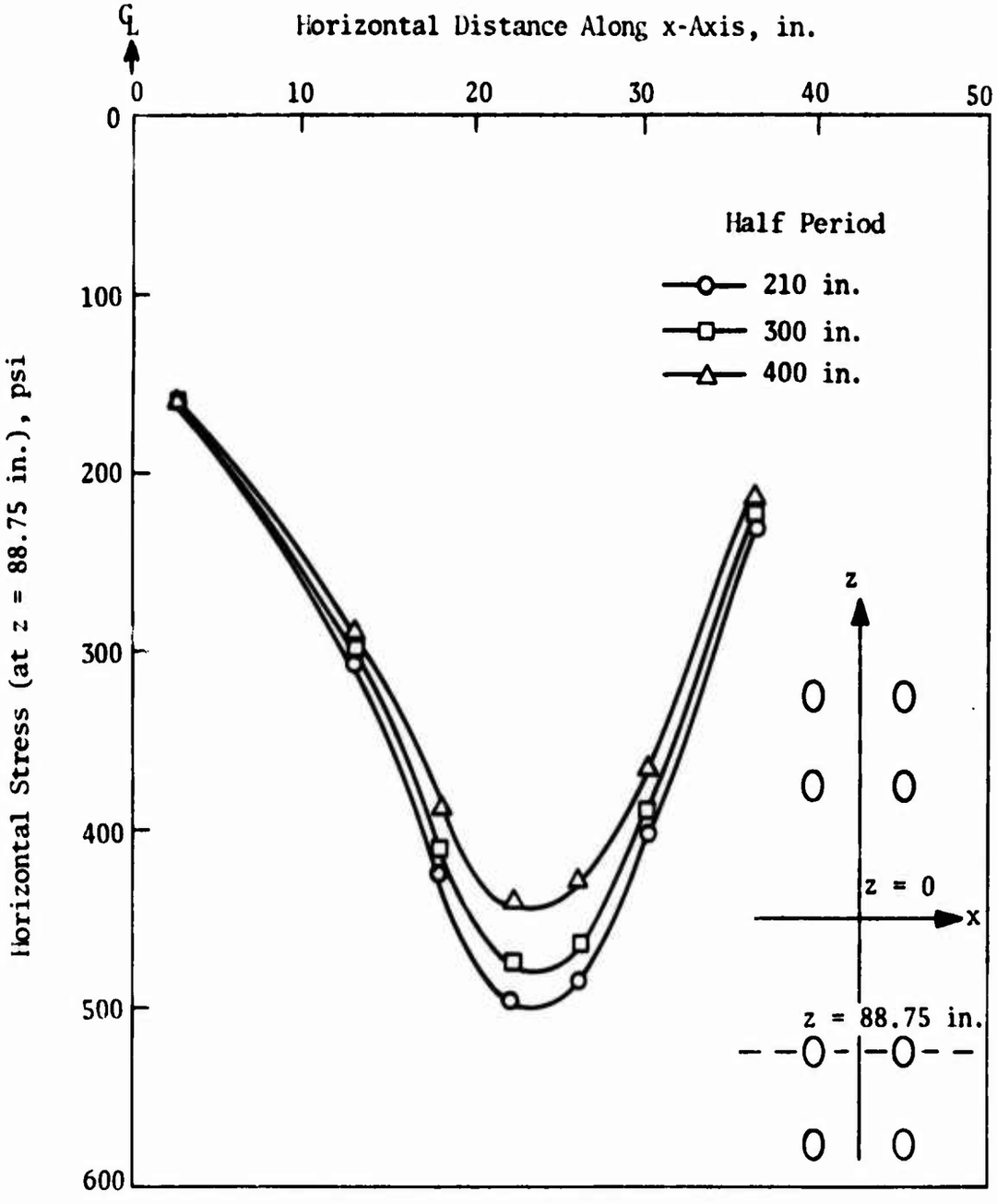

Figure 19. Effect of Period on Maximum Horizontal Stress of Rigid Pavement

This is just as significant as the selection of the characteristic length. It would be ideal if the entire width of the airfield pavement could be used when drawing up the finite element mesh; but, this is impossible because of the limitation on the number of nodes and elements imposed by computer capacity and cost. The problem of choosing a proper width for the idealized structure is, in fact, a part of the overall problem of the boundary conditions assumed at the two sides and at the bottom of the idealized pavement structure. As shown in figures 10 through 13, the bottom supports are assumed to allow no translational movement in either the x- or y-direction, and these supports could be at a depth of fifty to sixty times* the half-width of a wheel contact area. The sides are assumed to consist of roller supports which restrain movement perpendicular to the sides. The surface and base regions have vertical sides; the subgrade region has sloping sides (angle of slope = 30° to the vertical axis). The width of a flexible pavement structure could be obtained by assuming that the vertical rollers are at a distance of about 20 times the half-width of the outer wheel contact area; but, the width of a rigid pavement structure should be obtained by placing the vertical rollers as far away as possible from the outer wheel, say about 30 times the half-width of the wheel contact area. In this connection, it is noteworthy that the AFPAV code has an important advantage over the WIL67 and BISTRO codes which perform axisymmetric analyses of pavement systems. Whereas BISTRO and WIL67 cannot consider edge loading in the case of a rigid pavement system, the AFPAV code can analyze edge loading because it treats the structure as a prismatic solid.

An eight-wheel assembly of the main landing gear of a C-141A aircraft is assumed to load a pavement with the two sets of four wheels parallel to the edge of the pavement as shown in figure 20. Figure 21 shows the effect of the location of the load on the normal stresses at some selected points in an 8-in. Portland cement concrete slab resting on a 10-CBR subgrade. The contact pressure, p, is assumed to be 180 psi. The boundary conditions with concrete extending up to the vertical rollers on both sides (fig. 21a) represent an interior loading condition (i.e., one with the aircraft wheels located in the interior part of a wide airfield pavement). Figure 21b shows an edge loading

*If a rigid layer is known to exist at a lesser depth, the actual thickness of the subgrade should be used in the finite element idealization of the structure.

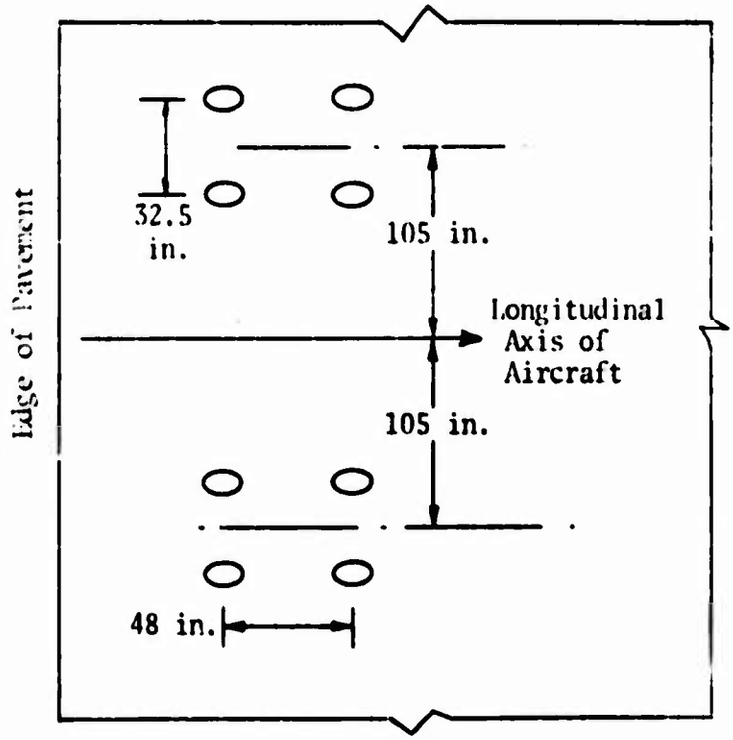

Figure 20. Location of Main Landing Gear of C-141A Aircraft for Boundary Condition Problem

condition (i.e., one with the set of rear wheels coming to the very edge of the slab). The top of the slab is assumed to be at the same level as the adjacent ground which has the same E-modulus as the subgrade beneath the slab.

There is a very significant difference in stress distribution between the interior loading and the edge loading conditions. In the former case, the maximum tensile stress in the longitudinal direction, σ_z, is about 500 psi (point B in fig. 21a). In the edge loading case, the maximum tensile stress in the longitudinal direction, σ_z, is about 630 psi (point A in fig. 21b). Considering the stresses at all the points in the slab, there is an increase of about 26 percent in the maximum horizontal tensile stress. Considering only the stresses at an interior point such as B under the front set of four wheels, there is no significant difference in the magnitude of normal stresses (fig. 21); but, the stresses at point A near the edge of the slab change dramatically, e.g., the value of σ_z changes from a compressive stress of 6.2 psi to a tensile stress of 630.4 psi. Again, only the AFPAV code can compute the stresses due to such edge loading. The BISTRO code or any other axisymmetric code can only determine the stresses due to interior loading and, therefore, this code would have underpredicted the maximum tensile stress caused by the C-141A aircraft in this problem.

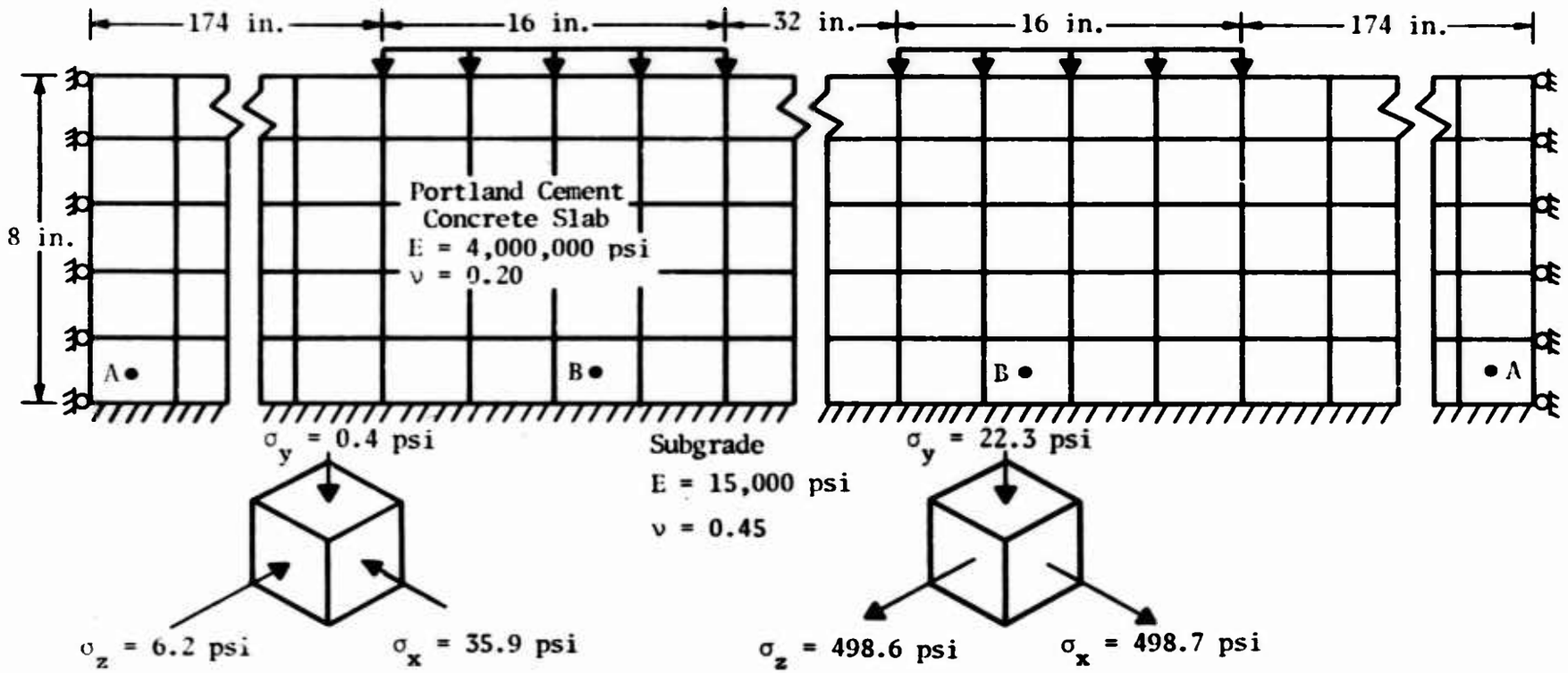

Notes: (1) Outward arrows denote tensile stresses.
(2) Shear stresses are not shown.
(3) Finite element grid is not drawn to scale; elements in the subgrade are not shown in this figure.

(a) Interior Loading

Figure 21. Effect of Load Location on Stresses in Rigid Pavement

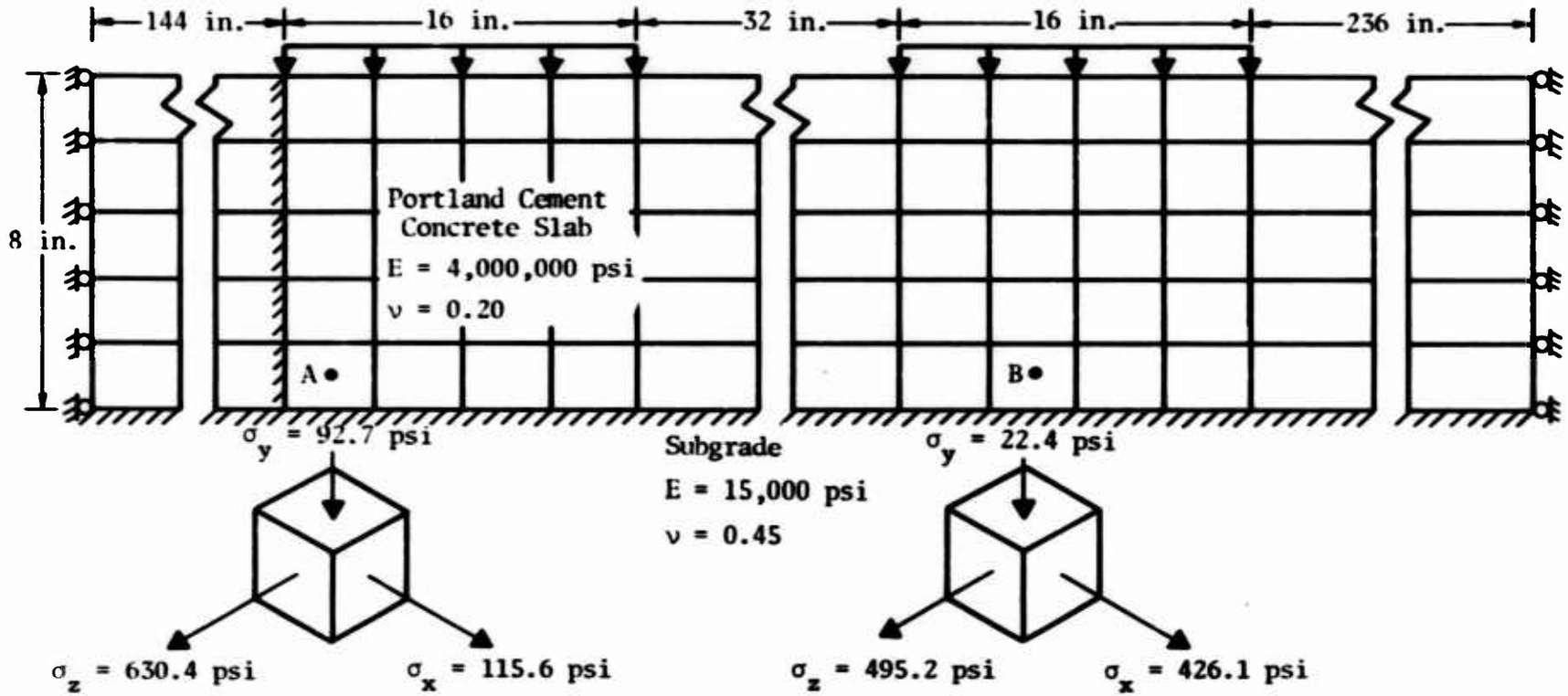

Notes: (1) Outward arrows denote tensile stresses.
(2) Shear stresses are not shown.
(3) Finite element grid is not drawn to scale; elements in the subgrade are not shown in this figure.

(b) Edge Loading

Figure 21---Concluded

SECTION IV

ANALYSIS OF MWHGL PAVEMENT TEST SECTIONS

A comprehensive experimental research project was jointly sponsored by the U.S. Air Force, the U.S. Army, and the Federal Aviation Administration to obtain data on the behavior of different pavement systems subjected to multiple wheel heavy gear loads. Flexible and rigid pavement sections (fig. 22) were constructed and tested at WES (ref. 15) to determine, among other things, the pavement response to (1) static loading and (2) trafficking of a prototype of a 12-wheel assembly (i.e., one main landing gear of a C-5A aircraft). The experimental data obtained from this full-scale pavement testing were compared with the theoretical response predicted by computer codes.

Before the AFPAV code was fully developed, the BISTRO, the WIL67, and the VISAB3 codes, along with the main program of the AFPAV code (without the preprocessor and the postprocessor) were used in the theoretical analysis of these test sections. The results of this analysis were compared with the experimentally determined values for the test sections (ref. 4). After the preprocessor and the postprocessor were added to the AFPAV main program, these test sections were again analyzed using all three parts of the AFPAV code as a check on the performance of the completed AFPAV code. While looking at the comparison of field observations and predicted data, the following two important facts must be kept in mind: (1) The original version of the AFPAV code used in this analysis was based on a linear elastic model for all of the components of the pavement systems; and (2) the elastic properties of the different layer materials were estimated in the absence of actual data obtained by procedures which would give properties corresponding to the strain levels pertaining to the applied loading (ref. 16).

1. FLEXIBLE PAVEMENT TEST SECTION

As seen in figure 22a, the flexible pavement test section consisted of five items. In all of these items the surface course was a 3-in.-thick asphalt cement concrete layer and the base course was a 6-in.-thick crushed stone layer; the thicknesses of the subbase and the subgrade of these items varied (fig. 22a).

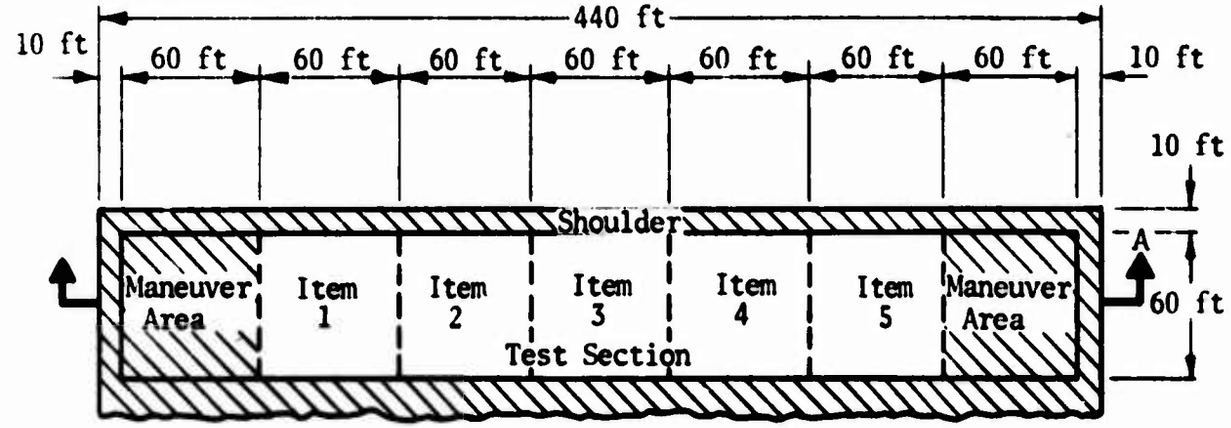

Transition Zone Between Test Sections
(See figure 22b.)

Plan View

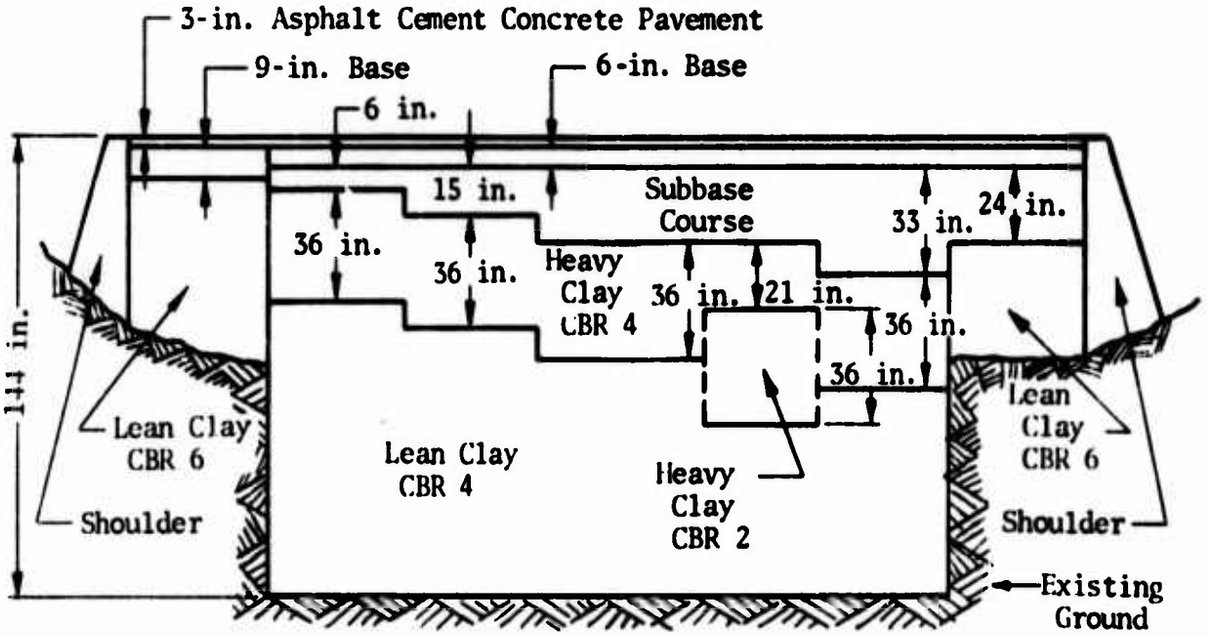

Section A-A

(a) Flexible Pavement

Figure 22. WES Test Sections

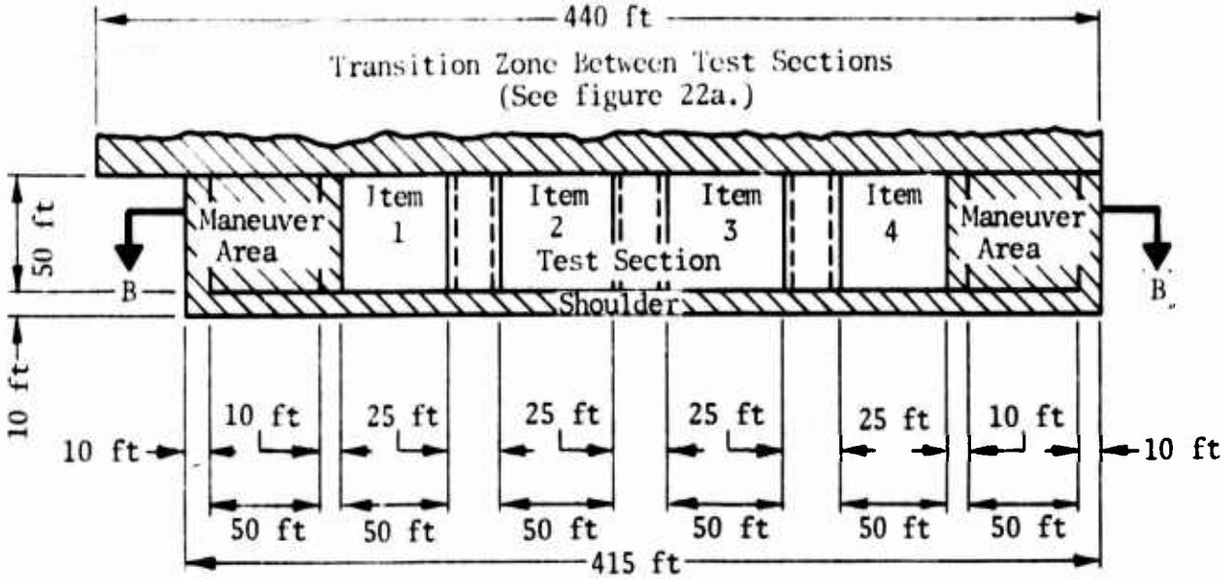

Plan View

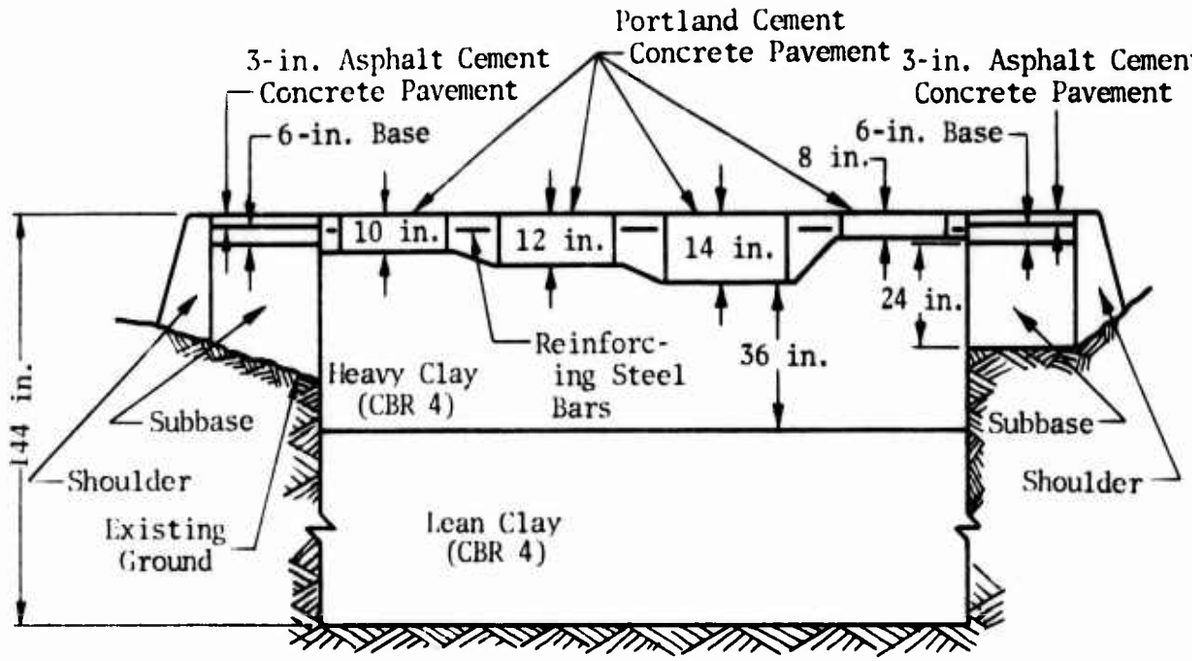

Section B-B

(b) Rigid Pavement

Figure 22---Concluded

Item 4 of the flexible pavement test section was analyzed using the main program of the AFPAV code and the theoretical response was compared with the preliminary experimental test data obtained at WES (ref. 4). Table I presents the layer properties that were used for the various layers of flexible item 4 in the analysis reported in reference 4. It was shown therein that the pavement response predicted by the linear elastic analysis did not vary significantly whether item 4 was considered to consist of seven layers as shown in figure 22a or to consist of only four layers as idealized in table I. Therefore, item 3 of the flexible test section was idealized as a four-layered pavement system and analyzed. The layer properties of item 3 are shown in table II. Since the value of 108,000 psi for the E-modulus of the crushed-stone base

Table I

LAYER PROPERTIES OF WES FLEXIBLE ITEM 4

Layer	Thickness, in.	Modulus of Elasticity, psi	Poisson's Ratio
Surface Course	3	150,000	0.25
Base Course	6	108,000	0.25
Subbase	24	22,500	0.35
Subgrade	∞	4,400	0.45

Note: Data are from reference 4.

Table II

ASSUMED LAYER PROPERTIES OF WES FLEXIBLE ITEM 3

Layer	Thickness, in.	Modulus of Elasticity, psi	Poisson's Ratio
Surface Course	3	150,000	0.25
Base Course	6	50,000	0.30
Subbase	24	25,000	0.35
Subgrade	∞	5,000	0.45

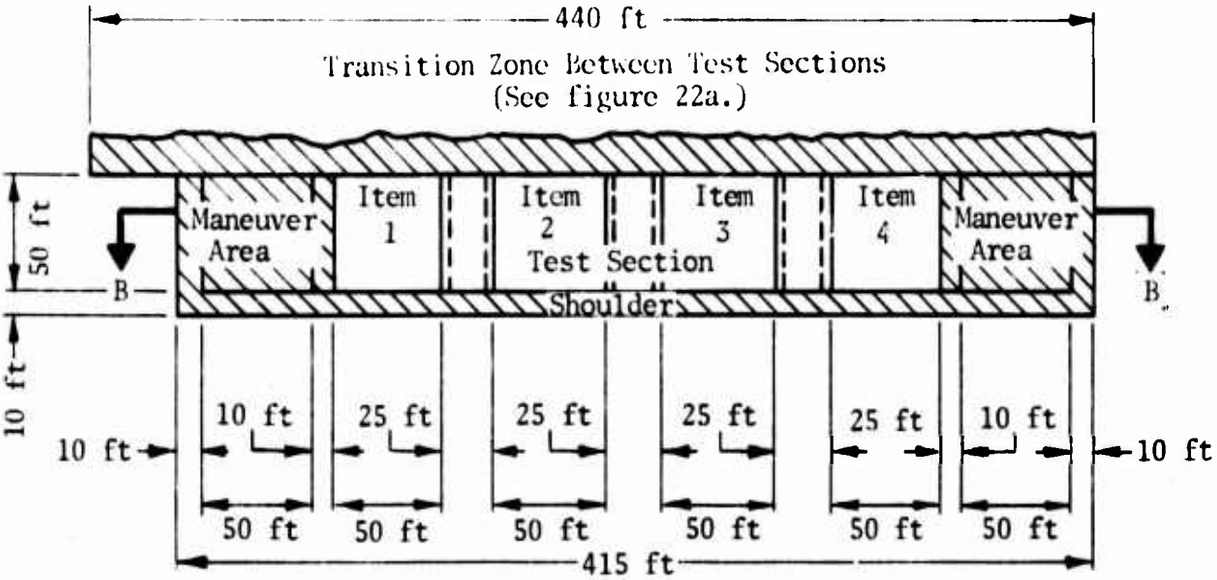

Plan View

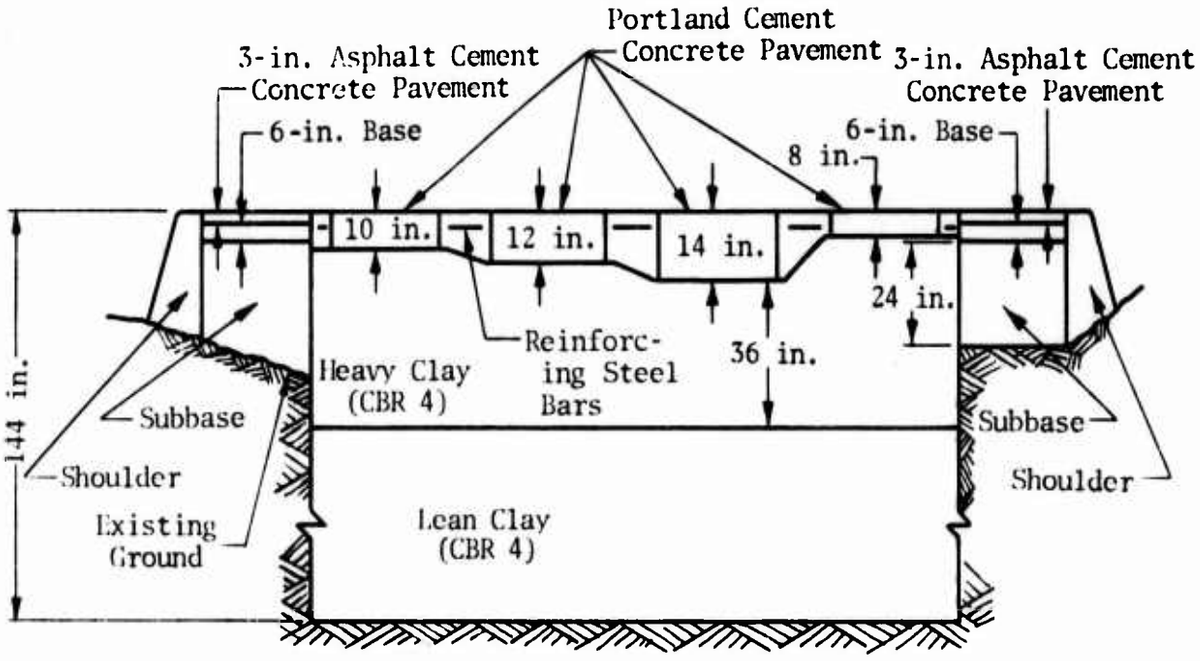

Section B-B

(b) Rigid Pavement

Figure 22---Concluded

Item 4 of the flexible pavement test section was analyzed using the main program of the AFPAV code and the theoretical response was compared with the preliminary experimental test data obtained at WES (ref. 4). Table I presents the layer properties that were used for the various layers of flexible item 4 in the analysis reported in reference 4. It was shown therein that the pavement response predicted by the linear elastic analysis did not vary significantly whether item 4 was considered to consist of seven layers as shown in figure 22a or to consist of only four layers as idealized in table I. Therefore, item 3 of the flexible test section was idealized as a four-layered pavement system and analyzed. The layer properties of item 3 are shown in table II. Since the value of 108,000 psi for the E-modulus of the crushed-stone base

Table I

LAYER PROPERTIES OF WES FLEXIBLE ITEM 4

Layer	Thickness, in.	Modulus of Elasticity, psi	Poisson's Ratio
Surface Course	3	150,000	0.25
Base Course	6	108,000	0.25
Subbase	24	22,500	0.35
Subgrade	∞	4,400	0.45

Note: Data are from reference 4.

Table II

ASSUMED LAYER PROPERTIES OF WES FLEXIBLE ITEM 3

Layer	Thickness, in.	Modulus of Elasticity, psi	Poisson's Ratio
Surface Course	3	150,000	0.25
Base Course	6	50,000	0.30
Subbase	24	25,000	0.35
Subgrade	∞	5,000	0.45

course in reference 4 was too high, a reduced E-modulus of 50,000 psi was assumed for this layer based on an empirical relationship given by Seed, et al. (ref. 17).*

Figure 23 shows a comparison of the theoretical stress distribution determined by the AFPAV code and the experimental stress distribution measured at WES in flexible item 3 (ref. 15). As in reference 4, the comparison was not satisfactory, probably because of the inadequacy of the linear elastic model currently used in the AFPAV code and the choice of elastic properties. It is hoped that by using the strain-dependent moduli obtained from Hardin's research (ref. 16) for the base and subgrade materials, it may be possible to achieve better correlation between the computed and the measured data; the AFPAV code is thus being modified to consider strain-dependent moduli.

Figure 24 shows a comparison of the theoretical elastic vertical deflections and the experimental data reported in reference 15. Although the agreement between computed deflections and experimental data is reasonably good at the upper layers the computed deflection curve does not have the marked change in curvature as does the measured deflection curve. Although it is difficult at this stage to pinpoint the reasons for the unsatisfactory correlation between the measured and the computed data, the following factors may be responsible to a greater or lesser degree for the discrepancies:

(1) The inability to define the most appropriate elastic properties of the various layers of the pavement system (for example, the dependence of the subgrade, subbase, and base course materials on the actual strain level is not considered in the linear elastic analysis performed in this investigation. The fact that the granular base course has little or no tensile strength is ignored in assuming a modulus of 50,000 psi in all directions);

(2) The subgrade with a modulus of 5,000 psi is assumed to extend to a depth of 50 ft from the surface in the finite element

*Even this reduced value is not correct since it should be zero in the horizontal direction where tensile stress is developed under the applied loading. Since, in the present version of the AFPAV code, different moduli values cannot be input in different directions, predicted response will be in error to some extent.

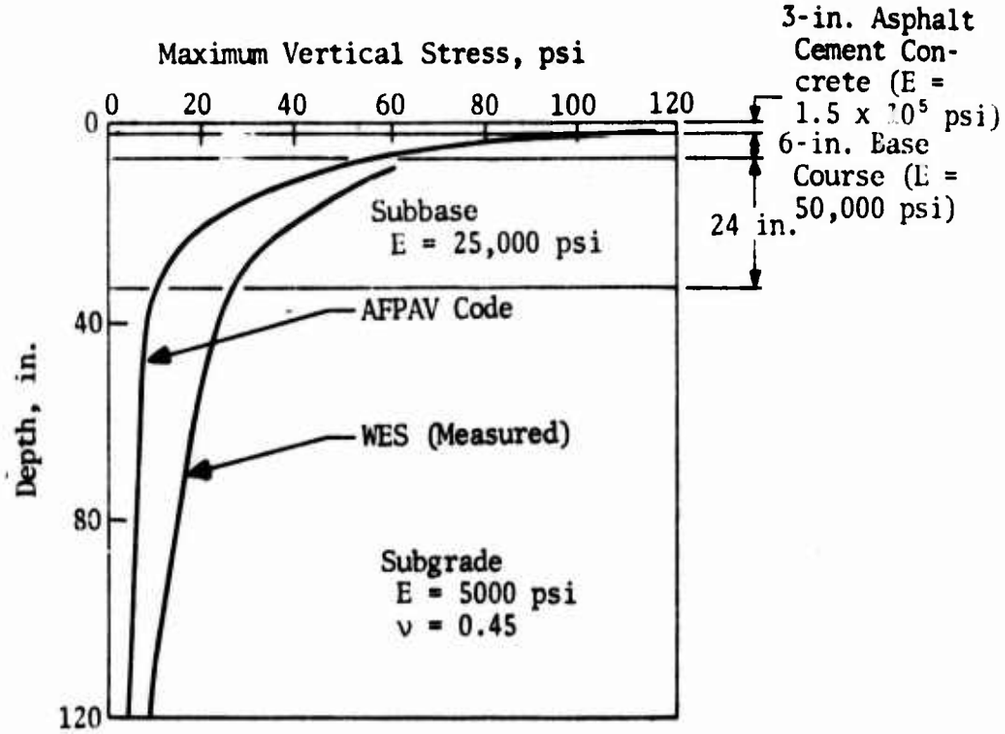

Figure 23. Comparison of Theoretical Stress Distribution and WES Field Test Data

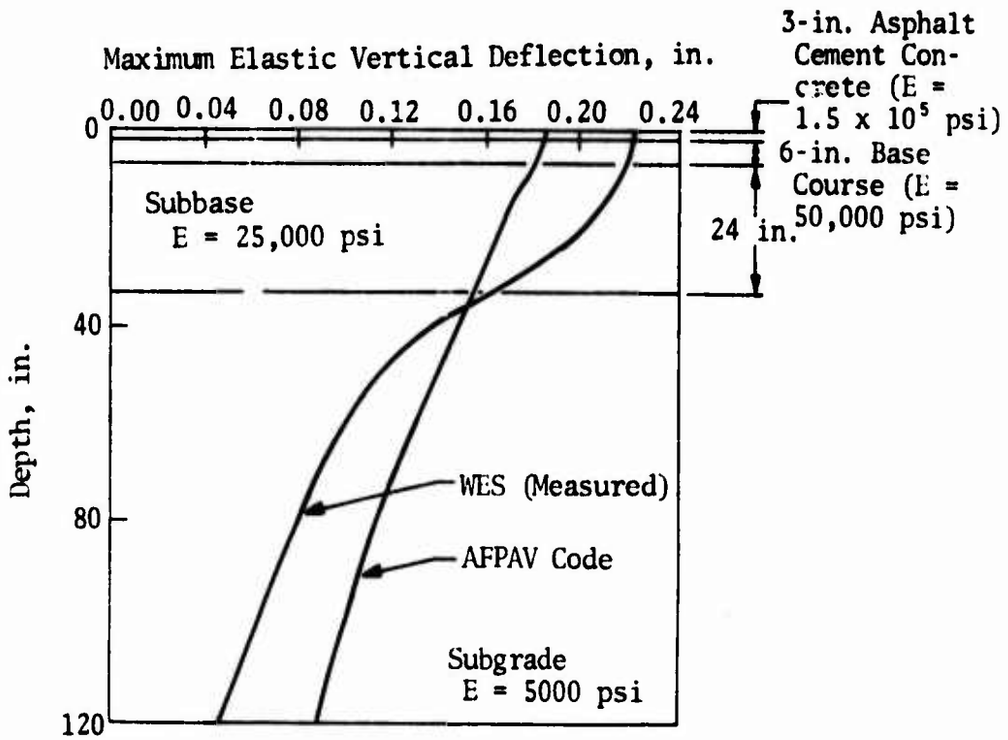

Figure 24. Comparison of Theoretical Elastic Vertical Deflections and WES Field Test Data

model while, in reality, the built-in subgrade with a CBR value of about 4 or less extends to a depth of only 12 ft from the top surface; and

(3) The actual modulus of the existing ground below 12 ft is not known, but it is probably higher than that of the CBR 4 subgrade. (If so, the actual deflection will be less than the computed values at greater depths.)

Suitable modification of the AFPAV code to account for the strain-dependent modulus of the subgrade, etc., and *no-tension* characteristic of the granular material is being made now to improve the match between the predicted values and the measured data.

A brief clarification is required to explain the qualifying term *maximum* in figures 23 and 24. The maximum stress or deflection means the maximum quantity at a given depth in the test item due to the 12-wheel assembly of the C-5A gear used in the WES tests. Each wheel carried a load of 30,000 lb with a contact pressure of about 106 psi. (The stress and deflection curves shown in figures 23 and 24, respectively, were referred to as *limiting* curves in reference 4.)

2. RIGID PAVEMENT TEST SECTION

Item 1 of the rigid pavement test section (fig. 22b) was analyzed to determine its response to static loading by a 12-wheel assembly of the C-5A gear. The layer properties used in this analysis are given in table III.

No measured vertical stress data from the rigid pavement section are available to compare with the computed values; however, strain data were received

Table III

LAYER PROPERTIES OF WES RIGID ITEM 1

Layer	Thickness, in.	Modulus of Elasticity, psi	Poisson's Ratio
Surface Course	10	6,600,000	0.20
Subgrade (CBR 4)	590	6,000	0.45

from CERL (ref. 18). A strain of 23 μin./in. was measured at the center of one of the panels of item 1 when it was statically loaded by a 12-wheel assembly of the C-5A gear. Each wheel had a load of 15 kips. One of the two inner wheels of the interior line of four wheels was located at the center of the slab (ref. 4). The computed strain at the corresponding location was 30 μin./in. for a 12-wheel assembly with a load of 15 kips in each wheel; this compares reasonably well with the measured value.

The measured *recoverable* deformation in item 1 of the rigid pavement section averaged about 0.11 in. at the start of traffic tests using the 12-wheel assembly of the C-5A gear at WES (ref. 15, p. 27). The *elastic* deflection of item 1 under the same loading computed by the AFPAV code was also 0.11 in. This shows that, when the pavement system follows a linear elastic law, as the layers of item 1 apparently did in this case, good correlation between theory and actual field behavior can be achieved with the AFPAV code. This statement is qualified by saying that the definition of the appropriate material properties plays a vital role in predicting the pavement response.

SECTION V

PARAMETRIC STUDY OF WES TEST SECTIONS

To demonstrate the fact that theoretical predictions of pavement response are only as good as the input of material properties and to show the relative importance of the various parameters of pavement systems, a parametric study of both flexible and rigid pavement systems was conducted.

1. FLEXIBLE PAVEMENTS

The five items of the full-scale MWHGL flexible pavement test section shown in figure 22a were used to select a representative list of pavement parameters. Item 3 of this test section, whose properties are given in table II, was chosen as a reference system. Table IV lists the parameter variations studied. Studying all possible combinations of the variables in this table obviously would be time consuming. Therefore, only one parameter at a time was varied, and the change in the pavement response due to that variation was studied.

In this parametric study, attention was focused on the changes noticed in surface deflections and in significant stresses due to changes in the properties of the pavement components. The computed pavement response due to the static loading of a 12-wheel assembly of the C-5A gear with 30,000 lb on each wheel was used. Tables V, VI, and VII list the changes in deflections and stresses due to the changes in the pavement parameters.

a. Effect of Young's Modulus

The surface elastic deflections were not changed significantly by variations in the E-modulus of the surface course, base course, and subbase within the range of values shown in table IV. But, variations in Young's modulus of the subgrade affected the surface deflection very significantly. For example, a 67 percent reduction in the E-modulus of the surface course (i.e., from 1,500,000 to 500,000 psi) resulted in an increase of only 8 percent in surface deflection, while a 50 percent reduction in the subgrade E-modulus increased the surface deflection by about 60 percent. This is because in layered pavement systems the softer subgrade contributes more to the surface deflection than the stiffer upper layers do (ref. 12). Figure 25 shows the effect of the subgrade E-modulus on surface deflections. Even though increased values of the E-modulus of the surface course reduced the vertical stresses in the base course

Table IV

FLEXIBLE PAVEMENT PARAMETER VARIATIONS STUDIED

Layer	Parameter Varied		Values of Parameter Varied		
	Symbol	Unit			
Surface Course	E	psi	1.5×10^6;	500,000;	150,000
Surface Course	ν	--	0.20;	0.25;	0.30
Surface Course	h	in.	3.0;	4.5;	6.0
Base Course	E	psi	75,000;	50,000;	37,500
Base Course	ν	--	0.25;	0.30;	0.35
Base Course	h	in.	6.0;	9.0;	12.0
Subbase	E	psi	37,500;	25,000;	12,500
Subbase	ν	--	0.30;	0.35;	0.40
Subbase	h	in.	15.0;	24.0;	33.0
Subgrade	E	psi	5,000;	2,500;	1,250
Subgrade	ν	--	0.40;	0.45;	0.495
Existing Ground Profile	E	psi	5,000;	50,000;	500,000

Note: h = layer thickness.

Table V

EFFECT OF PARAMETER VARIATIONS IN SURFACE COURSE ON FLEXIBLE PAVEMENT RESPONSE

Parameters			Pavement Responses			Remarks
E, psi	ν	h, in.	Maximum Elastic Surface Deflection in.	Maximum Horizontal Stress, psi		
				Compression	Tension	
1,500,000	0.25	3.0	0.157	435	191	E-modulus only varied
500,000	0.25	3.0	0.170	279	23	
150,000	0.25	3.0	0.183	166	0	
150,000	0.20	3.0	0.183	155	0	Poisson's ratio only varied
150,000	0.25	3.0	0.183	166	0	
150,000	0.30	3.0	0.182	179	0	
150,000	0.25	3.0	0.183	166	0	Thickness only varied
150,000	0.25	4.5	0.174	150	0	
150,000	0.25	6.0	0.168	136	0	

Note: The properties of the other layers are given in table II.

Table VI

EFFECT OF PARAMETER VARIATIONS IN BASE COURSE AND SUBBASE ON FLEXIBLE PAVEMENT RESPONSE

Parameters			Pavement Responses		Remarks
E, psi	ν	h, in.	Maximum Elastic Surface Deflection, in.	Maximum Vertical Stress in Subgrade, psi	
Base Course					
37,500	0.30	6	0.187	8.7	E-modulus only varied
50,000	0.30	6	0.183	8.5	
75,000	0.30	6	0.178	8.4	
50,000	0.25	6	0.183	8.5	Poisson's ratio only varied
50,000	0.30	6	0.183	8.5	
50,000	0.35	6	0.182	8.5	
50,000	0.30	6	0.183	8.5	Thickness only varied
50,000	0.30	9	0.174	7.7	
50,000	0.30	12	0.167	7.1	
Subbase					
12,500	0.35	24	0.207	9.5	E-modulus only varied
25,000	0.35	24	0.183	8.5	
37,500	0.35	24	0.171	8.0	
25,000	0.30	24	0.182	8.5	Poisson's ratio only varied
25,000	0.35	24	0.183	8.5	
25,000	0.40	24	0.183	8.6	
25,000	0.35	15	0.197	11.7	Thickness only varied
25,000	0.35	24	0.183	8.5	
25,000	0.35	33	0.168	6.7	

Note: The properties of the other layers are given in table II.

Table VII

EFFECT OF PARAMETER VARIATIONS IN SUBGRADE ON FLEXIBLE PAVEMENT RESPONSE

Parameters		Pavement Response	
E, psi	ν	Maximum Elastic Surface Deflection, in.	Remarks
5,000	0.450	0.183	E-modulus only varied
2,500	0.450	0.299	
1,250	0.450	0.493	
5,000	0.400	0.215	Poisson's ratio only varied
5,000	0.450	0.183	
5,000	0.495	0.141	

Note: The properties of the other layers are given in table II.

and subbase, they did not alter the subgrade stresses significantly (fig. 26). This also explains why changes in the surface course E-modulus within the ranges shown in table IV do not affect the surface deflection significantly. When the E-modulus was increased tenfold (from 150,000 psi to 1,500,000 psi), the decrease in surface deflection was only about 14 percent (table V).

The horizontal stress in the surface course was affected by its Young's modulus as shown in figure 27. With an E-modulus of 500,000 psi, a horizontal tensile stress of about 100 psi was developed, while with an E-modulus of 1,500,000 psi, a larger horizontal tensile stress (greater than 200 psi), was developed because of increasing beam action. There was no horizontal tensile stress in the surface course when the E-modulus of the layer was 150,000 psi. But this was true only when the E-modulus of the base course was 50,000 psi and the E-modulus of the subbase was 25,000 psi. An E-modulus of 150,000 psi for the surface course, with a base course E-modulus of 25,000 psi and a subbase E-modulus of 15,000 psi, produced a horizontal tensile stress of about 30 psi in the surface course (ref. 4). This shows that the modular ratios (i.e., ratios of Young's moduli) of the various pavement components are important parameters which influence the pavement response. The modular ratio of the surface course to the base course affects the shear stresses in these layers significantly (fig. 28).

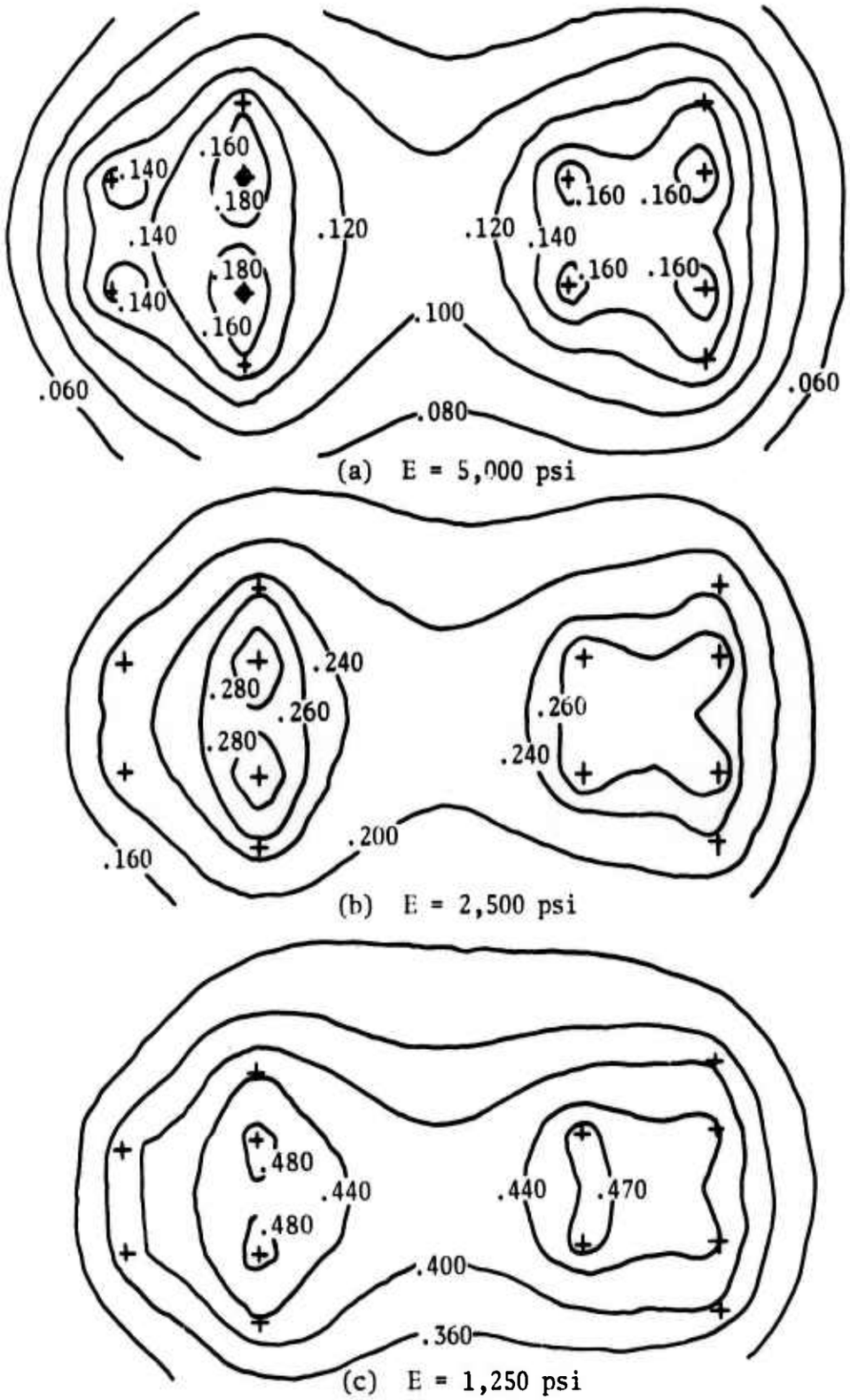

Note: + indicates the wheel position of the 12-wheel assembly of the C-5A gear.

Figure 25. Effect of Subgrade E-Modulus on Surface Deflection in Flexible Pavement

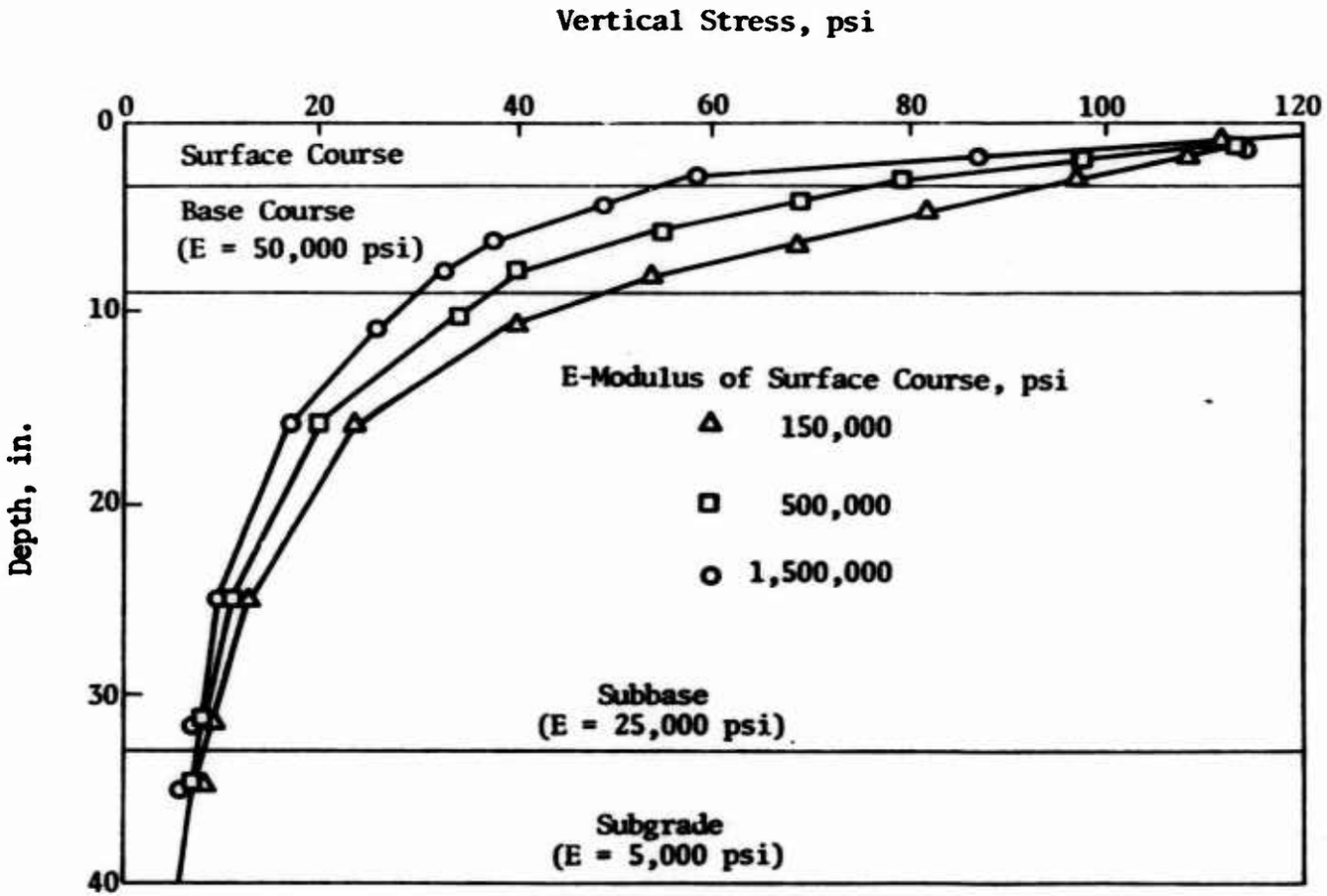

Figure 26. Effect of Surface Course E-Modulus on Vertical Stress in Flexible Pavement

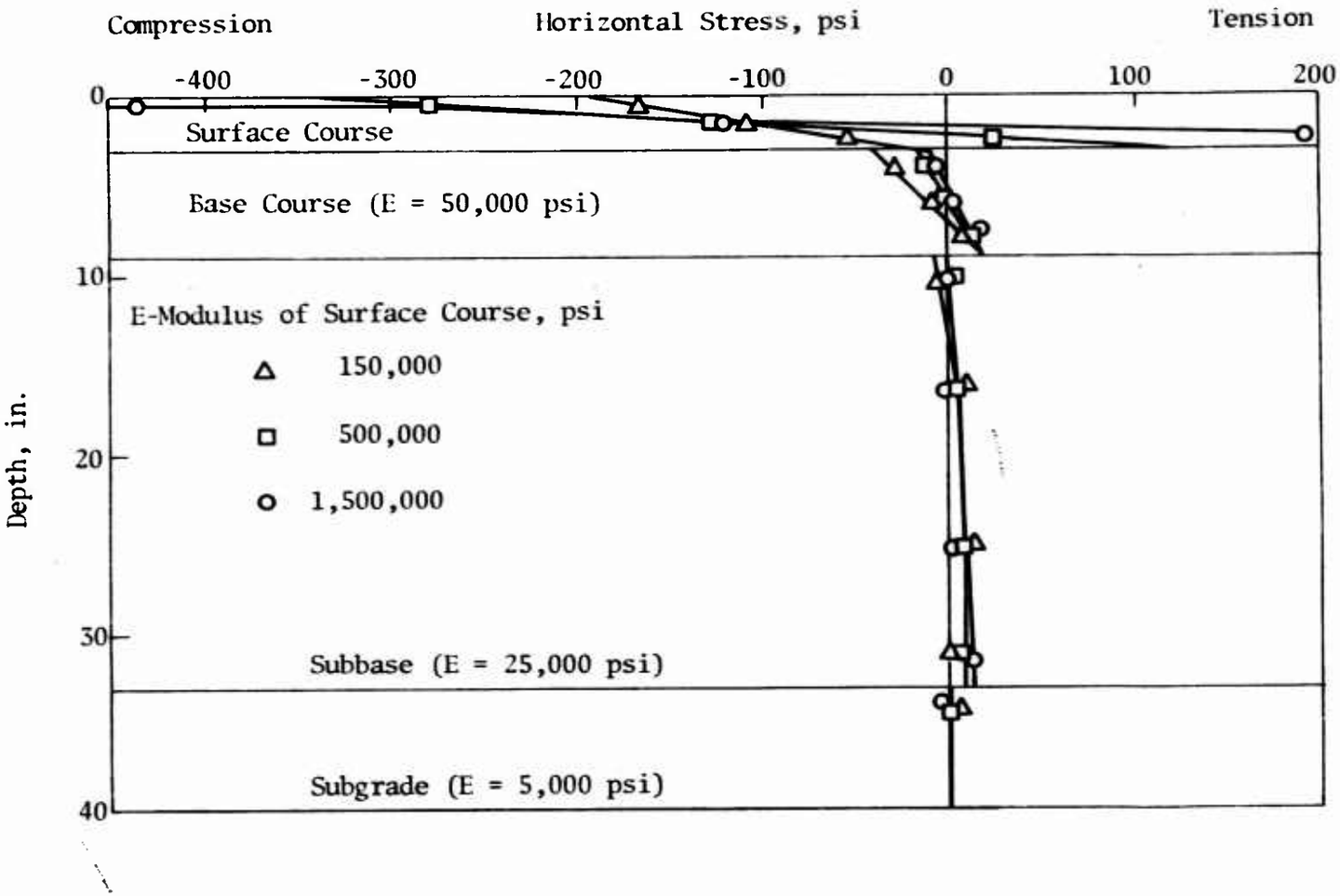

Figure 27. Effect of Surface Course E-Modulus on Horizontal Stress in Flexible Pavement

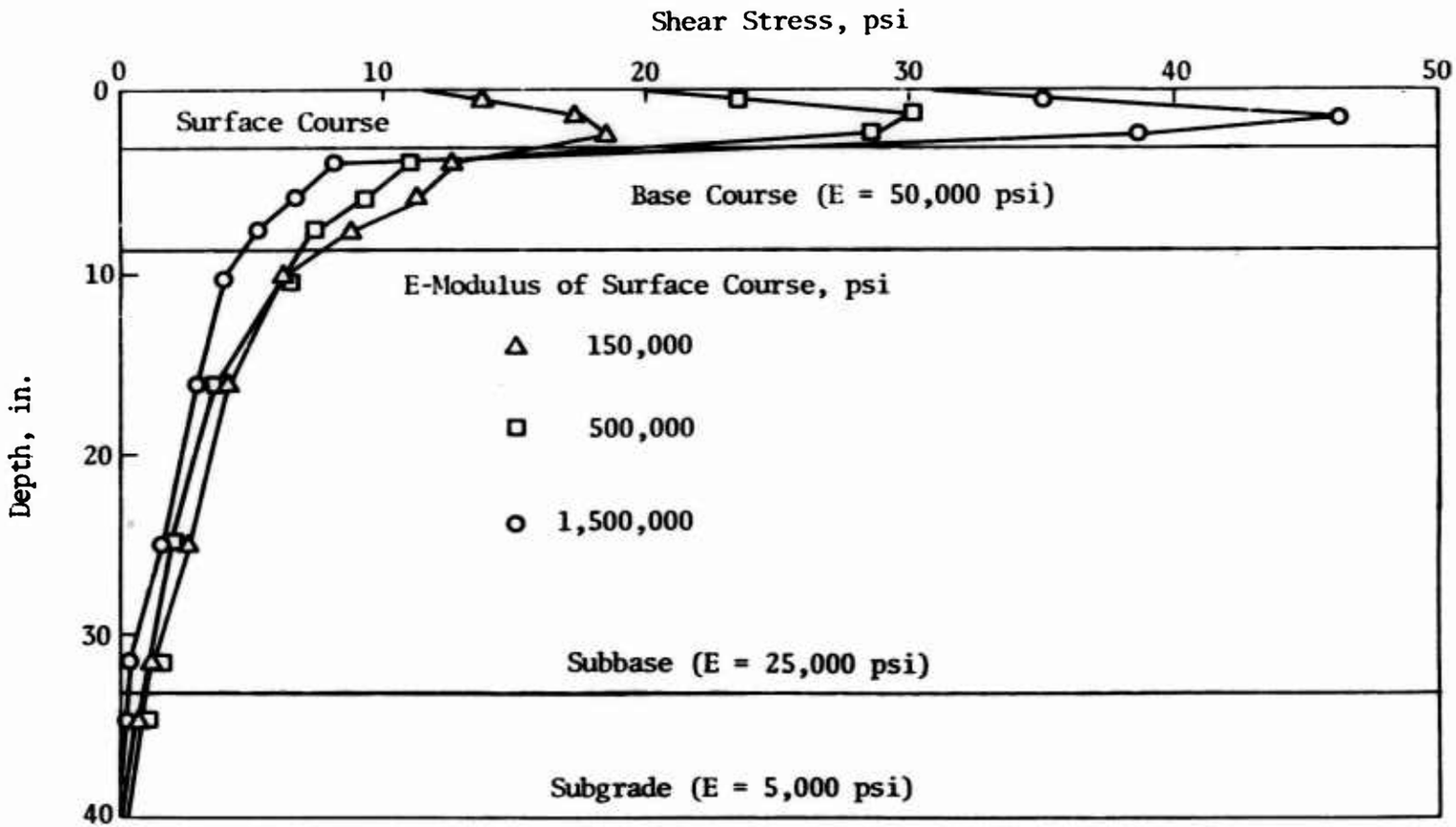

Figure 28. Effect of Surface Course E-Modulus on Shear Stress in Flexible Pavement

Even though the E-modulus values of the base course and subbase may not be very significant for surface elastic deflections, they are very important in determining the state of stress in the upper layers of the pavement system. Therefore, it is necessary to determine the E-moduli of the various layers as accurately as possible since structural failure of the pavement system can be caused by critical *load stresses* exceeding the inherent strength of the pavement materials.

b. Effect of Poisson's Ratio

Surface deflections were not significantly affected by Poisson's ratio of the surface course, base course, or subbase for the range of thicknesses studied; however, Poisson's ratio of the subgrade influenced the deflections significantly (fig. 29). A Poisson's ratio of 0.40 for the subgrade gave a maximum surface deflection of about 0.22 in., while a Poisson's ratio of 0.495 gave a maximum deflection of only 0.14 in. (These maximum values are shown in table VII).

c. Effect of Layer Thickness

Increasing the thicknesses of the upper pavement layers (i.e., the surface course, base course, and subbase) reduced the vertical stresses in the subgrade and, consequently, decreased the surface deflections. For example, when the subbase thickness (originally 24 in.) was altered to 15 and 33 in., the vertical stress at the top of the subgrade became 11.7 and 6.7 psi, respectively (fig. 30 and table VI). This results in a reduction of about 15 percent in surface deflection. The maximum elastic surface deflection was about 0.20 in. with a subbase thickness of 33 in., while it was 0.17 in. with a subbase thickness of 15 in. (table VI).

d. Effect of Young's Modulus of Existing Ground

In the finite element idealization of the pavement system, the total depth of the pavement structure was assumed to be 50 ft and the subgrade was considered to have a constant E-modulus. The total built-up depth of the WES flexible test section (fig. 22a) was only 12 ft. The E-modulus of the ground below the built-up subgrade was not known. However, based on the reported CBR value of 2 to 4, the E-modulus of the ground was assumed to be the same as that of the subgrade. To illustrate the importance of knowing the E-modulus of the existing ground below a depth of 12 ft, a parametric study assuming three

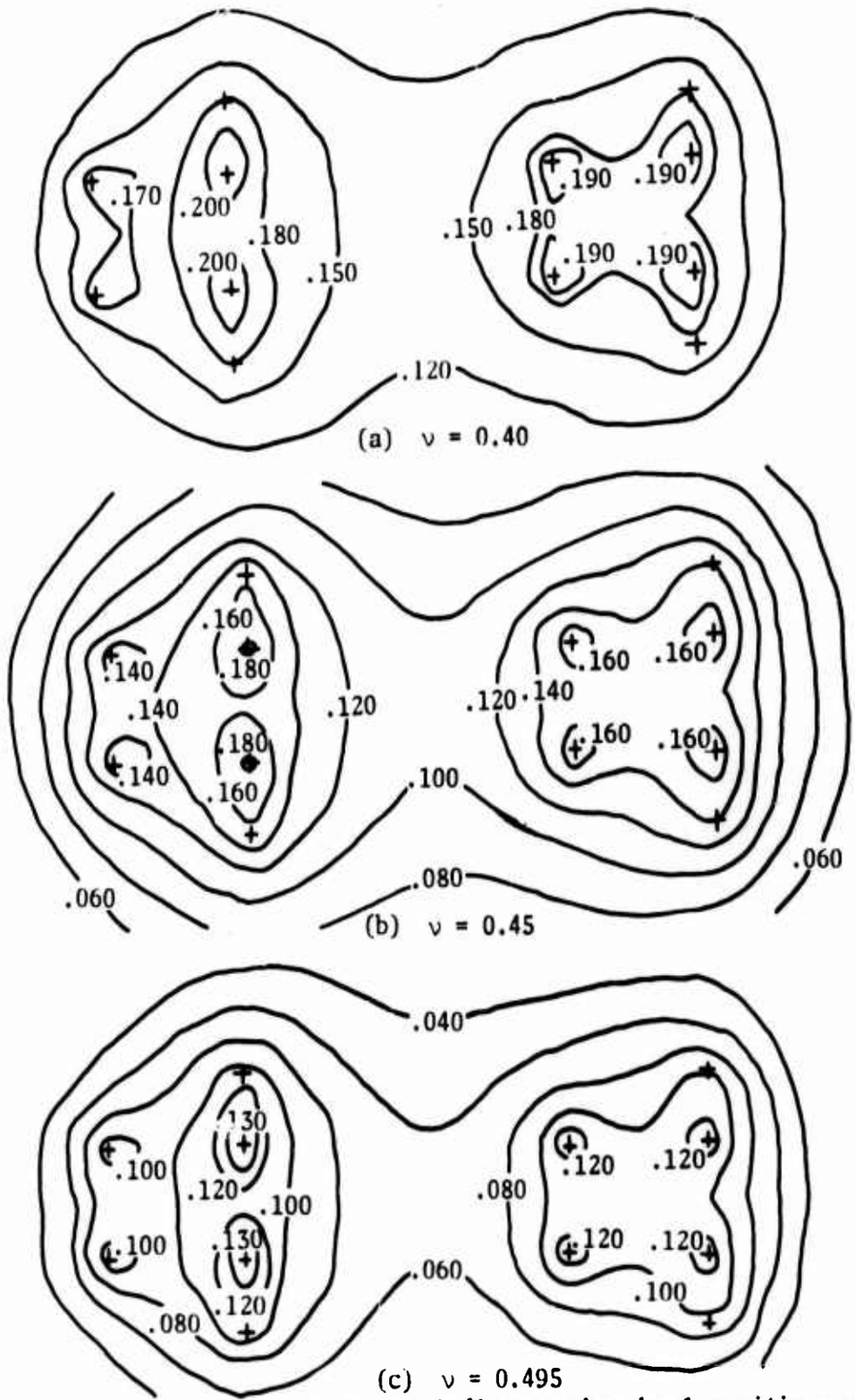

Note: + indicates the wheel positions of the 12-wheel assembly of the C-5A gear.

Figure 29. Effect of Subgrade Poisson's Ratio on Surface Deflection in Flexible Pavement

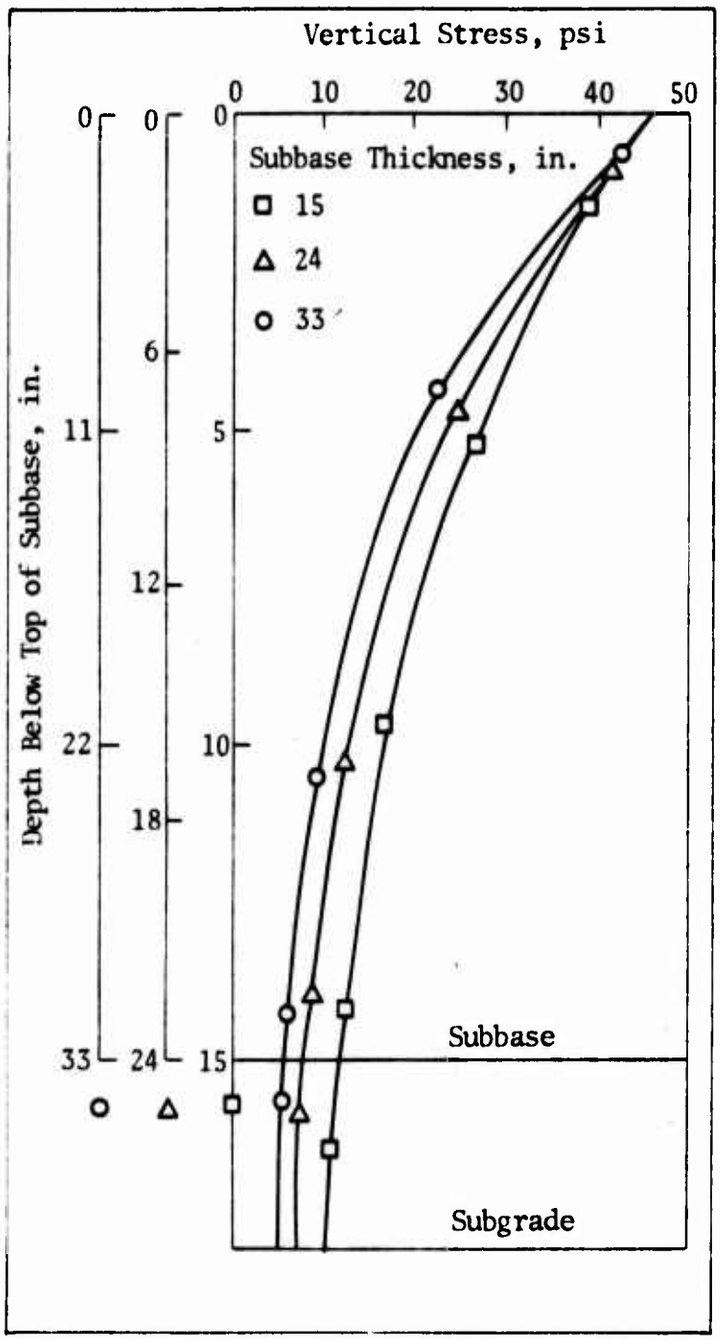

Figure 30. Effect of Subbase Thickness on Subgrade Stress in Flexible Pavement

different moduli values (5,000, 50,000, and 500,000 psi) was conducted. The maximum surface deflection of 0.183 in. with an E-modulus of 5,000 psi was reduced by one-third to 0.121 in. when the existing ground was assumed to have an E-modulus of 50,000 psi. An E-modulus of 500,000 psi below 12 ft further reduced the maximum surface deflection to 0.108 in., a reduction of about 40 percent (fig. 31). Therefore, it appears that it is necessary to determine the properties of the pavement system to an appreciable depth.

2. RIGID PAVEMENTS

Table VIII summarizes the various sets of layer properties used in the parametric study of rigid pavement systems. The computed pavement response due to the static loading of a 12-wheel assembly of the C-5A gear with 30,000 lb on each wheel was used. The effect of the parameter variations on two important responses, viz., the maximum surface deflections and the maximum tensile stresses in the surface course are listed in tables IX, X, and XI.

a. Effect of Young's Modulus of Surface Course

Figure 32 shows the effect of varying the E-modulus of the surface course on the deflection basin of the pavement structure caused by the static loading of the 12-wheel assembly of the C-5A gear. Decreasing the E-modulus of the surface course from 6,600,000 to 3,000,000 psi produced about an 18-percent increase in the maximum surface deflection.

Figure 33 shows how varying the E-modulus of the surface course affects the distribution of vertical normal stress, horizontal normal stress, and horizontal shear stress. In this analysis, the E-modulus of the subgrade was kept constant at 6,000 psi, and the thickness of the surface course was held constant at 10 in. Increasing the surface course E-modulus from 3,000,000 to 6,600,000 psi increased the maximum horizontal tensile stress in the surface course by about 25 percent (table IX). This increasing plate action of the surface course decreases the maximum vertical stress in the subgrade. No change in shear stress was noticed for the range of surface course E-moduli studied.

b. Effect of Layer Thickness

Increasing the thickness of the surface course from 10 to 12 and 14 in. decreased the maximum deflection by about 17 percent (table IX and fig. 34).

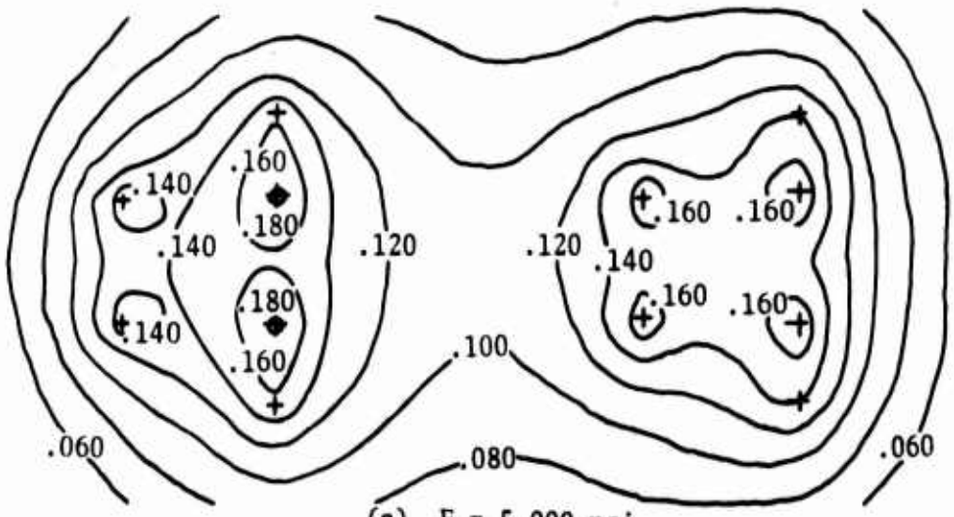

(a) E = 5,000 psi

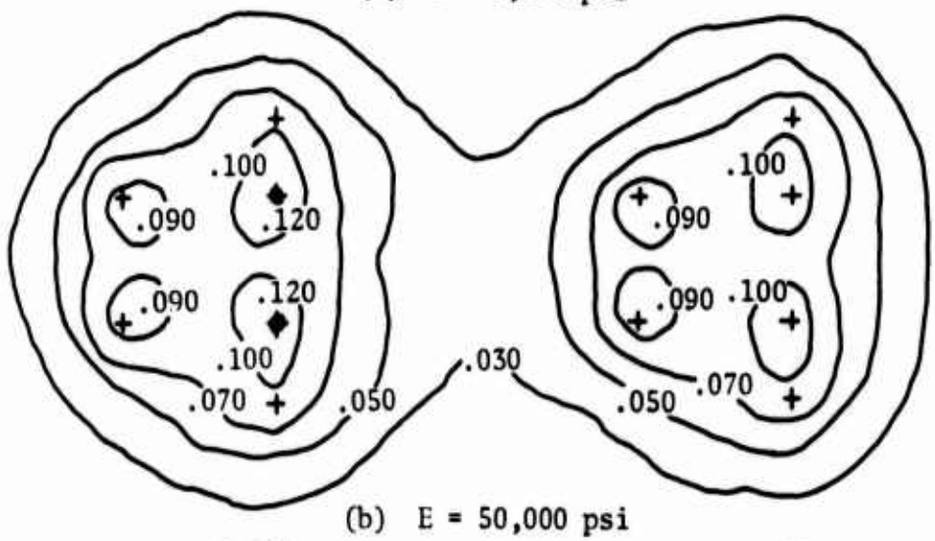

(b) E = 50,000 psi

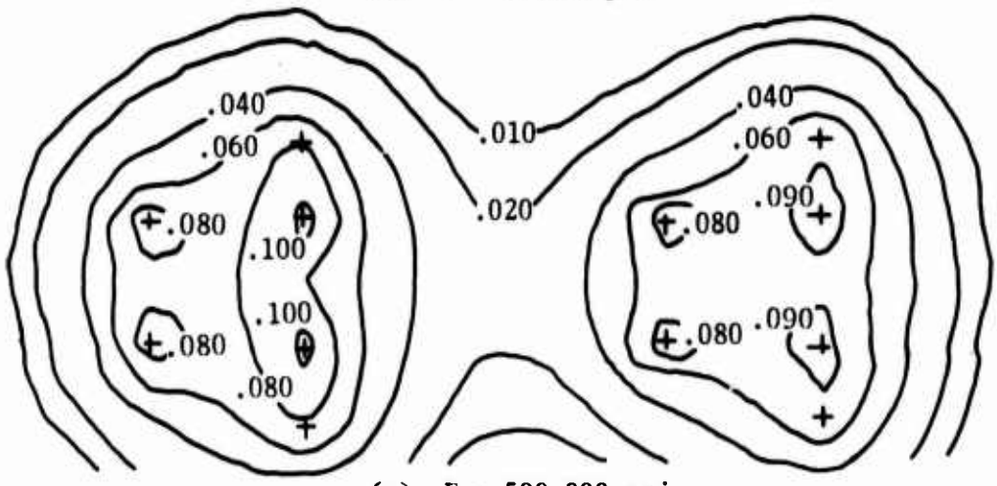

(c) E = 500,000 psi

Note: + indicates the wheel positions of the 12-wheel assembly of the C-5A gear.

Figure 31. Effect of Existing Ground (Below 12 Feet) E-Modulus on Surface Deflection in Flexible Pavement

Table VIII

RIGID PAVEMENT PARAMETER VARIATIONS STUDIED

Surface Course Parameters			Layer	Subgrade Parameters		
Thickness (h), in.	Modulus of Elasticity (E), psi	Poisson's Ratio (ν)		Thickness (h), in.	Modulus of Elasticity (E), psi	Poisson's Ratio (ν)
10.0	6.6×10^6	0.20	1	600	6,000	0.45
10.0	5×10^6	0.20	1	600	6,000	0.45
10.0	3×10^6	0.20	1	600	6,000	0.45
10.0	6.6×10^6	0.20	1	600	6,000	0.45
12.0	6.6×10^6	0.20	1	600	6,000	0.45
14.0	6.6×10^6	0.20	1	600	6,000	0.45
10.0	6.6×10^6	0.20	1	600	6,000	0.45
10.0	6.6×10^6	0.20	1	600	3,000	0.45
10.0	6.6×10^6	0.20	1	600	1,000	0.45
10.0	6.6×10^6	0.20	1	12	24,000	0.35
			2	588	6,000	0.45
10.0	6.6×10^6	0.20	1	18	36,000	0.35
			2	582	6,000	0.45
10.0	6.6×10^6	0.20	1	24	60,000	0.35
			2	576	6,000	0.45

Table IX

EFFECT OF PARAMETER VARIATIONS IN SURFACE COURSE ON RIGID PAVEMENT RESPONSE

Parameters		Pavement Responses		Remarks
E, psi	h, in.	Maximum Elastic Surface Deflection, in.	Maximum Horizontal Tensile Stress, psi	
6.6×10^6	10	0.098	418	E-modulus only varied
5.0×10^6	10	0.105	388	
3.0×10^6	10	0.116	335	
6.6×10^6	10	0.098	418	Thickness only varied
6.6×10^6	12	0.088	338	
6.6×10^6	14	0.081	278	

Note: The surface course rested directly on the subgrade; the E-modulus and Poisson's ratio of the subgrade were 6000 psi and 0.45, respectively.

Table X

EFFECT OF PARAMETER VARIATIONS IN SUBGRADE ON RIGID PAVEMENT RESPONSE

Parameters		Pavement Responses	
E, psi	ν	Maximum Elastic Surface Deflection, in.	Maximum Horizontal Tensile Stress, psi
6,000	0.45	0.098	418
3,000	0.45	0.166	488
1,000	0.45	0.387	579

Note: The surface course with $E = 6.6 \times 10^6$ psi and $\nu = 0.20$ rested directly on the subgrade.

Table XI

EFFECT OF BASE COURSE ON RIGID PAVEMENT RESPONSE

Base Course Parameters			Pavement Responses	
h, in.	E, psi	ν	Maximum Elastic Surface Deflection, in.	Maximum Horizontal Tensile Stress, psi
12	24,000	0.35	0.093	364
18	36,000	0.35	0.090	341
24	60,000	0.35	0.084	298

Note: The surface course parameters were $E = 6.6 \times 10^6$ psi, $\nu = 0.20$, and $h = 10$ in.; the subgrade parameters were $E = 6 \times 10^3$ psi, and $\nu = 0.45$.

In these two cases the properties of the subgrade as well as the elastic constants of the surface course remained unchanged.

Figure 35 shows the stress distribution in surface courses of varying thicknesses (10, 12, and 14 in.). The E-modulus of the surface course and that of the subgrade were held constant. The magnitude of maximum horizontal tensile stress in the 14-in.-thick surface course was only about two-thirds of that in the 10-in.-thick surface course. Similarly, the vertical normal stress at the 14-in.-thick surface course/subgrade interface was also reduced by about 25 percent (fig. 35) from that of the 10-in.-thick surface course, thus resulting in decreased deflection (table IX).

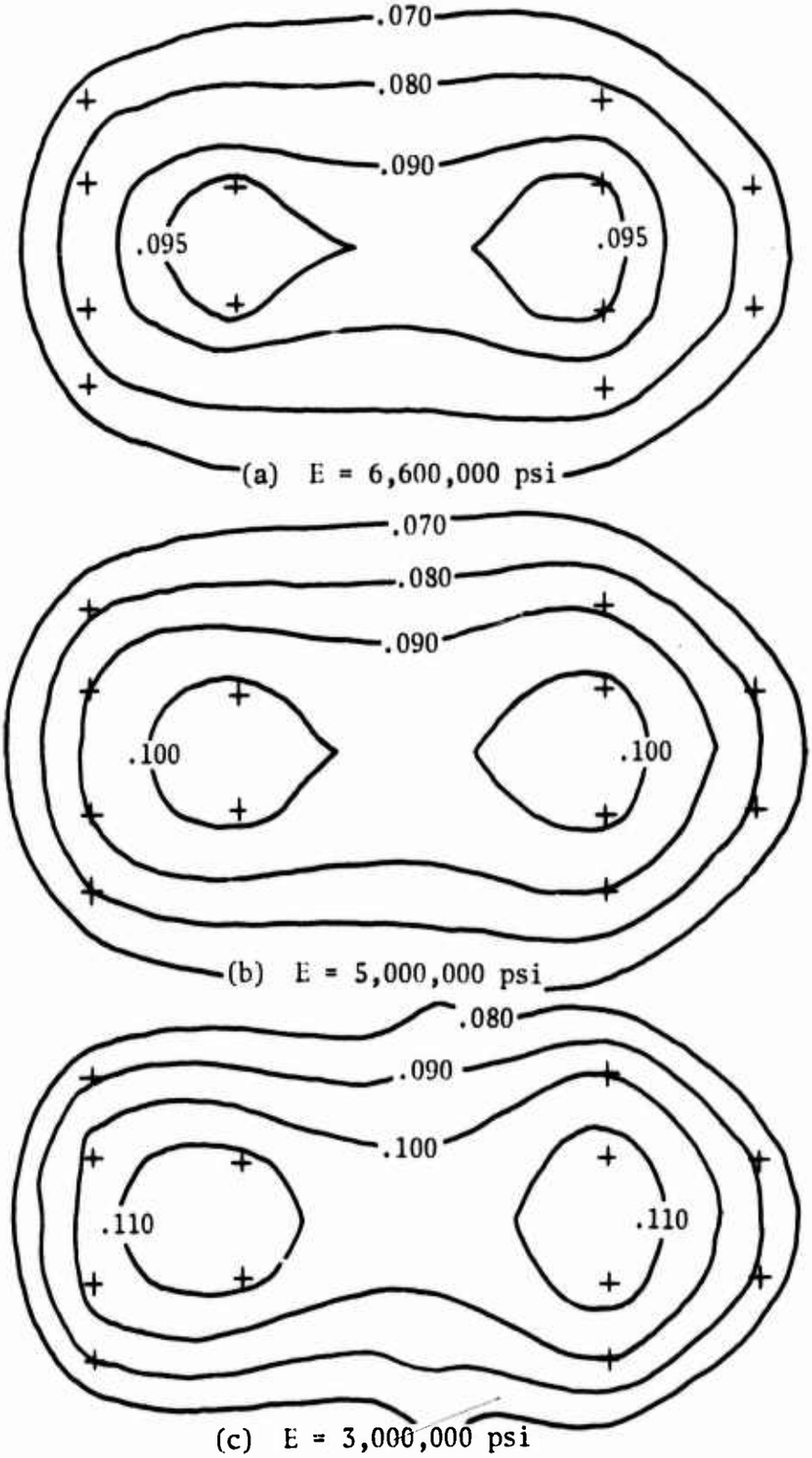

Note: + indicates the wheel positions of the 12-wheel assembly of the C-5A gear.

Figure 32. Effect of Surface Course E-Modulus on Surface Deflection in Rigid Pavement

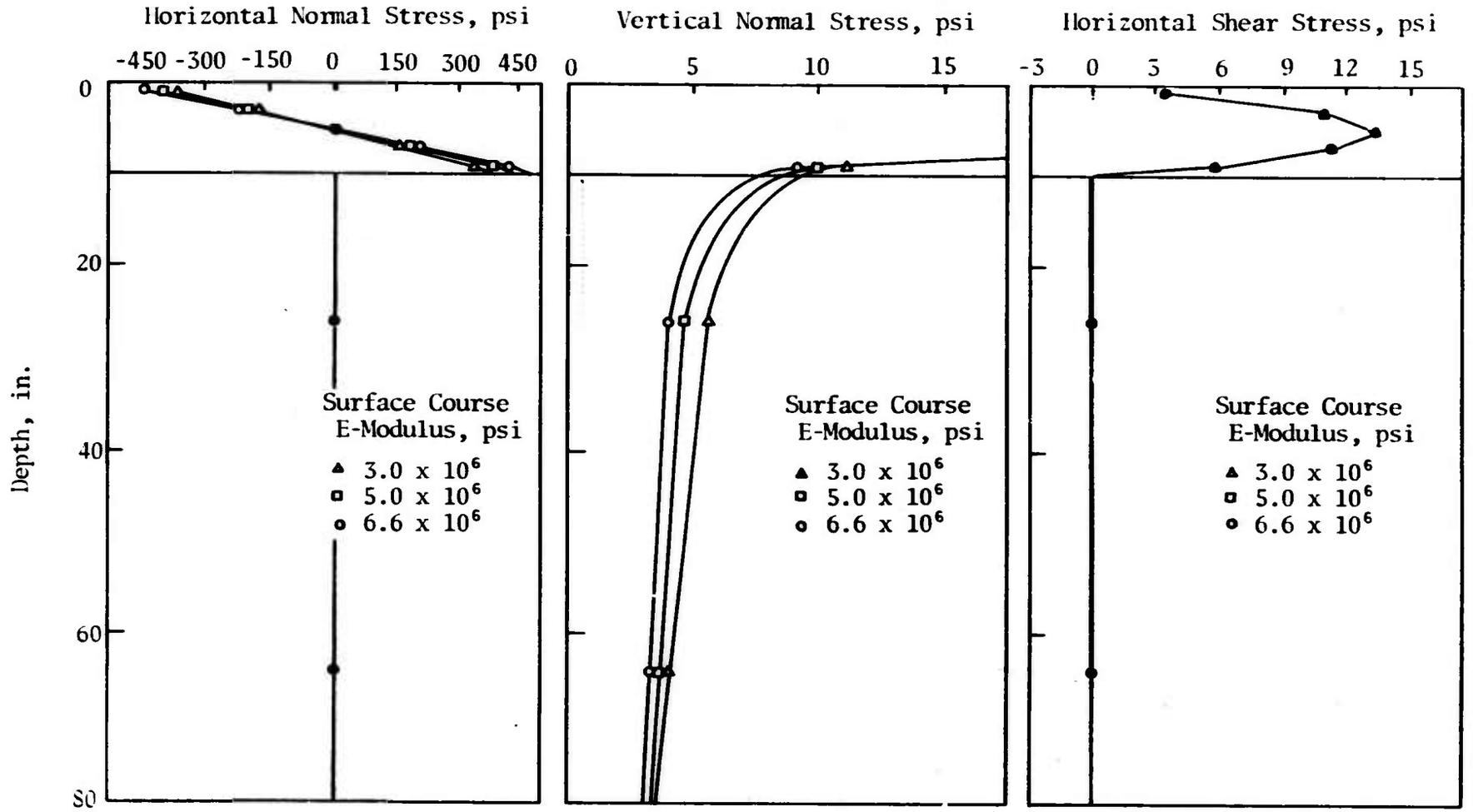

Note: • indicates identical response for the three E-moduli values considered.

Figure 33. Effect of Surface Course E-Modulus on Stress Distribution in Rigid Pavement

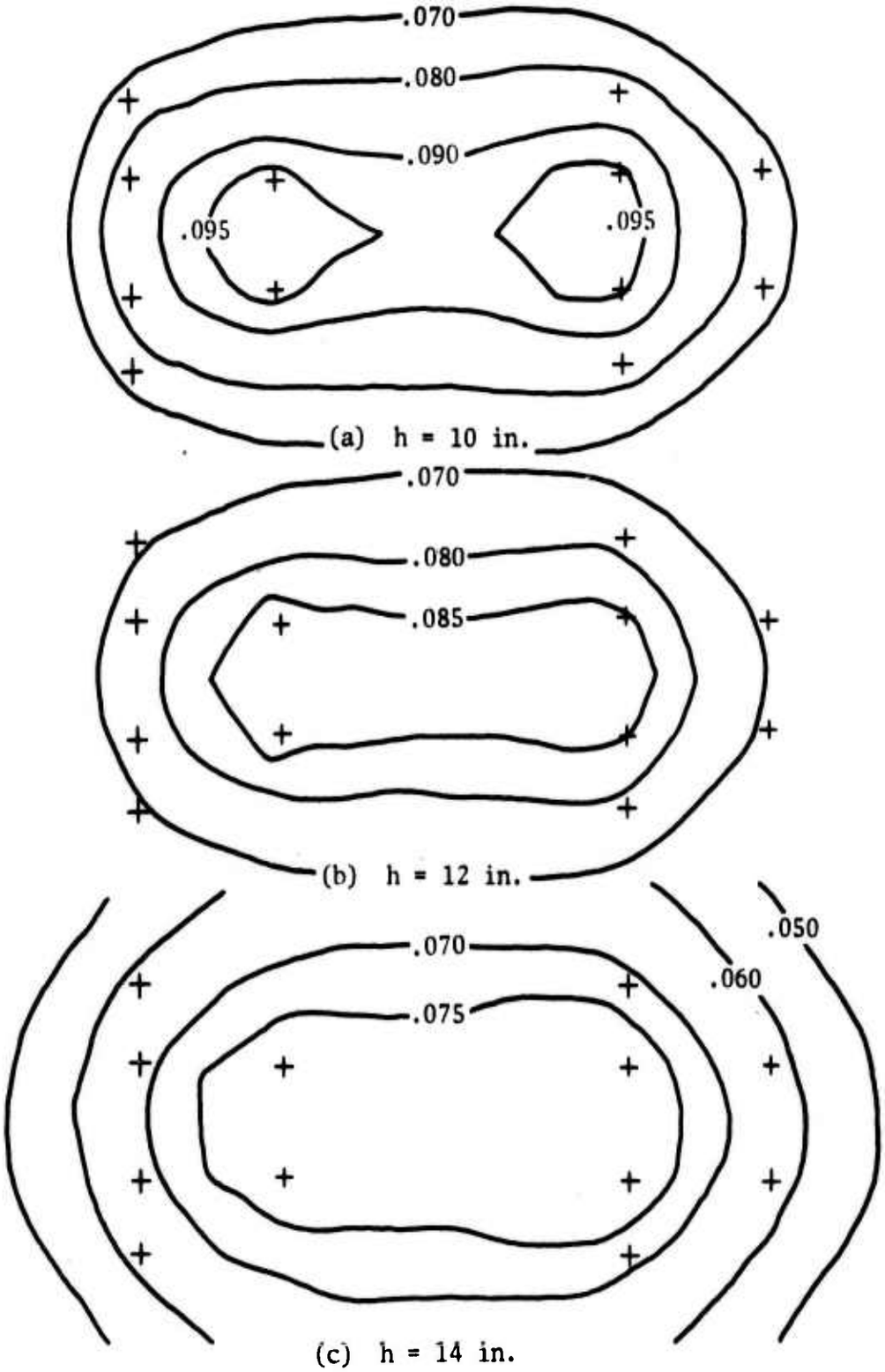

Note: + indicates the wheel positions of the 12-wheel assembly of the C-5A gear.

Figure 34. Effect of Surface Course Thickness on Surface Deflection in Rigid Pavement

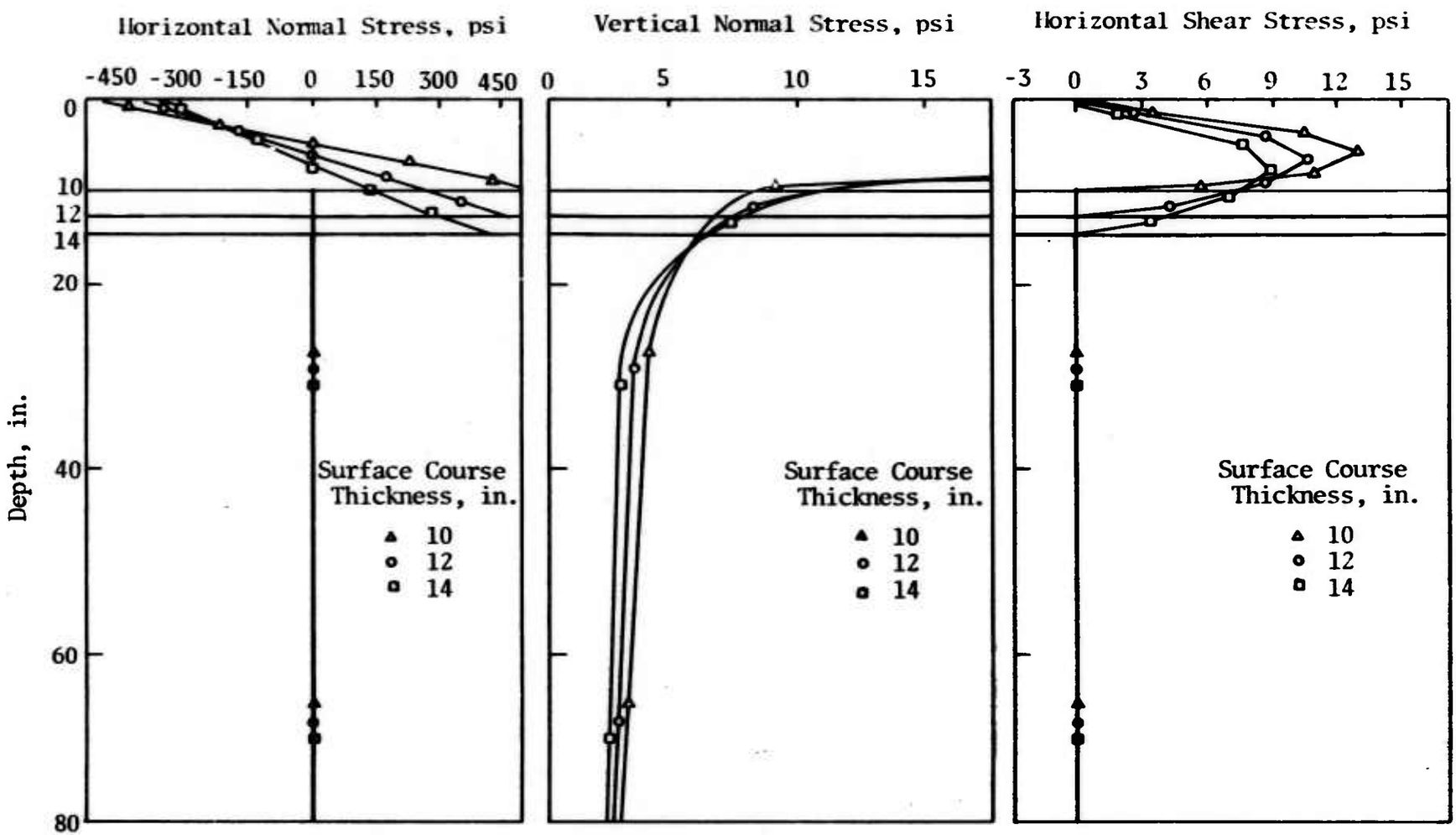

Figure 35. Effect of Surface Course Thickness on Stress Distribution in Rigid Pavement

c. Effect of Young's Modulus of Subgrade

Figure 36 shows the effect of changing the E-modulus of the subgrade while keeping the surface course properties constant. Reducing the subgrade stiffness from 6,000 to 3,000 psi increased the maximum deflection by about 70 percent, while reduction from 6,000 to 1,000 psi increased the maximum deflection by about 400 percent (table X).

Figure 37 shows the changes in stress distribution caused by variation of subgrade E-modulus from 1,000 to 6,000 psi. The weaker the subgrade the greater the horizontal normal stress in the surface course. The maximum horizontal tensile stress in the surface course was increased by about 40 percent when the subgrade E-modulus was reduced from 6,000 to 1,000 psi (table X). The vertical normal stress at the surface course/subgrade interface was reduced by about 25 percent for the same reduction in subgrade E-modulus. However, in spite of this reduction in subgrade stress, the surface deflection was increased by about 400 percent because of the reduction in subgrade E-modulus from 6,000 to 1,000 psi.

d. Effect of Base Course

Figure 38 and table XI show the manner in which the deflection basin of the surface course is affected when there is a base course below the surface course. While the deflection basin of the surface course resting on a 12-in.-thick base course with an E-modulus of 24,000 psi varied only slightly from that of a similar surface course resting directly on the subgrade, a 24-in.-thick base course with an E-modulus of 60,000 psi reduced the maximum deflection by about 10 percent and made the deflection basin somewhat flatter. In both cases, the E-modulus of the surface course was 6,600,000 psi and that of the subgrade was 6,000 psi.

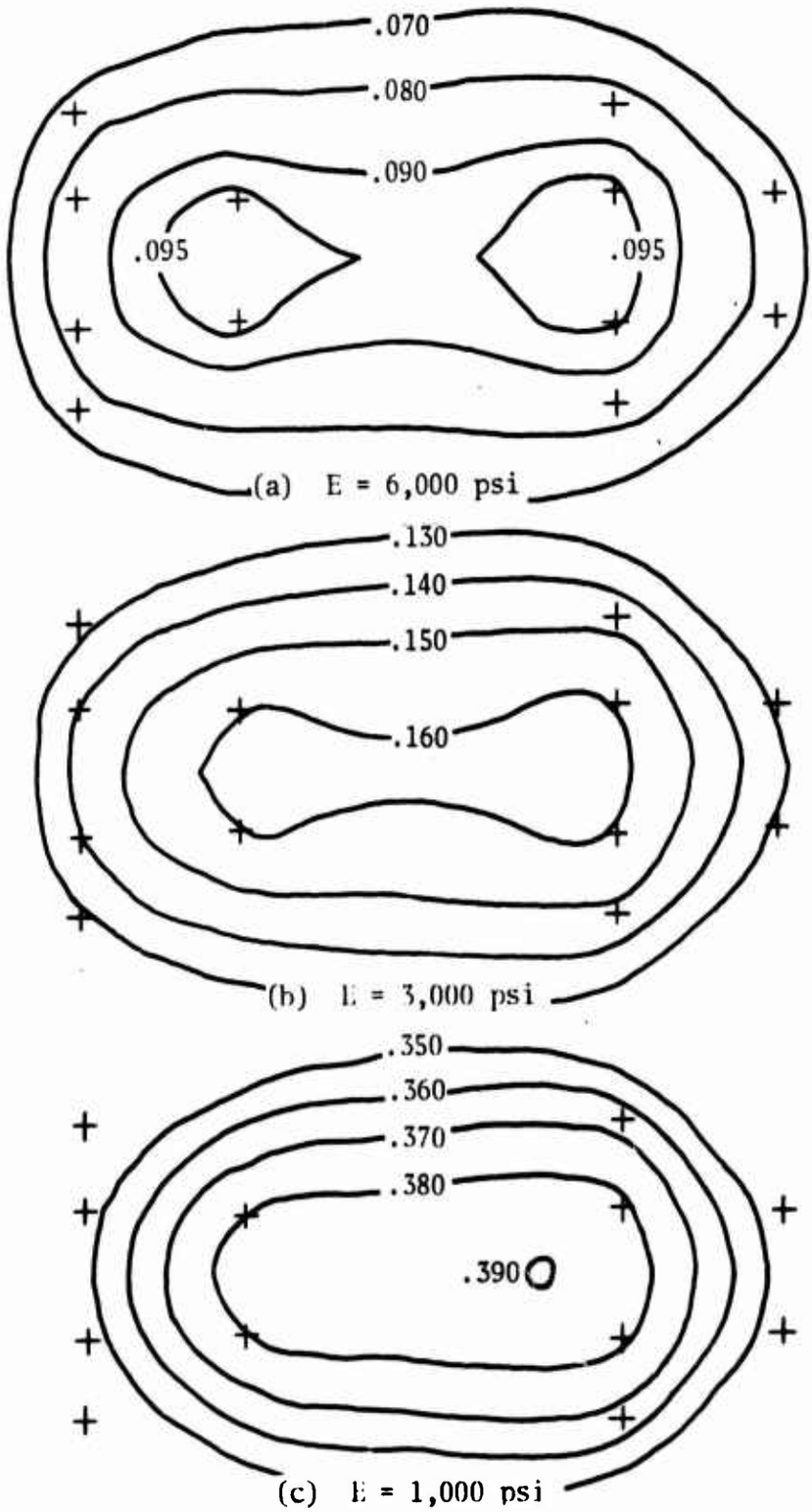

Note: + indicates the wheel positions of the 12-wheel assembly of the C-5A gear.

Figure 36. Effect of Subgrade E-Modulus on Surface Deflection in Rigid Pavement

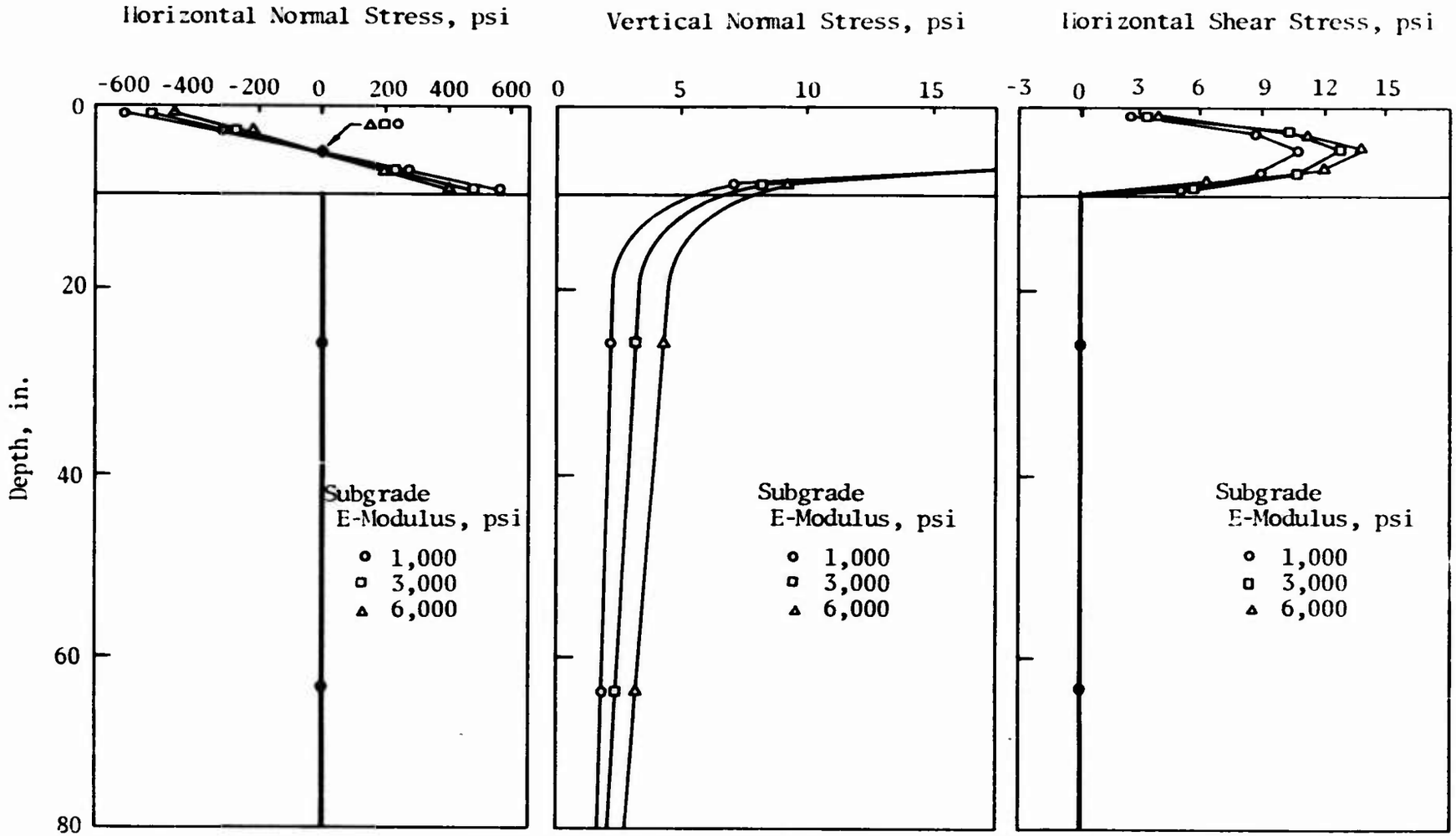

Note: • indicates identical response for the three E-moduli values considered.

Figure 37. Effect of Subgrade E-Modulus on Stress Distribution in Rigid Pavement

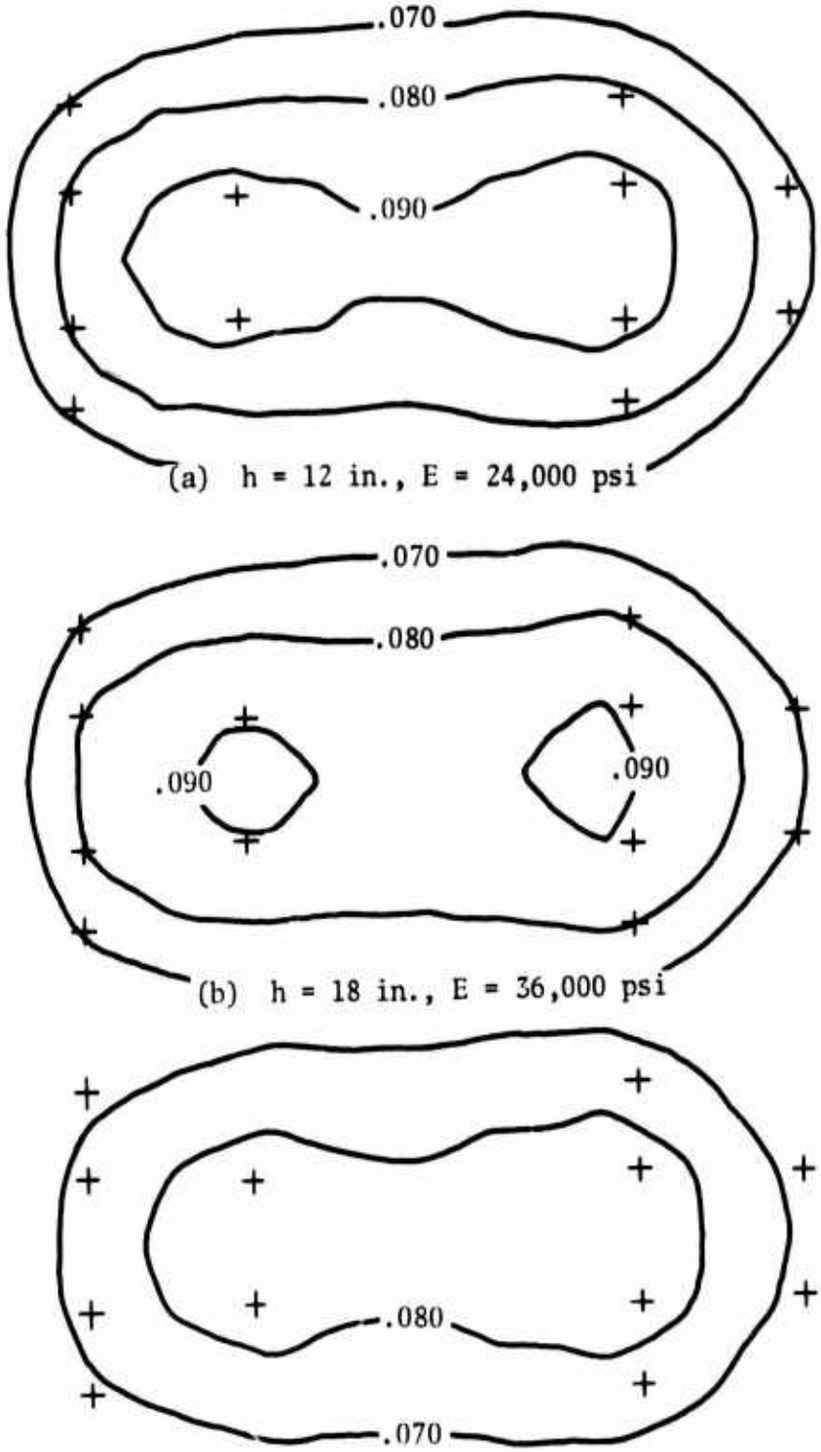

(a) h = 12 in., E = 24,000 psi

(b) h = 18 in., E = 36,000 psi

(c) h = 24 in., E = 60,000 psi

Note: + indicates the wheel positions of the 12-wheel assembly of the C-5A gear.

Figure 38. Effect of Base Course E-Modulus and Thickness on Surface Deflection in Rigid Pavement

SECTION VI

PARAMETRIC STUDY FOR AIR FORCE CIVIL ENGINEERING CENTER

The WES parametric study of both flexible pavement and rigid pavement systems (section V) was conducted from a theoretical point of view,* assuming some representative values of the pavement layer properties. In addition to this study, which was required by this research effort, another parametric study of a rigid pavement system was conducted at the request of the Civil Engineering Center (CEC) at Wright-Patterson AFB. This afforded an opportunity to demonstrate the practical use of the AFPAV code.

Figure 39 shows the pavement system parameters used in the study for the CEC. The objective of the study was the determination of the maximum horizontal tensile stress in the surface course when loaded by (1) the C-5A, (2) the Boeing 747, and (3) the C-141A aircraft. Figure 40 shows the configuration of the main landing gears of the C-141A and Boeing 747 aircraft; table XII compares the assumed wheel data for the three aircraft.

Figure 41 shows the effect of the surface course thickness on the maximum horizontal tensile stress in the rigid pavement system. The tensile stresses caused by the C-5A aircraft were lower than those caused by the other two aircraft because of the arrangement of the wheels of the landing gears (fig. 5) and the low tire pressure (table XII) of the C-5A aircraft. Although for thicknesses less than 12 in., the C-141A produced larger tensile stresses than did the Boeing 747 aircraft, this situation reversed when the thickness of the surface course was increased. In this analysis, as in most of the analyses included in this report, it was assumed that the loading was in the interior portion of a wide pavement system. Furthermore, the presence of joints in the surface course was also ignored.

*The results of this study have been published (refs. 19,20).

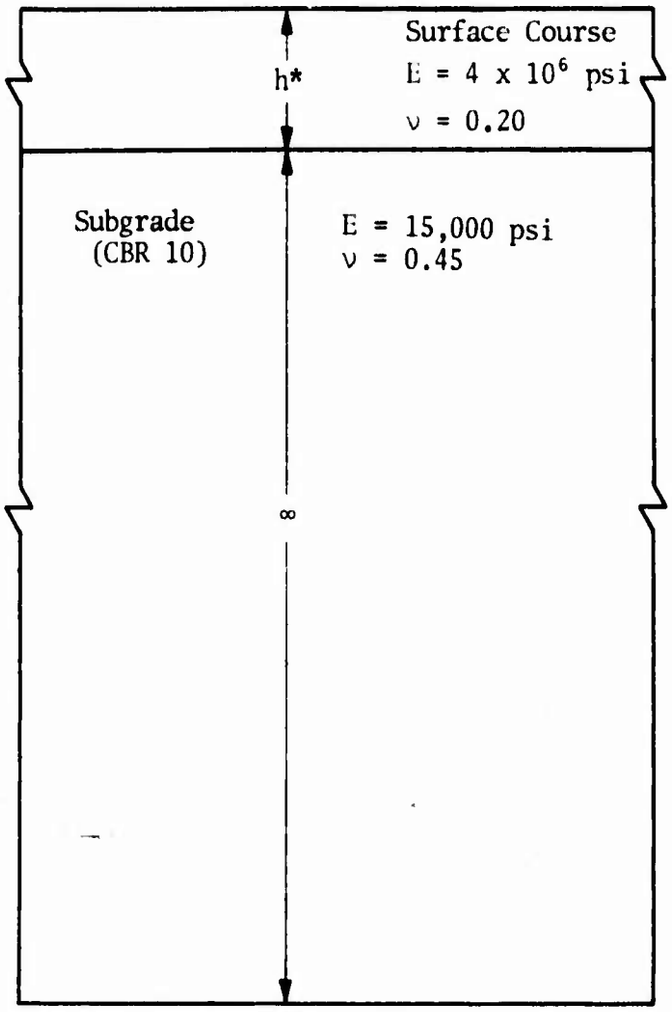

*Thickness of Surface Course

Problem	h, in.
1	8
2	10
3	12
4	14
5	18
6	20

Figure 39. Rigid Pavement System Analyzed for CEC

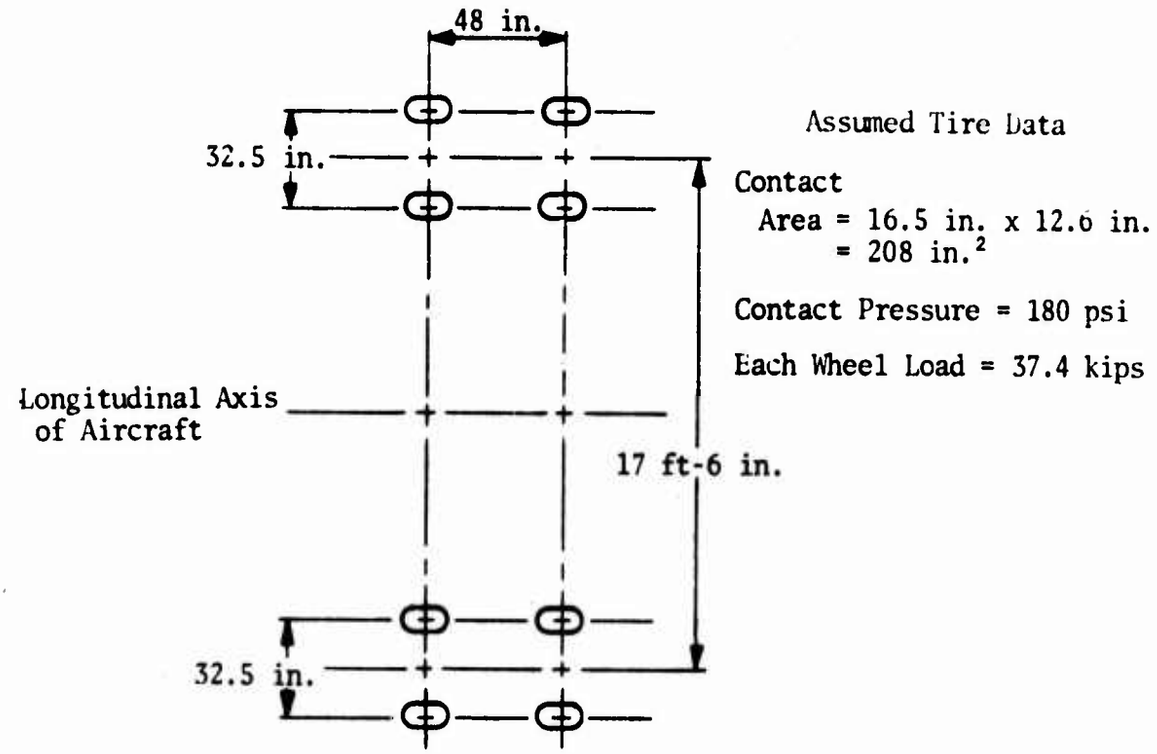

(a) C-141A Aircraft

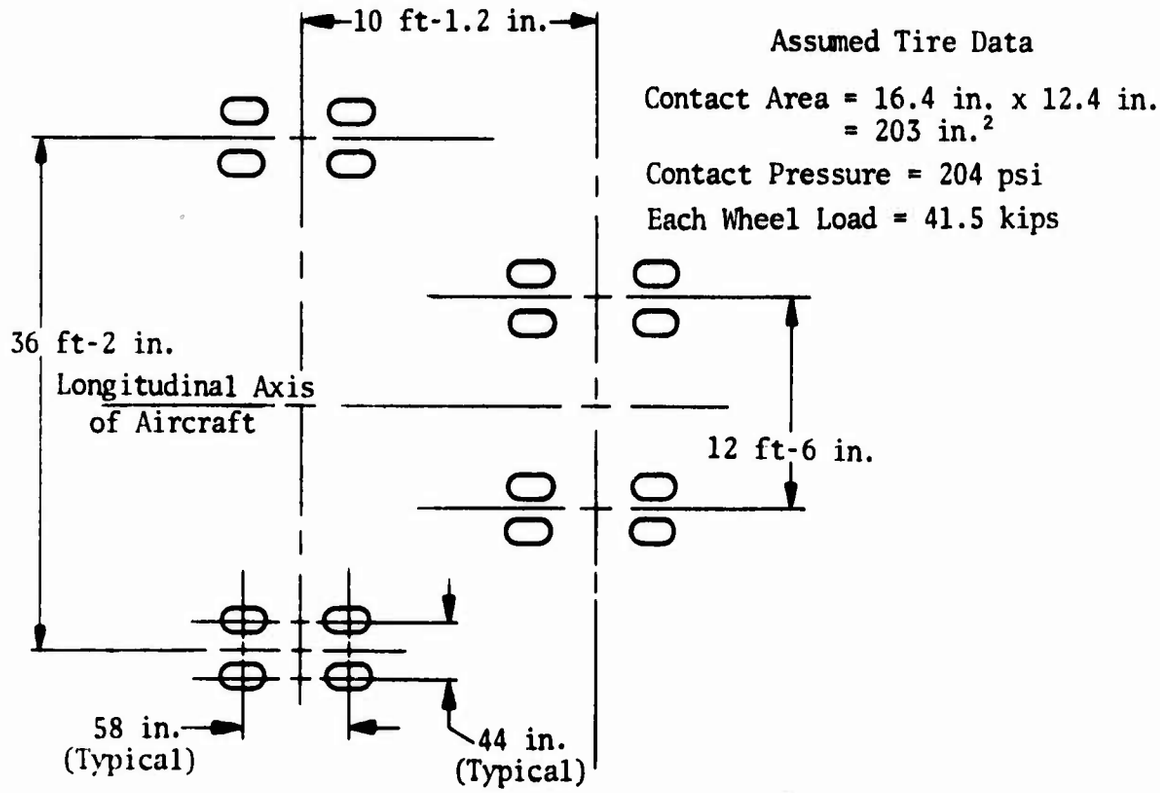

(b) Boeing 747 Aircraft

Figure 40. Main Landing Gear Configurations

Table XII

DATA FOR MAIN LANDING GEARS IN CEC STUDY

Aircraft	Number of Wheels	Contact Area,* $in.^2$	Contact Pressure,* psi	Wheel Load,* kips
C-5A	24	285	106	30.2
Boeing 747	16	203	204	41.5
C-141A	8	208	180	37.4

*Assumed data.

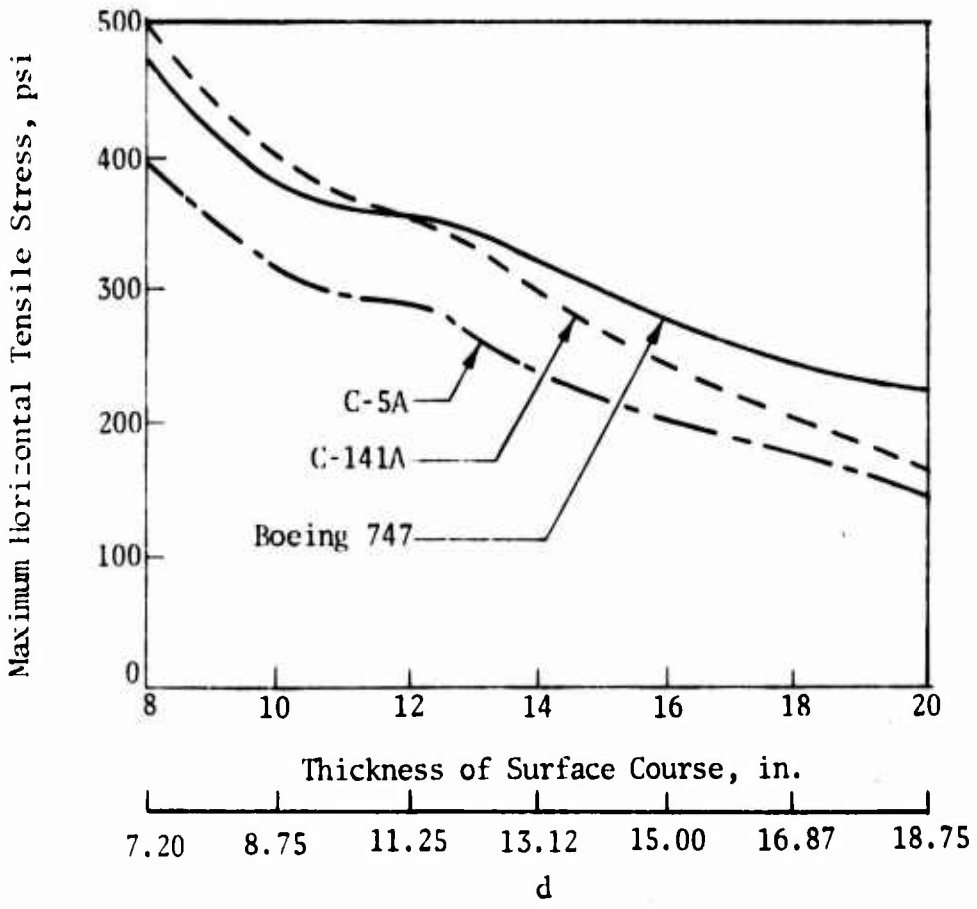

Note: d is the depth at which stresses shown in this figure existed.

Figure 41. Effect of Surface Course Thickness on Maximum Horizontal Tensile Stress in Surface Course of Rigid Pavement

SECTION VII

CONCLUSIONS AND RECOMMENDATIONS

1. CONCLUSIONS

Subject to the obvious limitations inherent in a linear elastic model of layered pavement systems, the AFPAV code appears to be a satisfactory analytical tool for predicting the pavement response due to the MWHGL of modern aircraft such as the C-5A. This is supported by the results of the analysis of the full-scale pavement sections (particularly the rigid pavement section) tested at WES.

Even though accurate predictions of pavement response may be difficult to make at present, either because of the limitations of the code or because of the engineer's inability to determine the proper input parameters pertaining to the different pavement layers, the AFPAV code is a very useful tool for parametric studies of pavement systems loaded by multiple wheels. The results of the parametric studies of both rigid and flexible pavements indicate the need for accurate determination of the following pavement system parameters for a linear elastic model:

(1) Moduli of elasticity of all pavement layers

(2) Poisson's ratio of the subgrade

(3) Thicknesses of the upper layers

(4) Elastic constants of the existing ground below the built-up subgrade

2. RECOMMENDATIONS

Experience in working with the AFPAV code indicates the need for the following improvements in the code:

(1) The code should be modified to consider the strain-dependent moduli values of the pavement layers.

(2) The phenomenon of *no-tension* in certain layers should be considered. (In such an analysis, the effects of the geostatic stresses (ref. 21) should be included.)

(3) The code should be modified to analyze the *sliding-plane* problem, both along vertical joints and along interfaces, when the pavement is loaded by multiple wheels.

(4) Viscoelastic behavior of asphaltic concrete layers as well as temperature effects should be analyzed.

(5) To predict permanent deformations, the unloading phenomenon should be analyzed. (So far attention has been paid only to the loading portion of the stress/strain relationships. This gives only the instantaneous, recoverable deformations.)

(6) Dynamic analyses of pavement response using the AFPAV code should be undertaken to see if there are any conditions which might be more critical than the static analyses.* (This may eventually lead to the refinement of analytical studies of runway roughness which at present do not consider the layered pavement systems.)

Modification of the AFPAV code to perform the analyses in (1), (2), and (3) is currently in progress. When the modified code becomes available, it should be possible to predict the three basic types of pavement response (i.e., deflection, strain, and stress) more accurately. Thus, the AFPAV code will be of great help in formulating workable pavement distress criteria for pavement evaluation.

*Lockheed-California Company has performed some research for the Federal Aviation Administration to predict the dynamic wheel load effects on airport pavements using the *plate on elastic solid* theory (ref. 22).

REFERENCES

1. U.S. Naval Civil Engineering Laboratory, *Rational Pavement Evaluation--Review of Present Technology*, AFWL-TR-69-9, Kirtland Air Force Base, N.Mex., October 1969.

2. Crawford, J. E., *An Analytical Model for Airfield Pavement Analysis (AFPAV)*, AFWL-TR-71-70, Kirtland Air Force Base, N.Mex., 1971.

3. Herrmann, L. R., "A Three-Dimensional Elasticity Solution for Continuous Beams," *Journal of the Franklin Institute*, Vol. 278, No. 2, August 1964.

4. Pichumani, R., *Theoretical Analysis of Airfield Pavement Structures*, AFWL-TR-71-26, Kirtland Air Force Base, N.Mex., July 1971.

5. Peutz, M. G. F., et al., *Layered Systems Under Normal Surface Loads, BISTRO Computer Program*, Koninklijke/Shell Laboratorium, Amsterdam, The Netherlands.

6. Pearre III, C. M., and Hudson, W. R., *A Discrete-Element Solution of Plates and Pavement Slabs Using a Variable Increment Length Model*, Research Report No. 56-11, Center for Highway Research, University of Texas, Austin, April 1969.

7. Wilson, E. L., "Structural Analysis of Axisymmetric Solids," *Journal of A.I.A.A.*, Vol. 3, 1965.

8. Herrmann, L. R., *User's Manual for PSA (Three-Dimensional Elasticity Analysis of Periodically Loaded Prismatic Solids)*, University of California, Davis, Calif., November 1968.

9. Wilson, E. L., *SAP--A General Structural Analysis Program*, Report No. UC SESM 70-20 to Walla Walla District, U.S. Engineer's Office, University of California, Berkeley, September 1970.

10. Pichumani, R., *Three-Dimensional Finite Element Analysis of Pile-Reinforced Pavement Structures*, DE-TN-72-001, Kirtland Air Force Base, N.Mex., February 1972.

11. Doherty, W. P., Wilson, E. L., and Taylor, R. L., *Stress Analysis of Axisymmetric Solids Utilizing Higher-Order Quadrilateral Finite Elements*, Report No. SESM 69-3, Structural Engineering Laboratory, University of California, Berkeley, January 1969.

12. Duncan, J. M., Monismith, C. M., and Wilson, E. L., "Finite Element Analysis of Pavements," Paper presented at the 47th Annual Meeting of the Highway Research Board, *Highway Research Record 228*.

13. U.S. Naval Civil Engineering Laboratory, *Layered Pavement Systems--Parts I and II*, Technical Report No. R763, April 1972.

14. Hay, D. R., *Aircraft Characteristics for Airfield Pavement Design and Evaluation*, AFWL-TR-69-54, Kirtland Air Force Base, N.Mex., October 1969.

15. Ahlvin, R. G., et al., *Multiple-Wheel Heavy Gear Load Pavement Tests*, AFWL-TR-70-113, Vol. I, Kirtland Air Force Base, N.Mex., November 1971.

16. Hardin, B. O., *Characterization and Use of Shear Stress-Strain Relations for Airfield Subgrade and Base Course Materials*, AFWL-TR-71-60, Kirtland Air Force Base, N.Mex., July 1971.

17. Seed, H. B., Mitry, F. G., Monismith, C. L., and Chan, C. K., *Factors Influencing the Resilient Deformations of Untreated Aggregate Base in Two-Layer Pavements Subjected to Repeated Loading.* Paper presented at the 46th Annual Meeting of the Highway Research Board.

18. Communication dated June 19, 1970, received from the Transportation Facilities Branch, CERL, Champaign, Ill.

19. Pichumani, R., "Applications of Computer Codes to the Analysis of Flexible Pavements," *Proceedings*, Third International Conference on the Structural Design of Asphalt Pavements, Vol. I, London, England, September 11-15, 1972.

20. Pichumani, R., and Triandafilidis, G. E., "Interaction Between Rigid Pavement Structure and Its Foundation," *Proceedings*, Symposium on the Interaction of Structure and Foundation, The Midland Soil Mechanics and Foundation Engineering Society, England, July 12-14, 1971.

21. Zienkiewicz, O. C., Valliappan, S., and King, I. P., "Stress Analysis of Rock as a 'No-Tension' Material," *Geotechnique*, Vol. 18, 1968.

22. Wignot, J. E., et al., *Aircraft Dynamic Wheel Load Effects on Airport Pavements*, Final Report No. FAA-RD-70-19 prepared by Lockheed-California Co., for FAA Systems Research and Development Service, Washington, D.C., May 1970.